Translocation of Botulinum Neurotoxins

By

Shihu Sun

A dissertation submitted in partial fulfillment of

the requirements for the degree of

Doctor of Philosophy

(Molecular and Cellular Pharmacology)

at the

UNIVERSITY OF WISCONSIN-MADISON

2012

Date of final oral examination: 04/30/12

The dissertation is approved by the following members of the Final Oral Committee:

Edwin Chapman, Professor, Department of Neuroscience

Meyer Jackson, Professor, Department of Neuroscience

Barry Ganetzky, Professor, Laboratory of Genetics

Elizabeth Craig, Professor, Department of Biochemistry

Eric Johnson, Professor, Department of Bacteriology

ACKNOWLEGEMENTS

Foremost I would like to thank Dr. Edwin Chapman, my thesis advisor. Dr. Chapman is an extremely intelligent scientist, and his passion for science and dedication to research are a lifetime inspiration to me. I also feel very grateful to have a mentor like him who gives me the best possible training in scientific thinking, data presenting and manuscript writing, and who also provides me a very supportive and motivating environment in which to work. His training over the past five years helps me to mature scientifically, and also greatly prepares me for future challenges.

I would like to thank my collaborators Dr. J. Michael Edwardson, Dr. Swetha Suresh for the AFM study, and Dr. William Tepp and Dr. Eric Johnson for providing me the toxins and antibodies. Their enduring support and generous help are paramount for the completion of the research presented in this thesis.

I want to thank my committee members, Dr. Elizabeth Craig, Dr. Barry Ganetzky, Dr. Meyer Jackson and Dr. Eric Johnson, for their guidance, insightful suggestions, valuable time and input throughout my graduate study.

I would like to thank all the past and current members in Dr. Chapman's laboratory for being great colleagues to work with and friends to spend time with. Especially Dr. Min Dong, who taught me basic experimentation skills and selflessly shared his insights in the field of botulinum toxin studies. He is like a big brother who helped me to adapt to life in the US, and I feel very fortunate to have him as a great friend. I also would like to give special thanks to Dr. Huisheng Liu for his support of my research with the patch clamp techniques and for being a fun and sincere friend.

I would like to thank the faculty, staff and students in the Department of Neuroscience, the Molecular and Cellular Pharmacology program for their support over the past five years. I would like to thank the Department of Biochemistry for recruiting me to this campus initially, and giving me the opportunity to study at this campus.

I would like to thank all my friends in Madison, for making my life in graduate school a great memory and for their support during my graduate school career. I would also like to thank many of my close friends and family members in other places in the US and those back in China, for always being just a phone call away during my graduate study, I feel very grateful to have them as a part of my life.

Finally, with all my love and gratitude, I would like to thank my dearest parents, my father Weizhu Sun and my mother Hongmei Fu. They raised and educate me with love and great effort, and their attitudes towards life and career also provide me the best guidance and inspiration. I would like to express my deepest thanks to my husband, Sean Daniel, for his endless support, patience and encouragement. This thesis is also dedicated to his love, care and devotion.

PREFACE

This thesis is dedicated to investigate how Botulinum Neurotoxins (BoNTs), the most potent toxins known to mankind, gain access to their targets in host cells. Generally, four steps are involved for BoNTs to intoxicate neurons: binding to receptors on cell surface, internalization via receptor-mediated endocytosis, translocation from endosomes into the cytosol, and cleavage of target proteins in cytosol. Previous studies have identified target proteins for all BoNTs; in addition, receptors for several serotypes of BoNTs were also revealed. However, how BoNTs translocate into the cytosol of neurons remains largely unknown. This thesis specifically focuses on studying the mechanisms underlying BoNT translocation.

In Chapter 1, I provide a general background of BoNTs: what are BoNTs and how BoNTs intoxicate host cells. Knowledge of BoNTs translocation based on previous studies is also intensively reviewed here. Despite the deadly natures of these toxins, BoNTs are currently used to treat a variety of human diseases. The first chapter will also provide an introduction to applications of BoNTs.

Chapter 2 focuses on mechanisms of translocation of BoNT/B. This serotype of BoNTs is currently used to treat human diseases, and here we use it as a model to study translocation of BoNTs. Previous studies indicate that low endosomal pH triggers the translocation of BoNTs; our data here further indicate that BoNT/B is a coincidence detector, that binding to the ganglioside GT1b, a co-receptor molecule of BoNT/B, enables the toxin to sense low pH to transform into a hydrophobic membrane channel that resembles other translocation machineries. As such, translocation of BoNT/B happens at the right time and place.

Our studies on BoNT/B revealed a novel model in BoNTs translocation, and in Chapter 3, we further test the model on BoNT/E. BoNT/E also causes botulism in humans. Here we directly compared pH-sensing activities of BoNT/E to BoNT/B, and common and unique features of BoNT/E translocation are revealed.

In Chapter 4, I summarize conclusions from current studies and also discuss directions of future studies.

Table of Contents

Abstract

Botulinum neurotoxins (BoNTs) are the most potent toxins known to humankind. They cause a fetal disease termed botulism, by specifically cleaving SNARE proteins to block neurotransmitter release at nerve terminals. This thesis is dedicated to elucidate how BoNTs translocate from endosomes into the cytosol of neurons, the least understood process during BoNT intoxication. Translocation of BoNT/B and E, two serotypes of BoNTs causing human botulism, were studied.

We found that binding to the ganglioside GT1b, a coreceptor for BoNTs, enables BoNT/B to sense low pH, undergo a significant change in secondary structure, and transform into a hydrophobic oligomeric membrane protein. Imaging of the toxin on lipid bilayers utilizing atomic force microscopy revealed donut-shaped channel-like structures that resemble other protein translocation assemblies. Toosendanin, a drug possessing therapeutic effects against botulism, inhibited GT1b-dependent BoNT/B oligomerization and in parallel truncated BoNT/B single-channel conductance, indicating that oligomerization plays a role in the translocation reaction. Thus, BoNT/B functions as a coincidence detector for receptor and low pH to ensure spatial and temporal accuracy for toxin conversion into a translocation channel.

We discovered that similar to BoNT/B, BoNT/E is also a coincidence detector for translocation, that binding to GT1b enabled BoNT/E to transform into a hydrophobic protein at the same low pH range as BoNT/B. However, BoNT/E exhibited some distinct properties from BoNT/B. BoNT/E translocated much faster than BoNT/B in neurons. Binding of GT1b enabled BoNT/E to assemble into oligomers even at neutral pH, potentially contributing to its fast

translocation. In the absence of GT1b, low pH altered the structure of BoNT/E to some degree that the toxin lost its ability to intoxicate neurons.

In summary, our studies indicate that BoNTs may function as coincidence detectors for low pH and GT1b for translocation, that in addition to the well-established role of low pH, receptor molecules may also play a role in shaping the behaviors of these deadly toxins.

Chapter 1

Background and Significance

1.1. Botulism

1.1.1. The Discovery

Botulism is a fetal disease that has probably accompanied mankind since dawn of our existence; however, it was not until the 19th century that it was first documented. In 1817, J.G. Steinbuch (1770-1818), a health officer in the village of Herrenberg in Germany, and Justinus Kerner (1786-1862), a German romantic poet and health officer, independently published two papers reporting lethal "sausage poisoning" occurring in the south of Germany (Kerner, 1817; Steinbuch, 1817). These papers, along with two monographs published by Kerner in the 1820s, gave the first accurate and complete clinical descriptions of symptoms of botulism (Figure 1-1) (Erbguth, 2004) .

1.1.2. The Organisms and Toxin Types

In 1897, the Belgian microbiologist Émile Pierre-Marie van Ermengem (1851–1932) consistently found an organism in botulism-causing ham, as well as in a culture of spleen from one botulism victim (Van Ermengem, 1897). He isolated the organism and named it *Bacillus botulinus,* after the Latin word *botulus* for sausage. The name was later changed to *Clostridium botulinum*; due to the anaerobic nature of toxigenic organisms, the genus *Clostridium*, rather than *Bacillus*, was adopted (Hatheway, 1990).

Clostridium botulinum includes a diverse group of spore-forming rod-shape anaerobic bacteria, and *Clostridium botulinum* strains are usually divided into four groups (i.e. groups I, II, III, and IV) based on physiologic characteristics (Hatheway, 1990). These organisms share a common property of producing botulinum neurotoxins (BoNTs) (Figure 1-2)， agents causing

botulism (Hill et al., 2007). Based on different anti-serum properties, seven distinct serotypes of BoNTs are identified, designated A-G (Table 1-1) (Hatheway, 1990). Together with tetanus toxin (TeNT), they are known as clostridial neurotoxins. In addition to *Clostridium Botulinum* (producing all serotypes of toxins), some other strains of clostridial species, including *Clostridium butyricum* (producing BoNT/E) (Aureli et al., 1986; McCroskey et al., 1986), *Clostridium baratii* (producing BoNT/F) (Hall et al., 1985) and *Clostridium argenetinense* (producing BoNT/G) (Suen et al., 1988), are also capable of elaborating BoNTs under anaerobic conditions. BoNT genes for serotypes A, B, E and F can be found within the bacterial chromosomes; BoNT/C and D are encoded by bacteriophages; BoNT/G genes are located to a plasmid within toxigenic strains (Hill et al., 2007).

1.1.3. Types and Symptoms of Botulism

Four main types of botulism are identified so far. They are categorized as: foodborne botulism, wound botulism, infant botulism and intestinal colonization of adults (Hatheway, 1990). Foodborne botulism is the most common form of botulism in the world. It is caused by consumption of foods contaminated by preformed toxins, and it starts with gastrointestinal symptoms of nausea, vomiting, and diarrhea in about one-third of cases. Symptoms typically develop within 18-36 hr after consumption of contaminated food, but can range from 2 hr to 8 days (Arnon, 1997). In 1943, wound botulism was discovered (Hatheway, 1990). *Clostridium botulinum* type A was identified in a mixture of bacteria cultured from the infected wound, suggesting that similar to tetanus, botulism can be caused by BoNTs produced by toxigenic organisms that reside in wounds. Wound botulism usually has a longer incubation time than

foodborne botulism, with an incubation time of 4-14 days (Johnson, 2000). Botulism caused by colonization of toxigenic organisms in intestinal tracts of infants (onset ranging from 1-63 weeks) (Hatheway, 1990) and adults (McCroskey and Hatheway, 1988) was discovered in 1976 and 1988, respectively, with infants botulism as the most prevalent botulism in the united states (~70% cases reported annually are infant botulism, according to CDC report) (Johnson, 2000).

All four types of botulism are characterized by symmetrical flaccid paralysis that first occurs and descends from the muscles of the head, face, mouth, and throat (Arnon, 1997). The sensorium remains clear, and the disease is not accomplished by fever or paresthesias. However, in severe conditions, death may also occur due to respiratory failure.

1.2. Botulinum Neurotoxins (BoNTs)

1.2.1. The Most Potent Toxin Known

The toxicity of BoNTs is measured by the median lethal dose (LD_{50}), which represents the dose required to kill half the population tested. BoNTs are the most potent toxin known to mankind, with LD_{50} ranging from 0.1-1 ng/kg (Gill, 1982). Human were said to be at least as sensitive as mice, with human LD_{50} calculated to be $\leqslant$ 1 ng/kg based on mice toxicities. As of today, the world population is estimated to be ~7 billion by the United States Census Bureau; if we assume an average body weight of 70 kg/person, $\leqslant$ 490 g BoNTs would be sufficient to eradicate humankind. Due to their extreme potency, BoNTs are listed as category A bioterrorism agents by the Center of Disease Control (CDC, see Section 1.4 for details) (Arnon et al., 2001).

1.2.2. Structures of BoNTs

BoNTs (150 kDa) are synthesized in the bacterial cytosol without a leader sequence, and released as protein aggregates only upon bacterial lysis (Schiavo et al., 2000). These aggregates, termed progenitor toxins, contain BoNTs nonconvalently associating with a nontoxic nonhemagglutinating (NTNH) protein, and up to six hemagglutinin proteins. Hemagglutinin proteins are named according to molecular mass (for instance, HA-70 possesses a molecular mass around 70 kDa), and are found in progenitor toxins of BoNT/A, B, C, D, G but not E and F (Hines et al., 2005). The association of BoNT, NTNH and various hemmagglutinin proteins results in different progenitor toxin masses (300-900 kDa) and sizes (categorized by sucrose density, 12-19 S), and progenitor toxins are classified into three types: M complex (300 kDa, 12 S), L complex (500 kDa, 16 S) and LL complexes (900 kDa, 19 S) (Hines et al., 2005).

Progenitor toxins significantly increase the oral toxicity of BoNTs (Ohishi and Sakaguchi, 1980; Ohishi et al., 1977). Reasons underlying such increase are not totally clear; one prevailing explanation is that progenitor toxins may help BoNTs to survive the harsh conditions in the stomach (Schiavo et al., 2000). Recent studies also revealed that progenitor toxins may facilitate the intestinal transepithelial delivery of BoNTs into the bloodstream (Matsumura et al., 2008; Niwa et al., 2007).

BoNTs are produced as inactive single-chain molecules, and have to be cleaved by a proteolytic enzyme, either endogenously or exogenously, to form active dichain toxins. The active BoNTs consist of an N-terminal light chain (LC, 50 kDa) and a C-terminal heavy chain (HC, 100 kDa), linked via a disulfide bond (Schiavo et al., 2000). The integrity of this disulfide bond is essential for toxicities of BoNTs *in vivo* (de Paiva et al., 1993). The HC also wraps

around the LC with a belt region (Montal, 2010). LC is a zinc-dependent protease, and is responsible for the toxicity of BoNTs. The HC assists the entry of LCs into cells, and HC is further divided into a N-terminal H_N domain (also known as the translocation domain (TD)), and a C-terminal H_C domain (also known as the receptor binding domain (RBD)). Functions of LC, H_N domain and H_C domain in intoxication of BoNTs are discussed in detail in Section 1.3.

Crystal structures of BoNT/A (PDB ID: 3BTA) (Lacy et al., 1998a), B (PDB ID: 1EPW) (Swaminathan and Eswaramoorthy, 2000) and E (PDB ID: 3FFZ) (Kumaran et al., 2009) holotoxins have been resolved. The sequences of these three toxins share significant homology, with 39% identity between A and B, 39.8% identity between A and E, and 37.2% identity between B and E, respectively (Swaminathan, 2011). Structures of BoNT/A and B are similar, but domain arrangement in BoNT/E is different with A and B. In the structures of BoNT/A and B, LC, H_N domain and H_C domain are clearly distinguishable, with the H_N domain locating in the middle and the LC and the H_C domain flanking on either side of the H_N domain in a linear fashion (Figure 1-3). There is no interface between the LC and the H_C domain in crystal structures of BoNT/A and B, and interactions between the H_N domain and the H_C domain are limited. In BoNT/E structure, however, the LC and the H_C domain locate on the same side of the H_N domain, and there are interfaces among all three domains (Figure 1-4) (Kumaran et al., 2009). Such unique domain arrangements in BoNT/E was also observed by electron microscopy (Fischer et al., 2008a).

Crystal structures of LCs of all BoNT serotypes were determined, and they shared a similar fold (Swaminathan, 2011). The fold is a compact globule composed of α helices and β sheets. The active sites of all BoNT LCs preserve high sequence conservation and have the

same geometry, and the zinc binding motif HExxH+H is found in all BoNT LCs. The zinc is coordinated by two histidines, one glutamate and by a water molecule that act as a nucleophile, in a large deep open cavity with a high negative electrical potential. The conserve sequences form identical interactions within 10 Å of the zinc, and mutagenesis studies demonstrate such conservation is required for catalytic activites of LCs (Swaminathan, 2011). In contrast, substrate interaction sides are high diverse among LCs of different BoNT serotypes, dictating specificities in substrate recognition (Swaminathan, 2011).

The H_N domain (TD) is proposed to be responsible for forming a membrane channel to conduct the translocation of LCs. The H_N domains of BoNT/A, B and E consist of two long helices ~100 Å long, and they form a coiled-coil (Swaminathan, 2011). The predicted transmembrane region within the H_N domain, locating at residues 650–672 in BoNT/A, residues 653–673 in BoNT/B and residues 638–658 in BoNT/E, respectively, is hydrophobic but does not have the helical conformation (Swaminathan, 2011). The N-terminal of the H_N domain is a loop called the "belt region" that wraps around the LC. Different from BoNT/A and B that the belt region only interacts with LC but not the H_C domain, the belt region in BoNT/E forms an interface between LC and the H_C domain (Kumaran et al., 2009).

The H_C domain is further divided into two domains with equal size: the H_{CN} domain and the H_{CC} domain. The H_{CN} domain forms a jelly-roll motif, and is highly conserved among BoNT serotypes. A recent study reported interactions between H_{CN} domain of BoNT/A with phosphatidylinositol phosphates (Muraro et al., 2009), but the function of H_{CN} domain is not clearly understood yet. The H_{CC} domain forms β-trefoil fold, and the sequences of the H_{CC} domain are highly diverse among different BoNT serotypes. The H_{CC} domain is responsible for

receptor binding of BoNTs on cellular surface, and this will be discussed in detail in Section 1.4 (Schiavo et al., 2000). The H_{CN} domain and the H_{CN} domain are connected by a short helix (Swaminathan, 2011).

1.3. Major Steps in BoNT Action

BoNTs exert their action by specifically block neurotransmitter release at nerve terminals. Depending on how BoNTs enter hosts, BoNTs take different routes to reach the general circulation that brings them to their final sites of action. In the most typical botulism, foodborne botulism, preformed BoNTs are ingested, go through the gastrointestinal tract and are absorbed primarily via small intestines; toxins are detected first in lymph then in blood after absorption (May and Whaler, 1958). How BoNTs penetrate membrane barriers from intestinal lumen to reach the general circulation is not fully understood; recent studies suggested a possible mechanism that BoNTs first bind to apical surface of epithelial cells, undergo receptor-mediated endocytosis and transcytosis, and are delivered to the basolateral surface of cells, which allow the toxins to reach the general circulation (Maksymowych and Simpson, 1998). This hypothesis is supported by observation of transcytosis of BoNT/A (Ahsan et al., 2005; Maksymowych and Simpson, 1998), B (Maksymowych and Simpson, 1998), C (Inui et al., 2010) and D (Niwa et al., 2010) in cultured epithelial cells; however, the molecular mechanisms underlying transcytosis still remains largely unknown.

At nerve terminals, four major steps are identified in BoNT action: binding to receptors on presynaptic terminals, receptor-mediated endocytosis, translocation of LCs across endosomal

membranes into the cytosol and cleavage of SNARE proteins by LCs in the cytosol (Figure 1-5). These four steps are reviewed in detail as below.

1.3.1. Neuronal Receptors for BoNTs

1.3.1.1. Double Receptor Model

Due to the extreme lethality of BoNTs, it is not surprising that identification of cellular receptors for these deadly toxins is of great interest to scientists for decades. However, the fact that there is so little tissue at peripheral nerve endings, the main sites of BoNT action, makes isolation and identification of BoNT receptors quite challenging (Simpson, 2004). Alternatively, toxin binding was studied in tissues like brain, and the research that characterized binding of radiolabeled toxins to isolated synaptosomes largely facilitated identification of BoNT receptors.

In a physiological medium, binding of radioiodinated BoNT/A to synaptosomes is biphasic, represented by a high affinity site (K_d= 0.6 nM, B_{max} = 60 fmol/mg) and low affinity sites (K_d > 25 nM) (Habermann and Dreyer, 1986; Williams et al., 1983). Similar binding was reported for radioiodinated BoNT/B, that the high affinity site has a K_d ~0.3-0.5 nM and B_{max} ~30-60 fmol/mg, and that the low affinity sites are heterogeneous in nature with K_d >16-21 nM and B_{max} » 3000 fmol/mg (Evans et al., 1986). These studies and others led to the hypothesis of double receptors for BoNTs in neurons (Montecucco et al., 1986), as detailed below.

1.3.1.2. Gangliosides

Gangliosides are glycosphingolipids that contain one or several sialic acid residues. Sialic acid(s) is (are) α-glycosidically linked to a neutral oligosaccharide core. Gangliosides present ubiquitously in vertebrate cells, and those in neurons are characterized by their unusually

structural complexity and high concentration (Ledeen, 1985). Based on their oligosaccharide core, gangliosides are categorized into different series (i.e. gala, hemato, ganglio, neolacto, globo and isoglobo series) (Tettamanti and Riboni, 1993); those predominant in the nervous system - GM1, GD1a, GD1b, GQ1b and GT1b - belong to the ganglio series, with *N*-acetylgalactosamme as the sugar attached to lactosylceramide via a GalNAc(β1–>4)Gal linkage (Figure 1-6). In neurons, the majority of gangliosides asymmetrically locate to the outer leaflet of the plasma membrane, accounting for ~5-10 % of total lipids in the plasma membrane (or ~10-20 % of lipids in the outer leaflet) (Ledeen, 1985). Rather than distributing evenly on cell surface, gangliosides may mainly exist in clusters surrounding membrane proteins as a functional aggregate (Aquino et al., 1985). In small amounts gangliosides are also found intracellularly, in organelles (such as mitochondria (Gillard et al., 1993), endoplasmic reticulum (Gillard et al., 1993) and synaptic vesicles (Ledeen et al., 1988)), in the cytosol (Sonnino et al., 1979) and even in nuclei (Saito and Sugiyama, 2002; Wu et al., 1995). They provide cell surface recognition sites, and they also play roles in neuritogenesis, neuronal differentiation and survival (Ledeen, 1985).

Numerous studies have demonstrated that BoNTs exhibit low affinity binding ($K_d > 10^8$ M) to gangliosides containing two or more sialic acids (i.e. complex gangliosides), with the highest affinity found in GT1b (Habermann and Dreyer, 1986; Kamata et al., 1986; Kitamura et al., 1980; Kozaki et al., 1998a; Nishiki et al., 1996b; Ochanda et al., 1986). In addition, preincubation with gangliosides at least partially inactivated BoNTs (Habermann and Dreyer, 1986; Simpson and Rapport, 1971a, b); removal of sialic acid residues from cell surface by neuraminidase treatment of adrenergic chromaffin cells (Marxen et al., 1989) and cultured cells

isolated from spinal cord (Bigalke et al., 1986) reduced toxicity of BoNT/A. These data suggest gangliosides may serve as receptors for BoNTs, and such receptor roles were confirmed by recently studies using ganglioside knockout (KO) mice. Disruption of $\beta_{1,4}$-*N*-acetylgalactosaminyltransferase (GM2/GA2/GD2 synthase) gene abolishes synthesis of all complex gangliosides (Kitamura et al., 1999; Liu et al., 1999), and toxicities of all BoNTs were reduced in these mice (Dong et al., 2007; Kitamura et al., 1999; Peng et al., 2011; Rummel et al., 2009). In addition, binding and functional entry of BoNT/A, B (Dong et al., 2007), C (Peng et al., 2011; Tsukamoto et al., 2005) and E (Dong et al., 2008b) was abolished in ganglioside KO cells, and intoxication was reduced for BoNT/ D (Peng et al., 2011) F (Peng et al., 2011) and G (Dong et al., 2007). Together, these data suggest that gangliosides play a crucial role in mediating entry of BoNTs.

Ganglioside binding site is confined to the H_{CC} domain of BoNTs (Binz and Rummel, 2009a; Lalli et al., 1999; Rummel et al., 2004b). A sialic acid binding motif H...SXWY...G within the H_{CC} domain, composing one of the two ganglioside binding cavities for TeNT (Binz and Rummel, 2009a), is largely conserved in the majority of BoNTs except for BoNT/C and D. Crystal structures of BoNT/A and B with GT1b analogs revealed that this motif forms the only ganglioside-binding pocket within these toxins (Stenmark et al., 2008; Swaminathan, 2011; Swaminathan and Eswaramoorthy, 2000); mutation of W1266L (BoNT/A) and W1262L (BoNT/B) within the motif resulted in reduction of BoNT toxicity (Binz and Rummel, 2009a; Rummel et al., 2004b). In BoNT/C, a conserved Typ (W1258) found in a nearby loop plays a critical in ganglioside binding (Tsukamoto et al., 2008), but no homologous Trp is identified as a key residue for ganglioside binding in BoNT/D (Binz and Rummel, 2009b).

1.3.1.3. Protein Receptors

In addition to gangliosides, many evidences, as summarized below, argued that BoNTs also need protein receptors for entry. Firstly, as pointed out above, binding of BoNTs to synaptosomes is biphasic; while binding of gangliosides ($K_d > 10^8$ M) explains the low affinity binding, it cannot explain the high affinity binding (K_d in subnanomolar range). Secondly, distribution of gangliosides is ubiquitous, but BoNTs only target a specific set of neurons (Habermann and Dreyer, 1986). Thirdly, treating synaptosomes with trypsin decreased the subsequent binding of BoNTs to membranes, and binding could not be restored by incorporation of gangliosides, indicating the existence of proteins receptors for BoNTs (Blasi et al., 1992; Ogasawara et al., 1991).

Isolation of a radioiodinated BoNT/B-binding protein from rat synaptosomes led to the identification of BoNT receptors (Nishiki et al., 1994). This protein was recognized as synaptotagamin I/II (syt) (Nishiki et al., 1994), the Ca^{2+} sensor for synaptic vesicle exocytosis (Chapman, 2002; Koh and Bellen, 2003). The dissociation constant for BoNT/B-syt was around 0.23 nM (Nishiki et al., 1996a), consistent with the high affinity binding of the toxin to synaptosomes (Evans et al., 1986). Further studies revealed that functional entry of BoNT/B into PC12 cells is dependent on syt I /II; binding of BoNT/B to syt II fragments blocked entry of the toxin into PC12 cells and rat diaphragm motor nerve terminals; and in conjunction with gangliosides, syt II fragment neutralized toxicity of BoNT/B in mice (Dong et al., 2003). These data demonstrate that syt I/II function as receptor for BoNT/B (Dong et al., 2003).

BoNT/B binding region is restricted to residues 47-60 in syt II (Chai et al., 2006; Dong et al., 2003). Crystal structures of BoNT/B with syt II segments containing this region revealed that syt II forms a short helix to bind BoNT/B within a hydrophobic groove in the H_{CC} domain (Chai et al., 2006; Jin et al., 2006), adjacent to the GT1b-binding pocket (Figure 1-7).

In addition to BoNT/B, BoNT/G also utilizes syt I/II as protein receptor for entry (Dong et al., 2007; Rummel et al., 2007b; Rummel et al., 2004a); however, this is not the case for other BoNTs. In 2006, protein receptor for BoNT/A was identified as SV2. SV2 is an integral membrane protein with 12 transmembrane regions, and it locates to synaptic and endocrine secretory vesicles in vertebrates (Dong et al., 2006). Significant increase of BoNT/A binding to neuromuscular junctions during high K^+ stimulation indicated that synaptic vesicle endocytosis might expose the protein receptor of BoNT/A to the cell surface, and screening binding activities of BoNT/A to various synaptic vesicle proteins allowed the identification of SV2. SV2 has three isoforms, SV2A, SV2B and SV2C; the binding activities of all isoforms to BoNT/A are contributed by the fourth loop of SV2. Binding and functional entry of BoNT/A in SV2 KO or knockdown cells were abolished or hampered, and were rescued by expression of SV2 isoforms; toxicity of BoNT/A in SV2B knocked out mice was also reduced. These data strongly suggest that SV2 is the protein receptor for BoNT/A (Dong et al., 2006). Similar to BoNT/B, BoNT/A causes human botulism (Arnon et al., 2001), and is also known as Botox® for medical and cosmetic uses, thus identification of the protein receptor for BoNT/A is a hallmark of BoNT research. Besides BoNT/A, BoNT/D (Peng et al., 2011) and BoNT/E (Dong et al., 2008b) also utilize SV2 as the protein receptor for entry; however, BoNT/E only binds SV2A/B but not

SV2C, and a N-glycosylation (at N573) within the fourth loop of SV2A/B is critical for binding and neuronal entry of BoNT/E (Dong et al., 2008b).

In summary, protein receptors mediating binding and entry of BoNTs – except for BoNT/C and F - into neurons have been resolved, and they are all synaptic vesicle proteins (Table 1-1). BoNT/A, D and E use SV2 as a receptor, and BoNT/B and G utilize syt I/II. BoNT/C and F share the highest sequence similarity to BoNT/D and E, respectively; however, lacking SV2 affected entry of neither toxin into rat hippocampal neurons, indicating BoNT/C and F may utilize a different protein receptor rather than SV2 for entry (Peng et al., 2011).

1.3.2. Receptor-Mediated Endocytosis

The idea that BoNTs utilize endocytosis for cellular entry was proposed by Lance L. Simpson in 1981 (Simpson, 1981), and was directly supported by visualization of internalized radioiodinated BoNT/A and B using electron microscopic autoradiography. Radioiodinated BoNT/A and B were exclusively found on the plasma membrane, and in intracellular compartments with morphologies consistent with those of synaptic vesicles and endosomes, at the motor nerve terminal (Figure 1-8) (Black and Dolly, 1986a, b). Internalization is a receptor-mediated process, as treating nerve terminals with excessive unlabeled BoNTs prevented subsequent binding and internalization of radioiodinated toxins. Internalization is also temperature- and energy- dependent (Black and Dolly, 1986a, b). These observations, in accord with earlier studies that nerve stimulation which accelerates endocytosis (Ceccarelli et al., 1973) increased binding of toxins to presynaptic membrane, as well as accelerated intoxication of BoNTs (Hughes and Whaler, 1962) (Simpson, 1980), suggest that BoNTs are internalized into

neurons via receptor-mediated endocytosis. This idea was confirmed by later studies, as discussed in detail in the previous section, that synaptic vesicle proteins serve as receptors for BoNTs to mediate uptake of these toxins during recycling of synaptic vesicles.

1.3.3. BoNT Translocation

1.3.3.1. Acidification of Synaptic Vesicles and endosomes

Currently, two endocytosis pathways are proposed for synaptic vesicles: a clathrin-independent fast pathway (kiss and run), in which vesicles briefly open and close again, and the intact vesicles are quickly retrieved from the plasma membrane to reload neurotransmitters; and a clathrin-mediated slow pathway, after which vesicles may fuse with endosomes during cycling (Figure 1-9) (Chapman, 2008). In synaptic vesicles and endosomes, the vacuolar (H+)-ATPases (V-ATPases) pumps protons into the lumen of these organelles to maintain an acidic pH and establish an electrochemical gradient cross membranes (Nishi and Forgac, 2002). Such electrochemical gradient powers transport of neurotransmitters into synaptic vesicles (Gasnier, 2000), and the low pH triggers dissociation of ligands in endosomes thus allowing recycling of receptors (Nishi and Forgac, 2002).

1.3.3.2. Trasnlocation of BoNT LCs Requires Low endosomal pH

Once internalized via receptor-mediated endocytosis, BoNTs need to translocate their LCs from the lumen of synaptic vesicles / endosomes into the cytosol. However, translocation

remains to be the most mysterious step during neuronal intoxication by BoNTs, and how the translocation of BoNTs occur remains largely unknown (Montal, 2010).

It is now generally accepted that low endosomal pH is required for BoNT translocation. Treating neuromuscular junctions with agents that neutralize acidic endosomal pH, such as chloroquine, ammonia chloride and methylamine, antagonized onset of muscle paralysis caused by BoNTs (Simpson, 1982, 1983; Simpson and Dasgupta, 1983). Specific inhibitors of V-ATPase, such as bafilomycin A1 or concanomycin A, prohibited action of BoNT on neuromuscular junctions (Simpson et al., 1994b), as well as blocked functional entry of BoNTs into cultured neurons (Keller et al., 2004).

Electrophysiological studies also lend strong support to the requirement of low pH. When exposed to low pH and oxidizing side of the membrane, BoNTs are capable to induce channel activities on planar bilayers (BoNT/A, B, E) (Hoch, 1985; Hoch et al., 1985; Koriazova and Montal, 2003), membrane patches excised from PC12 cells (BoNT/A and E) (Sheridan, 1998) and N2A cells (BoNT/A and E) (Fischer et al., 2008a; Fischer and Montal, 2006, 2007a, b; Fischer et al., 2009). Regardless of membrane sources and toxin serotypes, several properties are shared by BoNT channels: firstly, a pH gradient across the membrane is required, and BoNTs need to be on the low pH side of the membrane. Secondly, the channel activity is restricted to the HC (Hoch et al., 1985; Koriazova and Montal, 2003), and is further narrowed down to the TD (the H_N domain) within the HC (Fischer et al., 2012). Thirdly, the channel conductance of BoNT holotoxins always starts from a small value (10-50 pS, depending on recording conditions), then grows over time until a maximum value is reached (ranging from 60 pS to several hundred pS, depending on recording conditions); In order to reach this maximum conductance state, the

disulfide bond linking the LC and the HC must remain intact (Fischer and Montal, 2007a); the HC alone, in contrast, reaches the maximum conductance state immediately without going through the small conductance state (Brunger et al., 2007; Koriazova and Montal, 2003). Fourthly, BoNT channel is likely to be oligomeric, as the rate of channel formation on membranes was shown to depend on the square of the toxin concentration, indicating cooperative assembly may occur (Donovan and Middlebrook, 1986; Hoch, 1985). Based on these observations, it is proposed that low pH in the endosomes triggers BoNT HC to form a channel that conducts and chaperones LC translocation (Montal, 2010).

However, this hypothesis is hampered by the lack of direct support from biochemical studies. BoNTs are soluble proteins, and formation of membrane channels must involve major structural changes in the toxins; however, there is no strong evidence to support that BoNTs undergo such significant structural change at low pH. In fact, structures of BoNT/B at pH 7.4 and pH 4.4 are nearly identical (Eswaramoorthy et al., 2004), arguing against the idea that low pH alone triggers conformational changes in the toxin.

In addition, despite that crystal structures of BoNTs in their soluble state are resolved (Swaminathan, 2011), the hydrophobic channel state of the toxins remains completely elusive. BoNTs are never captured in their hydrophobic state, and the molecular architecture of the translocation-competent BoNT channels remains entirely unknown.

In summary, it is generally accepted that low endosomal pH is required for translocation of BoNTs, possibly by triggering HC to form membrane channel to conduct LC translocation, but the exact mechanisms underlying how this process occurs are still largely unknown.

Translocation remains as the most elusive step during action of BoNTs in neurons (Montal, 2010; Schiavo et al., 2000).

1.3.4. Cleavage of SNARE Proteins in the Cytosol

After translocation, LCs cleave SNARE (soluble NSF attachment protein receptor) proteins in the cytosol thereby blocking neurotransmitter release at nerve terminals (Table 1-1). In this section, I will give a brief introduction of SNARE proteins, and then discuss the specificities of the LCs towards SNARE proteins.

1.3.4.1. SNARE-Mediated Exocytosis

Neurotransmitter release is achieved by exocytosis of synaptic vesicles at presynaptic terminals, and synaptic vesicles need to overcome a high energy barrier to fuse with the plasma membrane during the process. SNARE proteins assemble into the core fusion machinery (Weber et al., 1998), and such assembly also release energy to drive fusion (Li et al., 2007). Three SNARE proteins mediate synaptic exocytosis: synaptobrevin (syb, also known as vesicle-associated membrane protein (VAMP)), SNAP-25 and syntaxin. Syb, the vesicle-SNARE, is a 18 kDa protein that anchors on synaptic vesicles with one transmembrane domain near the C-terminus. SNAP-25 (25 kDa) and syntaxin (33 kDa) are known as target-SNAREs locating on the plasma membrane. SNAP-25 attaches to the plasma membrane via palmitoylation of a central cysteine-rich cluster, and syntaxin anchors to the membrane via the C-terminal transmembrane domain. During fusion, these three proteins assemble in to a parallel four-helix bundle in which syb and syntaxin each contributes one helix, and SNAP-25 contributes two (Poirier et al., 1998; Sutton et al., 1998). The SNARE assembly proceeds from the membrane distal N-termini to the

membrane-proximal C-termini (zipper-like assembly), thereby pulling the membranes into close proximity to initiate fusion (Melia et al., 2002).

1.3.4.2. Cleavage of SNARE Proteins by BoNT LCs

BoNTs are long known to exert their toxicity by blocking neurotransmitter release (Simpson, 1981); sequencing of these toxins allowed identification of a highly conserved His-Glu-Xaa-Xaa-His zinc-binding motif of zinc-endopeptidases within LCs, leading to the hypothesis that BoNTs may achieve such blockade by cleaving proteins critical for neurotransmitter release (Schiavo et al., 2000). This hypothesis was directly supported by identification of syb, the v-SNARE, as the protease target for BoNT/B in neurons (Schiavo et al., 1992). SNARE proteins were later identified as proteolytic targets for all BoNTs: BoNT/B, D, F, G cleave cytosolic domain of syb at different sites (Schiavo et al., 1992; Schiavo et al., 1993a; Schiavo et al., 1993c; Yamasaki et al., 1994a; Yamasaki et al., 1994b); BoNT/A, E, and C cleave SNAP-25 within the region essential for SNARE-complex assembly (Binz et al., 1994; Blasi et al., 1993a; Blasi et al., 1993b; Schiavo et al., 1993a; Schiavo et al., 1993b); BoNT/C also cleaves syntaxin (Blasi et al., 1993b; Foran et al., 1996; Schiavo et al., 1995). BoNTs are highly specific enzymes for SNAREs, and no other proteins are identified as targets for these toxins so far. They seemed to recognize tertiary but not primary structures of SNAREs, and they bind to a conserved nine-residue-long motif, termed SNARE motif, found in all three SNARE proteins (Rossetto et al., 1994). The SNARE motif always locates within a α helix, and is characterized by containing three carboxylate residues alternated with hydrophilic and hydrophobic ones (Schiavo et al., 2000). Two copies of the motif are found within syb and syntaxin, four copies within SNAP-25.

Cleavage of SNAREs by most BoNTs affects neurotransmitter release but not neuron survival, but BoNT/C is an exception that it also causes neuronal death (Kurokawa, 1987; Kurokawa et al., 1987; Williamson and Neale, 1998).

1.4. Applications of BoNTs

"*Poisons can be employed as means for the destruction of life or as agents for the treatment of the sick.* "

Claude Bernard

La science expérimentale, 1895

1.4.1. BoNTs as Potential Biological Weapons

Due to their extreme potency (LD_{50} 0.1-1 ng/kg), BoNTs are considered as potential biological weapons and are also categorized as category-A bioterrorism agents by CDC (Arnon et al., 2001; Rotz et al., 2002).

Attempts to weaponize BoNTs started in 1930s, when Japanese radical nationalist Shrio Ishii initiated the Japanese biological weapon program (Unit 731), intending to develop formidable agents to assist Japan's imperialistic plans (Arnon et al., 2001; Frischknecht, 2003). During Japan's invasion in China in World War II, this program utilized Chinese captives and unsuspecting civilians as subjects of human experiments, and killed as many as 600 people a year in just one of its 26 centers. The Japanese also deliberately poisoned thousands of wells in Chinese villages. Some the epidemics caused by these agents continued for years and killed more than 30000 people in the year 1947 alone, long after the Japanese has surrendered (Frischknecht,

2003). BoNTs are among at least 25 disease-causing agents that they tested; pure cultures of *C. Botulinum* were fed to Chinese captives, with devastating effects.

In the concern that Germany may have weaponized BoNTs, the U.S. produced BoNTs during the World War II along with more than a million doses of vaccines against BoNTs (Arnon et al., 2001). Similar attempts were made in Soviet Union. Several other nations, including Iraq, Iran, North Korea, Syria, are listed by the US government as "sponsor for terrarism", and they are believed to have generated, or attempted to weaponize BoNTs (Arnon et al., 2001).

Two possible ways could be used to deliver BoNTs during terrorist attacks: contamination of food and aerosol dissemination, although constraints of concentrating and stabilizing BoNTs limit the potential of delivering the toxins by aerosol dissemination. In the U.S., a well-established surveillance system for human botulism is maintained by the CDC in the purpose to promptly detect any BoNT outbreaks (Arnon et al., 2001). A licensed trivalent antitoxin, containing antibodies against BoNT/A, B and E, is also available from the CDC via local health departments; US Army also possess a heptavalent antitoxin, containing antibodies against all seven BoNT serotypes, for treatment of patients.

1.4.2. BoNTs as Therapeutic Agents

Medical application of BoNTs was pioneered by collaborative work between Edward Schantz, a professor at University of Wisconsin, and Alan B. Scott, a surgeon in San Francisco, California, in the 1970s (Schantz and Johnson, 1992). In 1989, crystalline BoNT/A (Botox®, Allergan Inc.) was approved by the U.S. Food and Drug Administration for treatment of human muscle disorders including strabismus, hemifacial spasm and blepharospasm in patients at least

12 years of age (Schantz and Johnson, 1992). In 2000, BoNT/A and BoNT/B (Myobloc® in the U.S., Neurobloc® in the European Union) were both approved for treatment of cervical dystonia, and BoNT/A (Botox® Cosmetic) for treatment of forehead wrinkles. The number of disorders treated by BoNTs have been expanded dramatically in recent years, and the global market of BoNTs is predicted to reach $4.3 billion by 2018 (Global Industry Analyst, 2012).

In addition to their widest use in abnormal and excessive muscle contractions, BoNTs are now used for treatment of more than 50 kinds of ailments, such as orthopaedic, ophthalmological, gastrointestinal, urological, dermatological, secretory disorders and pain (Table 1-2) (Jankovic, 2004a). They are also used cosmetically to treat wrinkles. The toxins are administered by intramuscular injections directly to the sites of desired actions; the potencies and clinical effects vary among different commercial preparations. The effects usually last 3-6 months, and treatment is repeated as needed. Most patients continue to respond to repeat treatment, although some patients exhibit BoNTs resistance due to development of neutralizing antibodies (Jankovic, 2004a).

1.5. Significance

BoNTs are the most deadly toxins known to humankind (Schiavo et al., 2000), and are listed as category-A bioterrorism agents by the Centers for Disease Control (e.g. it has been estimated that one gram of toxin can kill more than one million people) (Arnon et al., 2001; Rotz et al., 2002). Paradoxically, BoNTs were the first biological toxins approved for medical use on humans due to their ability to inhibit neurotransmitter release and thereby abate musculoskeletal disorders, chronic pain, and other conditions (Jankovic, 2004a). This has grown into a worldwide multi billion-dollar industry that affects the health of a large number of human patients. As such,

elucidating the means by which BoNTs gain access to the cytosol of neurons to exert their effects is crucial for developing therapeutic agents against these deadly toxins. Moreover, an understanding of this process will uncover new ways to tailor aspects of toxin function for future therapeutic applications.

Previous studies indicate that BoNTs first enter endosomes of neurons via receptor-mediated endocytosis (Dong et al., 2008a; Dong et al., 2003; Dong et al., 2007; Dong et al., 2006; Mahrhold et al., 2006; Nishiki et al., 1994; Nishiki et al., 1996c; Peng et al., 2011; Rummel et al., 2007a; Rummel et al., 2004a). However, the molecular mechanism by which these toxins translocate from endosomes into the cytosol of neurons remains enigmatic (Montal, 2010; Schiavo et al., 2000); for example, how the toxins (which are hydrophilic soluble proteins) form translocation-competent channels remains unknown, and virtually nothing is known concerning the molecular architecture of the toxins in their translocation-competent state.

The work presented in this thesis uncovers a novel and surprising role for the toxin co-receptor molecule, GT1b, in the translocation reaction. We found that GT1b facilitates the ability of BoNT/B and E, two serotypes of BoNTs causing human botulism (Schiavo, 2006), to sense a drop in endosomal pH and thereby transform from a soluble protein into a membrane-bound channel-like structure. Our atomic force microscopy images provide the first glimpses into the structure of a BoNT in its low-pH membrane-bound form, and we found that these structures resemble other distantly related translocation machines including the mitochondrial TOM and TIM complexes, and PhoE porin in *E. coli*. We also discovered that toosendanin, a Chinese drug which blocks BoNT translocation, hindered GT1b-dependent assembly of BoNT/B oligomers, indicating that oligomerization may be required for optimal BoNT/B translocation. Our data

revealed that BoNT/E is also a coincidence detector for GT1b and low pH, but BoNT/E also exhibited some unique features regarding translocation.

BoNTs are unique in that they both pose a significant public health risk worldwide, yet also have tremendous therapeutic potential to treat a variety of human diseases. These qualities, in conjunction with our novel findings regarding a critical step in entry of BoNTs into host neurons, indicate that results represented in this thesis will be of significant interest to scientists studying bacterial toxins.

1.6. Tables

Table 1-1. Properties of BoNTs †

BoNT Serotype	Discovery (year, event)	Pathogenic Species″	Primary Species Affected	Receptors (lipid, protein)	Target Proteins
A	1919, human botulism (United States)	*C. botulinum*	human	gangliosides, SV2	SNAP-25
B	1919, human botulism (United States)	*C. botulinum*	human, cattle, horses	gangliosides, syt I/II	syb
C	1922, chicken botulism (United States), cattle botulism (Australia)	*C. botulinum*	birds, farmed chickens and pheasants, cattles, horses, mink	gangliosides, unknown	SNAP-25, syntaxin
D	1928, cattle botulism (South Africa)	*C. botulinum*	cattle, sheep	gangliosides, SV2	syb
E	1934, human botulism (United States, Ukraine)	*C. botulinum, C. butyricum*	human, salmonid fish	gangliosides, SV2A/B	SNAP-25
F	1960, human botulism (Denmark)	*C. botulinum, C. baratii*	human	gangliosides, unknown	syb
G	1970, organism isolated from soil (Argentina)	*C. botulinum, C. argentinense*	unknown	gangliosides, syt 1/II	syb

″ *C* stands for *Clostridium* in this column.

† Note: Please check related text for references.

Table 1-2. Medical Applications of BoNTs †

Dystonia	Blepharospasm and lid apraxia
	Oromandibular-facial-lingual dystonia
	Cervical dystonia (torticollis)
	Laryngeal dystonia (spasmodic dysphonia)
	Limb dystonia
	Task specific dystonia (eg, writer's or other occupational cramps)
	Other focal/segmental dystonias (primary, secondary)
Other involuntary movements	Hemifacial spasm
	Limb, head, voice, chin tremor
	Palatal myoclonus
	Motor and phonic tics (including coprolalia
	Nystagmus and oscillopsia
	Myokymia
Inappropriate muscle contractions	Spasticity (stroke, cerebral palsy, head injury, multiple sclerosis)
	Painful rigidity
	Strabismus
	Bruxism and temporo-mandibular joint syndrome
	Stuttering
	Chronic tension (muscle contraction) headaches

	Lumbosacral strain and back spasms
	Radiculopathy with secondary muscle spasm
	Myofascial pain syndromes
	Achalasia (lower oesophageal sphincter spasm)
	Spasm of the inferior constrictor of the pharynx
	Spasm of the sphincter of Oddi
	Spastic bladder, detrusor sphincter dyssynergia
	Anismus
	Vaginismus
Other applications	Protective ptosis
	Hyperlachrymation
	Drooling (sialorrhoea)
	Hyperhidrosis
	Gustatory sweating
	Anal fissure
	Constipation
	Obesity (distal stomach)
	Cosmetic (wrinkles, brow furrows, frown lines, ‘‘crow’s feet’’, platysma lines, facial asymmetry)
	Tennis elbow and other sports injuries

† Note: this table is adapted from (Jankovic, 2004a)

1.7. Figures and Legends

Figure 1-1.

Neue

Beobachtungen

über

die in Würtemberg so häufig vorfallenden tödtlichen Vergiftungen durch den Genuß geräucherter Würste.

Von

Dr. Justinus Kerner,

Oberamtsarzt zu Weinsberg.

Tübingen,

bei C. F. Osiander.

1820.

Figure 1-1. Justinus Kerner and His First Monograph on Sausage Poisoning.

(A) A portrait of Justinus Kerner by Alexander Bruckmann, 1844.

(B) Justnus Kerner's first monograph on sausage poisoning (botulism).

Note: This figure is adapted from (Erbguth, 2004).

Figure 1-2

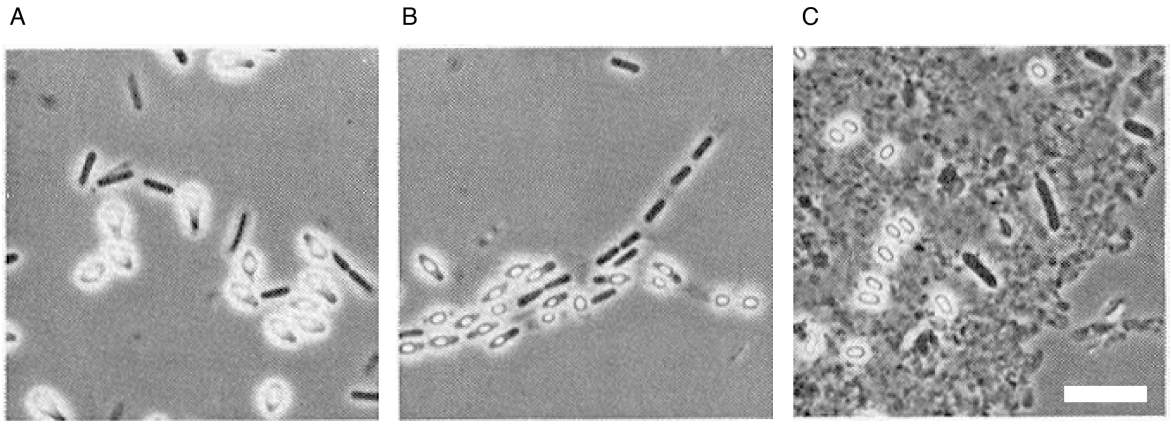

Figure 1-2. Morphology of *Clostrium botulinum* Viewed by Phase-Contrast Microscopy.

(A) *Clostrium botulinum* type A.

(B) *Clostrium botulinum* type B.

(C) *Clostrium botulinum* type E.

Scale bar: 10 μm.

Note: This figure is adapted from (Hatheway, 1989).

Figure 1-3

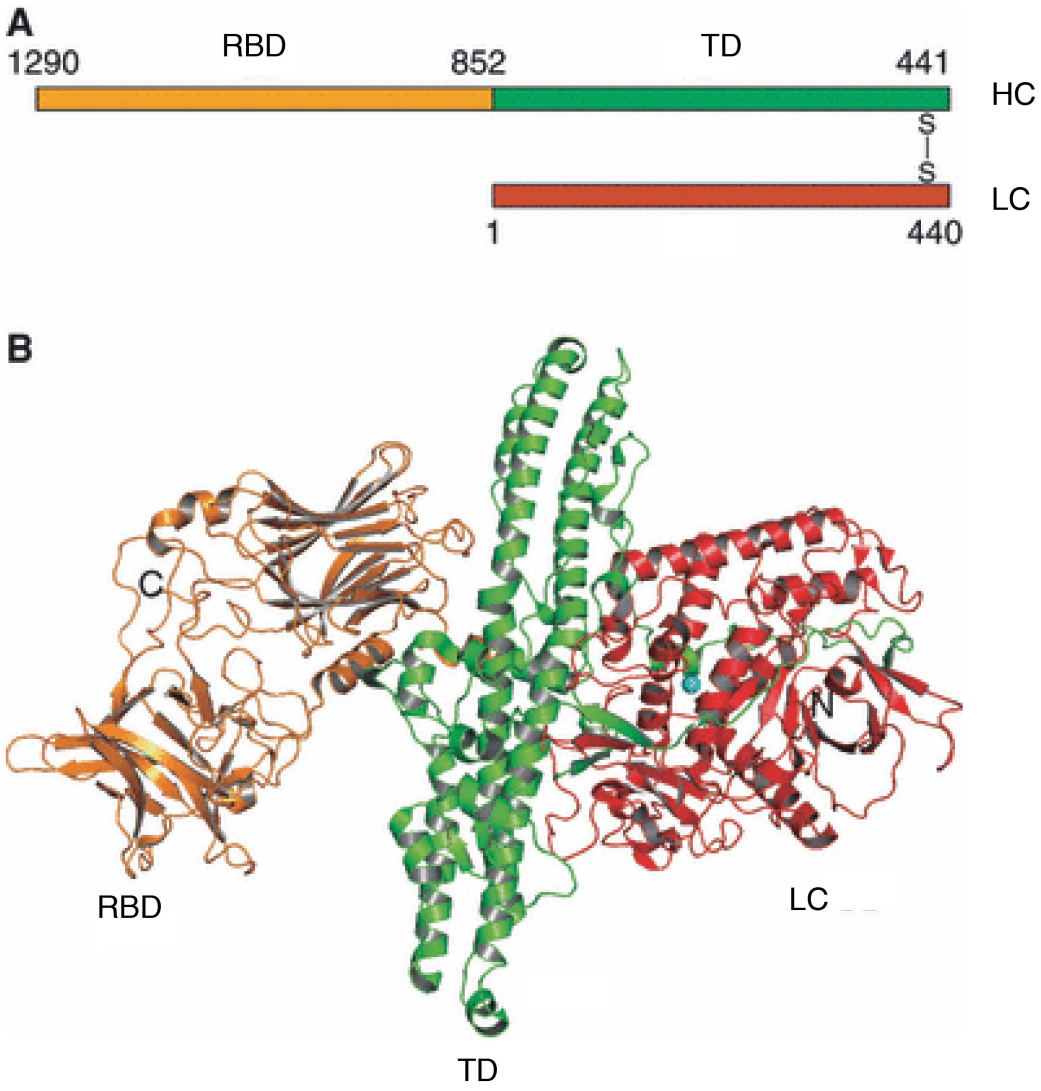

Figure 1-3. Structure of BoNT/B

(A) Illustration of domain organization in BoNT/B. BoNT/B is composed of a N-terminal LC (red) and a C-terminal HC. HC is divided into a RBD (orange, also known as the H_C domain) and a TD (green, also known as the H_N domain), and TD is linked to LC via a disulfide bond. (B) Ribbon representation of the crystal structure of BoNT/B. RBD and LC are flanked on either side of TD in a linear fashion, and RBD and LC share no interface. LC is a zinc-dependent protease (zinc shown as a cyan ball), and is wrapped by TD via a belt region. N-terminal and C-terminal are marked as N and C, respectively.

The crystal structure of BoNT/A shares similar folds as BoNT/B.

Note: this figure is adapted from (Swaminathan, 2011).

Figure 1-4

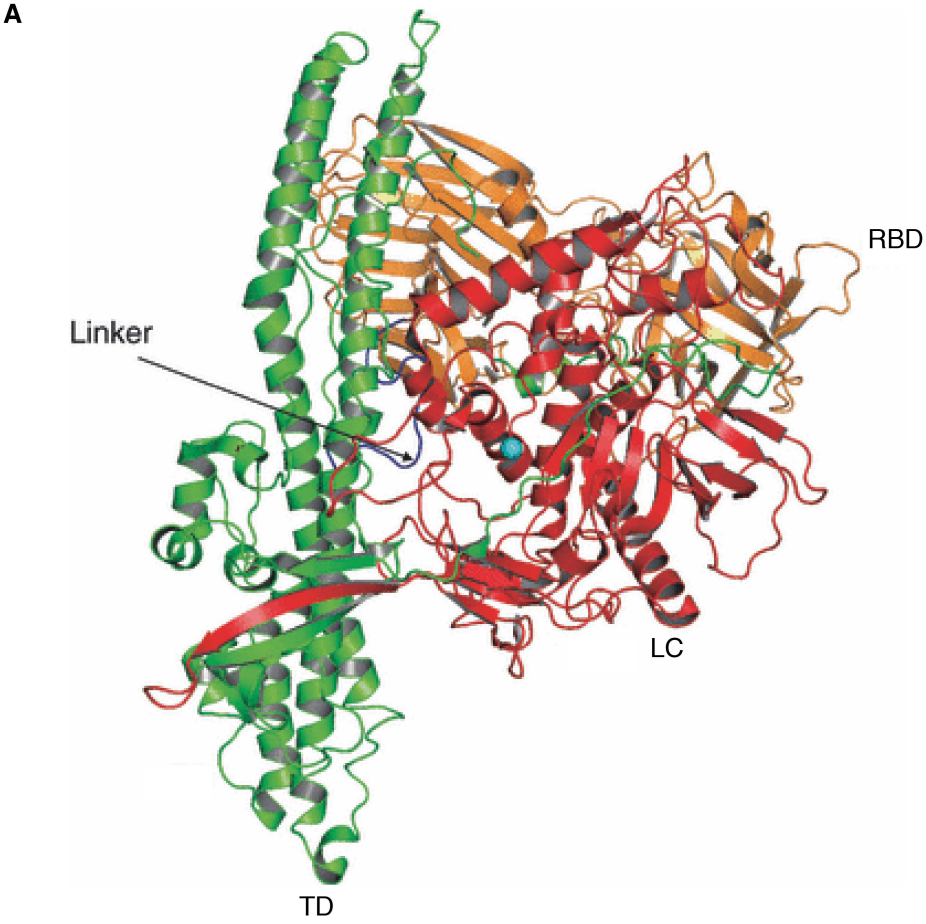

Figure 1-4. Domain Organization in BoNT/E

(A) Ribbon representation of the crystal structure of BoNT/E. RBD (orange) and LC (red) locate on the same side of TD (green), and all three domain share interfaces with each other. The linker region connecting RBD and TD is a loop (residues 830-845) that allows the RBD to swing around to the side of the LC. LC is a zinc-dependent protease (zinc shown as a cyan ball).
(B) Representative cryo-electron microscopy images of BoNT/E at neutral pH. Scale bar, 20 nm.
Note: this figure is adapted from (Swaminathan, 2011) and (Fischer et al., 2008a).

Figure 1-5

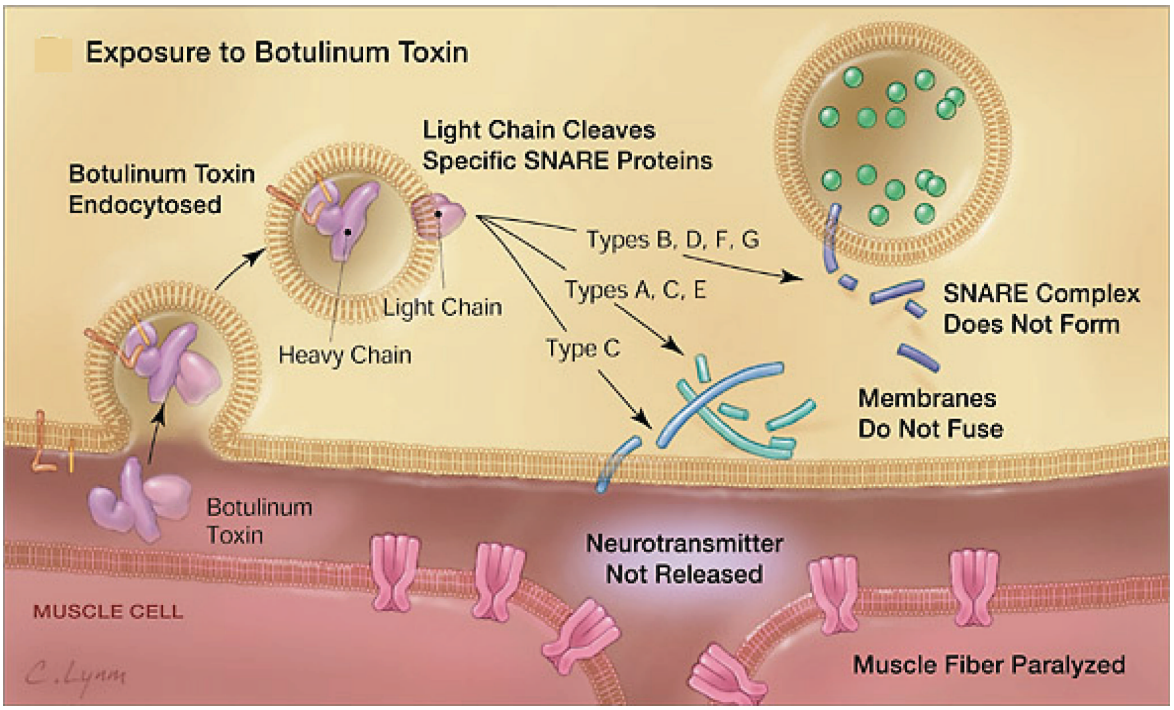
Exposure to Botulinum Toxin
Botulinum Toxin Endocytosed
Light Chain Cleaves Specific SNARE Proteins
Light Chain
Heavy Chain
Types B, D, F, G
Types A, C, E
Type C
SNARE Complex Does Not Form
Membranes Do Not Fuse
Botulinum Toxin
Neurotransmitter Not Released
MUSCLE CELL
Muscle Fiber Paralyzed
C. Lynn

Figure 1-5. Major Steps in BoNT Action at Nerve Terminals.

BoNTs bind to receptors located on presynaptic terminals, and are internalized via receptor-mediated endocytosis. BoNT LCs are translocated from vesicle / endosomal lumen into the cytosol. LCs then act as proteases to cleave SNARE proteins, thereby inhibiting neurotransmitter release. Such blockade results in flaccid paralysis at neuromuscular junctions.

Note: This figure is adapted from (Arnon et al., 2001).

Figure 1-6

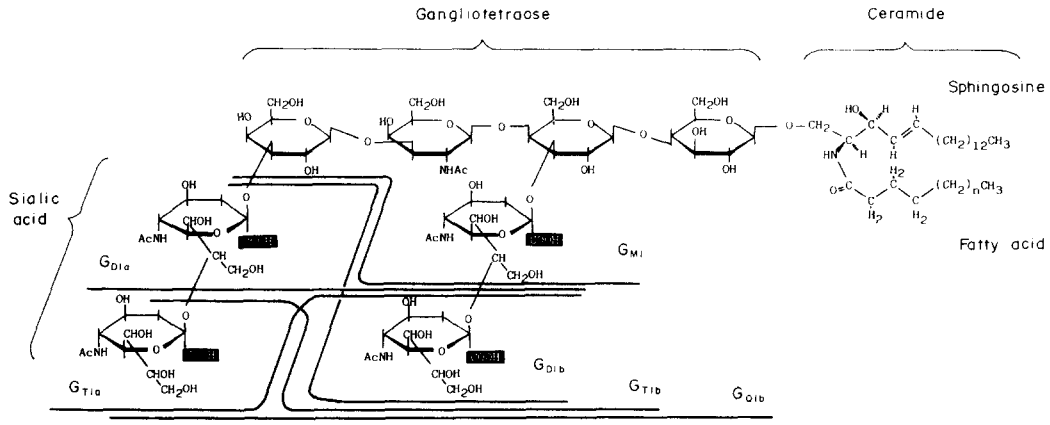
Gangliotetraose
Ceramide
Sphingosine
Fatty acid
Sialic acid
G_{D1a}
G_{M1}
G_{D1b}
G_{T1a}
G_{T1b}
G_{Q1b}

Figure 1-6. Structure of the Most Abundant Gangliosides in the Adult Mammalian Nervous System.

Gangliosides are named according to (Svennerholm, 1980). Briefly, G stands for gangliosides; M, D, T or Q indicates the ganglioside including mono-, di-, tri- or quad-sialic acid. The number 1, 2, or 3 refers to the carbohydrate sequence attached to the ceremide. In some cases, a lowercase letter is included at the end of the designation to indicate the position of sialic acid(s) attached. Note: This figure is adapted from (Ando, 1983).

Figure 1-7

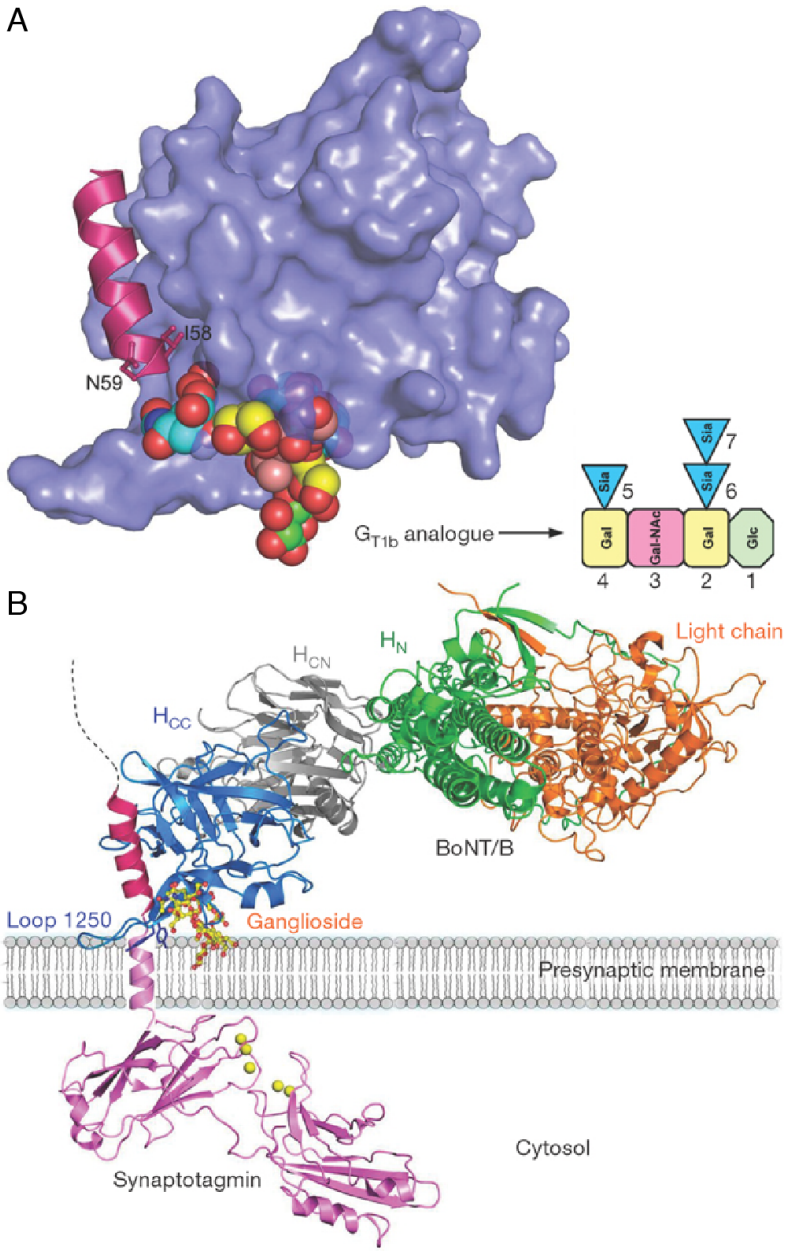
A
I58
N59
G_{T1b} analogue
Sia
Sia
Gal
Gal-NAc
Gal
Glc
7
5
6
4
3
2
1
B
H_{CN}
H_N
Light chain
H_{CC}
BoNT/B
Loop 1250
Ganglioside
Presynaptic membrane
Cytosol
Synaptotagmin

Figure 1-7. Model of BoNT/B Binding to Syt II and GT1b.

(A) Surface representation of H_{CC} domain of BoNT/B showing that BoNT/B (blue) binds syt II (magenta) within a hydrophobic groove in the H_{CC} domain of the toxin, and the binding site is adjacent to the GT1b-binding site (binding as modeled).

(B) Model of double receptor binding of BoNT/B on neurons. Binding to syt II (magenta, structure modeled based on (Cheng et al., 2004) and (Sutton et al., 1999)) and GT1b (yellow) anchors H_{CC} domain of BoNT/B to the plasma membrane, positioning H_N domain (TD) tangential to the membrane.

Note: This figure is modified from (Chai et al., 2006).

Figure 1-8

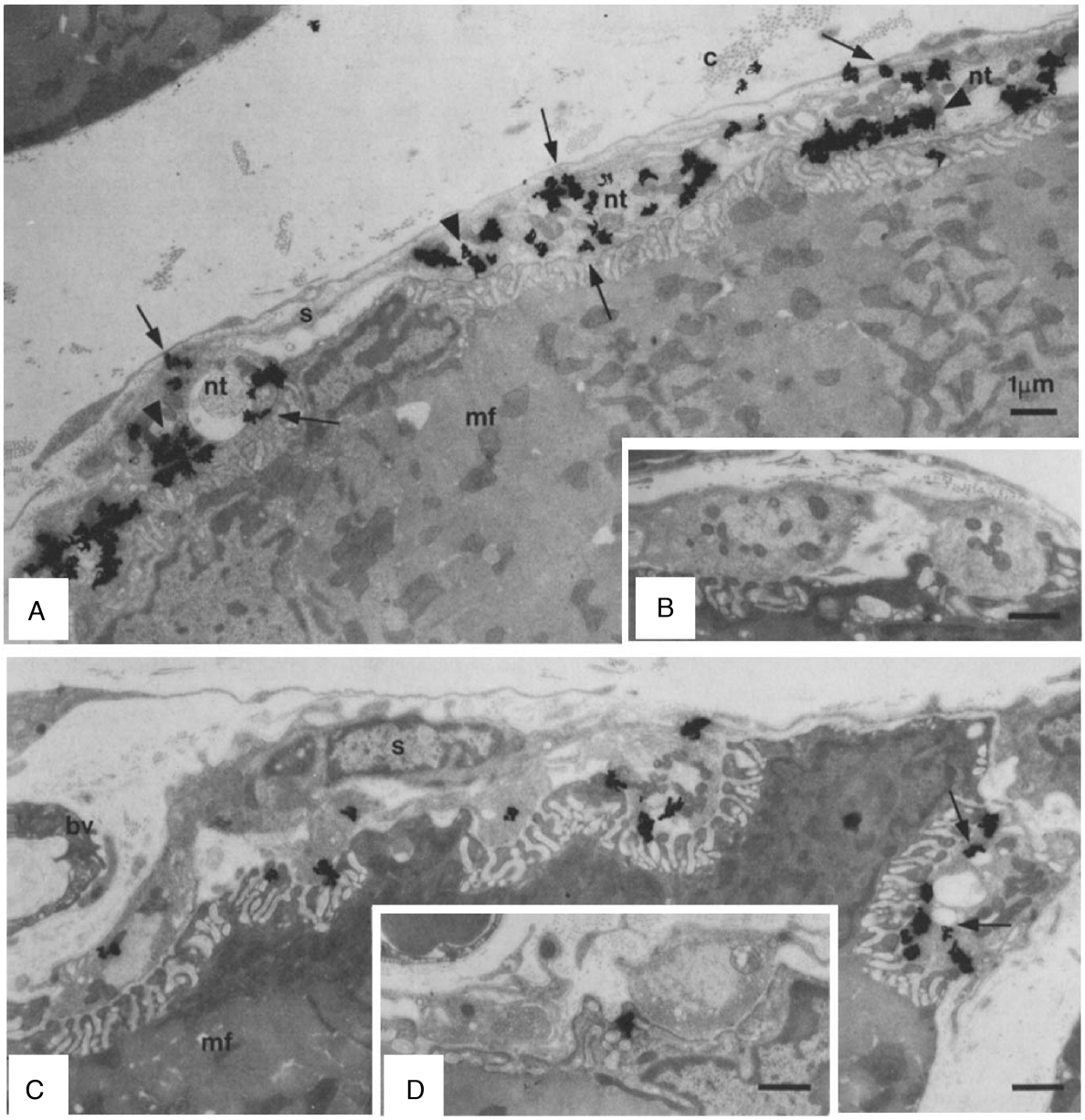

Figure 1-8. Interactions of Radioiodiniated BoNT/A and B with the Mouse Motor Nerve Terminal Monitored by Electron Microscopic Autoradiography.

(A and B) Radioiodinated BoNT/A (15 nM) was added to motor nerve terminals (nt) from a mouse diaphragm, and sections were exposed for 3 weeks. Silver grains are seen on the plasma membrane (arrows) and associated with vacuolar structures in the cytosol (arrowheads) (A). Control preparation treated as in (A) in the presence of 100-fold excess of unlabeled BoNT/A was devoid of silver grains (B), indicating internalization of the toxin is a receptor-dependent process.

(C and D) Radioiodinated BoNT/B (10 nM) was added to five synaptic boutons from a nerve-muscle preparation in the absence (C) or in the presence of 100-fold excessive unlabeled BoNT/B (D). Sections were exposed for 11 days. In the cytosol, radioiodinated BoNT/B were often associated with vacuolar structures (arrows).

Mf stands for muscle fibers, and S for schwann cells.

Note: This figure is adapted from (Black and Dolly, 1986a).

Figure 1-9

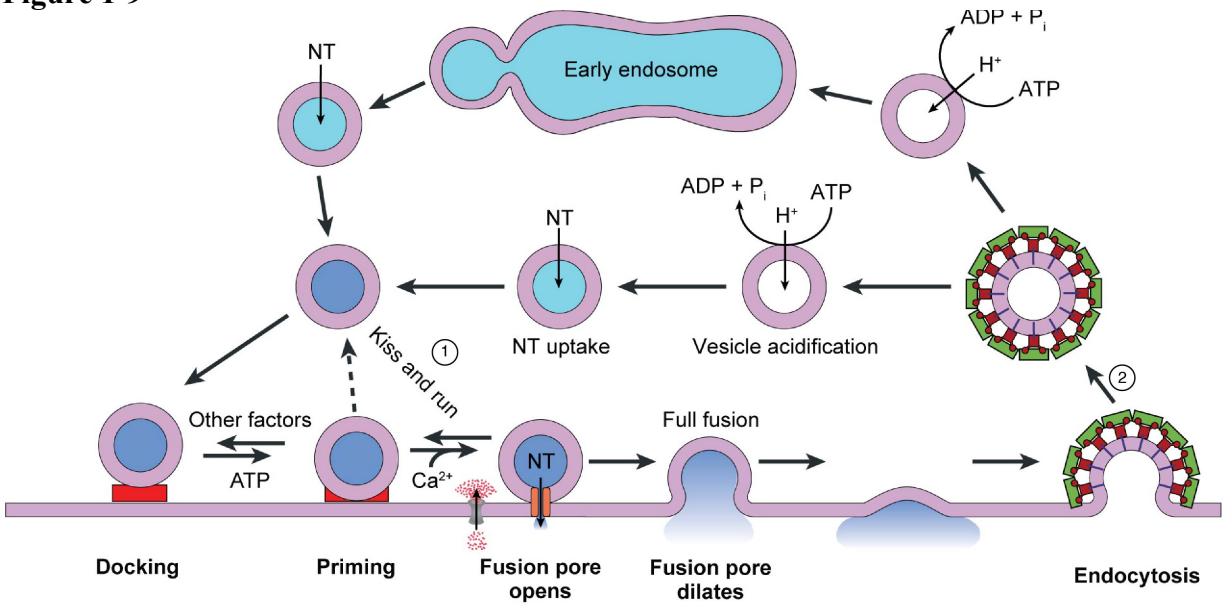
NT
Early endosome
ADP + P$_i$
H$^+$
ATP
ADP + P$_i$
ATP
H$^+$
NT
NT uptake
Vesicle acidification
Kiss and run
1
2
Other factors
ATP
Ca^{2+}
NT
Full fusion
Docking
Priming
Fusion pore opens
Fusion pore dilates
Endocytosis

Figure 1-9. The Synaptic Vesicle Cycle

Upon release of neurotransmitters (NT) during Ca^{2+}-triggered exocytosis, synaptic vesicles: either close fusion pore without further dilution, and undergo clathrin-independent endocytosis (kiss and run, ①); or finish full fusion before retrieved via clathrin-mediated endocytosis (②). Fusion with endosomes may occur as one part of the cycle process after clathrin-mediated endocytosis. V-ATPase pumps proton into synaptic vesicle / endosomal lumen to maintain an acidic pH in these organelles, and also establishes an electrochemical gradient to drive active transport of NT into synaptic vesicles. Vesicles loaded with NT then target to active zones, where they become bound or docked to the plasma membrane. ATPase and other factors further convert vesicles into priming steps, after which vesicles are rendered competent for fusion. Arrival of an action potential triggers opening of voltage-gated Ca^{2+} channels; influxed Ca^{2+} binds to Ca^{2+} sensor on vesicles, resulting in fusion pore opening and release of NT.

Chapter 2

Receptor Binding Enables Botulinum Neurotoxin B to Sense Low pH for Translocation Channel Assembly

2.1. SUMMARY

Botulinum neurotoxins (BoNTs, serotypes A-G), elaborated by *Clostridium botulinum*, can induce lethal paralysis and are classified as category-A bioterrorism agents. However, how BoNTs translocate from endosomes into the cytosol of neurons to gain access to their intracellular targets remains enigmatic. We discovered that binding to the ganglioside GT1b, a toxin co-receptor, enables BoNT/B to sense low pH, undergo a significant change in secondary structure, and transform into a hydrophobic oligomeric membrane protein. Imaging of the toxin on lipid bilayers using atomic force microscopy revealed donut-shaped channel-like structures that resemble other protein translocation assemblies. Toosendanin, a drug with therapeutic effects against botulism, inhibited GT1b-dependent BoNT/B oligomerization, and in parallel truncated BoNT/B single-channel conductance, suggesting that oligomerization plays a role in the translocation reaction. Thus, BoNT/B functions as a coincidence detector for receptor and low pH to ensure spatial and temporal accuracy for toxin conversion into a translocation channel.

2.2. HIGHLIGHTS

- Gangliosides are required for cell surface entry of BoNT/B at low pH
- The ganglioside GT1b enables BoNT/B to sense low pH and change conformation
- BoNT/B assembles into channel-like structures on GT1b-containing bilayers at low pH
- TSN, a botulism therapeutic, inhibits GT1b-dependent BoNT/B oligomerization at low pH

See also visual abstract (Figure 2-A1).

2.3. INTRODUCTION

Botulinum neurotoxins (BoNTs) are the most deadly toxins known, and cause the disease botulism (Schiavo et al., 2000). This family of toxins - of which there are seven serotypes (BoNT/A-G) - are potential biological weapons, and are categorized as category-A bioterrorism agents by the Centers for Disease Control (CDC) (Arnon et al., 2001; Rotz et al., 2002). Despite their extreme potency and lethality, BoNTs possess great therapeutic potential. For instance, two serotypes, BoNT/A and B, are widely used in a broad range clinical applications (Montecucco and Molgo, 2005), including the treatment of muscle dysfunction and neurological pain.

Each BoNT consists of an N-terminal light chain (LC, 50 kDa) and a C-terminal heavy chain (HC, 100 kDa) (Schiavo et al., 2000). The LC acts as a zinc-dependent protease that cleaves SNARE (soluble NSF attachment protein receptor) proteins in the cytosol of pre-synaptic nerve terminals, thereby blocking neurotransmitter release. Loss of neurotransmission can result in paralysis and death. The HC is connected to the LC via a disulfide bond; the HC also wraps around the LC via a single stranded “belt” loop (Montal, 2010). The HC is composed of an N-terminal translocation domain and a C-terminal receptor binding domain. The receptor binding domain interacts with specific receptors on the surface of presynaptic nerve terminals, and the toxin is endocytosed, usually via recycling synaptic vesicles (Chai et al., 2006; Dong et al., 2008b; Dong et al., 2003; Dong et al., 2006; Rummel et al., 2007b; Schiavo et al., 2000). In order to access SNARE proteins, the LC must be translocated from the lumen of endosomes/synaptic vesicles into the cytosol. This process, translocation, is the least understood step in the action of BoNT on target cells (Montal, 2010; Schiavo et al., 2000).

Low pH in the lumen of endosomes/synaptic vesicles serves as the trigger for BoNT LC translocation. Presumably, low pH converts the translocation domain within the BoNT HC into a membrane channel that mediates LC translocation (Schiavo et al., 2000). Evidence for this model includes the well-established single-channel activity of BoNTs in planar bilayers and in membranes excised from PC12 or N2A cells (Hoch et al., 1985; Sheridan, 1998); Montal, 2010). Addition of BoNTs to the low-pH, oxidizing side of a membrane results in the formation of single-channel conductances that are initially small but grow over time, reaching a plateau. It was suggested that the early low conductance state represents a HC channel that is partially occluded by the nascent, translocating LC, and that the large conductance state at the plateau represents an un-occluded channel after the LC has left (Montal, 2010). Despite these advances, the mechanisms underlying LC translocation are still poorly understood. For instance, the mechanism by which BoNT transforms from a soluble to an integral membrane protein is unclear, and the molecular architecture of the toxin translocation channel is completely unknown.

The goal of the current study was to use a combination of cell biological, biochemical, structural and electrophysiological approaches to probe the assembly of the BoNT translocation channel. We focused on BoNT/B, a clinically-used serotype (Montecucco and Molgo, 2005), for which the crystal structure has been determined (Swaminathan and Eswaramoorthy, 2000), and for which interactions with co-receptors, the ganglioside GT1b and synaptotagmin (syt) I/II, have been well characterized (Chai et al., 2006; Dong et al., 2003; Jin et al., 2006; Nishiki et al., 1996b). The data reported here indicate that BoNT/B must interact with its neuronal co-receptor, GT1b, in order to sense the low pH in endosomes/recycling synaptic vesicles and transform into a membrane associated oligomeric channel-like structure. The ability of BoNT/B to act as a

coincidence detector for receptor and low pH ensures that the toxin converts into a translocation machine at the right time and place.

2.4. RESULTS

2.4.1. Low-pH Pretreatment Does Not Inactivate BoNT/B

Low pH in the lumen of endosomes/synaptic vesicles triggers the transformation of BoNTs from soluble proteins into translocation-competent membrane channels (Montal, 2010; Schiavo et al., 2000). For some bacterial toxins that also utilize low endosomal pH to translocate, such as anthrax toxin, exposure to low extracellular pH prior to binding to cellular receptors results in conformational changes - that would normally underlie translocation - in solution, leading to aggregation such that the toxin becomes inactive (i.e. enters an "off-pathway", Figure 2-1A) (Gupta et al., 2001; Sun et al., 2007; Young and Collier, 2007). To test whether BoNT/B responds to low extracellular pH and enters an off-pathway, we preincubated BoNT/B for 2 h in high-K^+ buffer at either pH 7.4 or pH 4.4, before treating rat hippocampal neurons with the toxin in the same buffers. High-K^+ buffer stimulates synaptic vesicle recycling, thus facilitating uptake of BoNT/B into neurons (Dong et al., 2003; Schiavo et al., 2000). BoNT/B that was not taken up by neurons was washed away, and translocation was monitored by assaying cleavage of synaptobrevin II (syb), the intracellular target of BoNT/B (Schiavo et al., 2000). We found that pH 4.4-pretreatment had no effect (Figures 2-1B and 2-1C), and thus does not drive BoNT/B into an off-pathway. Either the isolated toxin is unable to sense the drop in pH, or pH-induced conformational changes - unlike the case of anthrax toxin - failed to inactivate the toxin.

2.4.2. Gangliosides are Required for Efficient Cell Surface Entry of BoNT/B

The ideal sites to study BoNT/B translocation are endosomes/synaptic vesicles, where translocation normally occurs. However, it is difficult to measure and manipulate pH inside these organelles. Therefore, in order to study the effect of pH on the behavior of BoNT/B, we devised a method to reconstitute BoNT/B translocation across the plasma membrane of cultured rat hippocampal neurons. To this end, normal translocation of BoNT/B from the vesicle lumen into the cytosol was blocked by addition of bafilomycin (Figure 2-2A), a specific inhibitor of vacuolar H^+-ATPase (Keller et al., 2004; Simpson et al., 1994a). Neurons were then treated with BoNT/B in extracellular buffers of varying pH, and LC translocation into the cytoplasm was determined, again, by monitoring cleavage of syb (Figure 2-2B). After exposure of neurons to BoNT/B at an extracellular pH of 7.4 for 8 min, the toxin efficiently cleaved syb in the absence, but not the presence, of bafilomycin during a subsequent 24-h incubation. As extracellular pH was lowered, cleavage in the presence of bafilomycin increased progressively; at pH 4.4, which was the lowest pH value possible without compromising cell viability, cleavage of syb reached ~50% (Figures 2-2B and 2-2C). Hence, BoNT/B LC can be translocated across the plasma membrane at low pH.

We note that the time-averaged pH value reported for synaptic vesicles is 5.6 (Miesenbock et al., 1998). However, given the minute volume of these organelles (diameter of ~42 nm) (Heuser and Reese, 1981), the instantaneous intra-luminal pH will be significantly altered by the flux of even a single proton, and pH values of 4.4 - or lower - seem likely to occur, at least for brief periods.

BoNT/B normally enters neurons via receptor-dependent endocytosis (Schiavo et al., 2000), but whether interactions with receptor molecules play a role in the translocation reaction is a question that has not been addressed. To begin to study this problem, we monitored translocation in neurons lacking gangliosides, the low-affinity co-receptors for BoNT/B (Schiavo et al., 2000). For this purpose, we used both ganglioside knockout (KO) mouse hippocampal neurons (Figure 2-2D, quantified in Figure 2-2E) and rat hippocampal neurons treated with fumonisin B1 (FB1) (Figure 2-2F, quantified in Figure 2-2G). FB1 effectively inhibits synthesis of gangliosides in cultured rat neurons without impairing axonal growth; the ganglioside GT1b is decreased to ~26% of control level in the presence of 25 μM FB1 (de Chaves et al., 1997). In both ganglioside KO and FB1-treated neurons, BoNT/B - in low pH extracellular buffer - failed to translocate across the plasma membrane to cleave syb (Figures 2-2D to 2-2G). Hence, gangliosides are required for efficient surface translocation of BoNT/B. We note that in a previous study, it was shown that loading ganglioside KO neurons with exogenous gangliosides rescued the entry of BoNT/B (Dong et al., 2007).

2.4.3. Ganglioside GT1b Enables BoNT/B to Change Conformation and Transform into a Hydrophobic Membrane Protein at Low pH

One fundamental question regarding BoNT/B translocation concerns the mechanism by which BoNT/B transforms from a soluble protein into a membrane channel in response to low pH. The cell surface translocation/entry experiments described above indicate that gangliosides facilitate efficient translocation of BoNT/B across membranes. We therefore tested whether

binding to the ganglioside GT1b, the lipid receptor of BoNT/B, triggers conformational changes in the toxin that allow it form a membrane channel at low pH.

Channel formation by pore-forming toxins, such as anthrax toxin, is associated with secondary structural rearrangements at low pH, which can be probed by circular dichroism (CD) spectroscopy (Kintzer et al.; Vernier et al., 2009). At pH 7.4, the CD spectra of BoNT/B with or without GT1b largely overlapped from 197 nm to 260 nm (Figure 2-3A, left panel), and the helical content estimated from molar ellipticity at 222 nm (Chen et al., 1972) was ~20% both for BoNT/B alone, and for BoNT/B plus GT1b. BoNT/B alone yielded similar spectra at pH 7.4 and pH 4.4, with a helical content of ~23% at pH 4.4 (Figure 2-3A, right panel). These findings are in agreement with crystallography studies indicating that exposure to low pH alone does not cause a structural change in BoNT/B (Eswaramoorthy et al., 2004), and are also consistent with the lack of effect of low pH in our off-pathway assays. However, addition of GT1b at pH 4.4 resulted in a significant shift in the spectrum, with a large reduction in signal at ~208 nm, and a reduction in helical content to only ~12%. These results indicate that BoNT/B undergoes a major structural rearrangement in the presence of GT1b at pH 4.4, a pH value that enables efficient translocation.

To further test whether the GT1b-dependent structural rearrangement of BoNT/B at low pH enables it to transform into a hydrophobic protein, we examined the interaction of BoNT/B with membranes. We found that the toxin did not cosediment with GT1b-free liposomes at either pH 7.4 or pH 4.4 (Figure 2-3B), consistent with the notion that low pH alone is insufficient to convert BoNT/B into a hydrophobic species. When the liposomes contained GT1b, only low

levels of binding were observed at pH 7.4; however, at pH 4.4 efficient cosedimentation of BoNT/B with GT1b-containing liposomes occurred.

To characterize the interactions that mediate cosedimentation at pH 4.4, we collected the BoNT/B-bound liposomes and performed extraction experiments with either 1M NaCl at pH 4.4 or Na_2CO_3 at pH 11.0 (Figure 2-3C). Typically, only peripheral proteins, and not transmembrane or lipid-anchored proteins, are extracted by these reagents (Bai et al., 2000; Fujiki et al., 1982). Interestingly, 1M NaCl failed to extract BoNT/B from liposomes, but Na_2CO_3 caused complete extraction. These results suggest that GT1b enables BoNT/B to sense low pH and tightly associate with membranes, and further, that the interaction can be reversed by exposure to higher pH. Consistent with this idea, incubation of the liposomes in a buffer (phosphate-buffered saline; PBS) at pH 7.4 caused partial extraction of the BoNT/B (Figure 2-3C). As expected, BoNT/B was completely extracted by treatment of the liposomes with Triton X-100. We further tested whether the observed partial reversibility in the liposome co-sedimentation assay was related to conformational changes in BoNT/B via CD, and found that ~76% of the measured-conformational change triggered by GT1b and pH 4.4 was reversed at pH 7.4 (Figure 2-3D).

To further test whether BoNT/B is converted into a hydrophobic species in the presence of GT1b at low pH, we performed Triton X-114 partitioning assays. Triton X-114 is a detergent that is homogeneous at 0°C in solution, but partitions into aqueous and detergent phases above 20°C. This behavior provides a simple way to distinguish integral or lipid-anchored proteins (which partition into the detergent phase), from soluble or peripheral proteins (which partition into the aqueous phase) (Bordier, 1981). We found that in the presence of GT1b, BoNT/B partitioned into the aqueous phase at pH 7.4, but was almost equally divided between the two

phases at pH 5.4, and was found exclusively in the detergent phase at pH 4.4 (Figure 2-3E). In contrast, the toxin remained in the aqueous phase at all pH values when GT1b was absent. As controls, a known membrane protein, syb, remained in the detergent phase, whereas the cytoplasmic domain of syb (cd-syb) remained predominantly in the aqueous phase. The partitioning of BoNT/B into the detergent phase at low pH in the presence of GT1b was not due to more avid binding of the toxin to GT1b at low pH, as the receptor binding domain of BoNT/B (HCR/B) (tested at the same concentration as BoNT/B in Triton X-114 partitioning assay) exhibited similar GT1b binding activity at pH 7.4 and 4.4 (Figure 2-S1) in a solid-phase binding assay (Schmitt et al., 2010). In addition, the interaction of another BoNT serotype with gangliosides is known to be less, rather than more, avid at low pH than at neutral pH (Kamata et al., 1988). We also note that BoNT/B was stable under all conditions tested; the partitioning behavior of BoNT/B at low pH in the presence of GT1b was not due to degradation or aggregation of the toxin. Together, the experiments reported in this section reveal that BoNT/B is converted into hydrophobic species in the presence of GT1b at low pH.

2.4.4. BoNT/B Assembles into Oligomeric Channel-like Structures in GT1b-containing Bilayers at Low pH

To visualize the structure adopted by BoNT/B on GT1b-containing bilayers at low pH, we turned to atomic force microscopy (AFM). This technique offers single-molecule resolution under near-physiological conditions (i.e. under fluid) (Saslowsky et al., 2002; Suresh and Edwardson). We first imaged BoNT/B holotoxin adsorbed onto mica in air. The toxin appeared as homogenous particles, which consisted of adjoined large and small components, likely

representing the HC and the LC (Figures 2-4A and 2-4C). We measured the dimensions of a number of particles and calculated their molecular volumes, using Equation 1, as detailed in Experimental Procedures. The frequency distribution of molecular volumes had a peak around 250 nm^3 (Figure 2-4B), consistent with the predicted molecular volume for a 150-kDa protein (around 285 nm^3, according to Equation 2).

We next examined the interaction of BoNT/B with lipid bilayers via AFM imaging under fluid. Both at pH 7.0 and pH 5.0, the mean molecular volume of the particles was around 300 nm^3, very close to the value for holotoxin. Although the measured molecular volume suggests that the toxin bound to the bilayer predominantly as monomers, it is unwise to rely too heavily on volume measurements to deduce stoichiometry. For instance, it is well known that the geometry of the scanning AFM probe introduces a tendency to overestimate particle radii, a convolution that becomes especially significant when imaging under fluid, because fluid-imaging tips are blunter than air-imaging tips. In addition, volume measurements of particles bound to lipid bilayers do not take into account penetration of the bilayer by the protein, which is likely to be an issue here (see below). At pH 5.0, BoNT/B holotoxin appeared as a dome-shaped structure on GT1b-containing bilayers (Figure 2-4D, left panel). When the LC was released by reduction of the toxin with DTT, the appearance of some of the BoNT/B particles changed from dome-shaped to donut-shaped, channel-like structures (Figure 2-4D, right panel). The presence of GT1b in the bilayers clearly promoted the formation of these donut-like structures. Specifically, 33% (218 of 650) of bound particles were donuts in the presence of GT1b, compared with 19% (42 of 225) without GT1b.

Sections through single donuts were used to construct frequency distributions for various dimensions (Figures 2-4E and 2-4F). The peak height above the bilayer was 0.3 nm (Figure 2-4G); the peak depth of the hole was 0.2 nm (Figure 2-4H); the peak radius of the donut was 17 nm (Figure 2-4I); and the peak radius of the hole (at the highest point of the donut) was 7 nm (Figure 2-4J). We note that the radius of the donut is very similar to the radius of the holotoxin, indicating that donut formation does not require oligomerization of the toxin. The rather small protrusion of the toxin molecule from the bilayer surface (0.3 nm) suggests that the toxin is embedded in the bilayer. Consistent with this finding, increasing the pH from pH 5.0 to pH 7.0 resulted in the dissociation of some of the toxin particles, leaving indentations where toxin molecules were previously bound (Figure 2-S2). This result provides direct support for the idea that BoNT/B inserts, at least partially, into membranes at low pH.

Some of the donuts self-associated to form dimers and trimers (Figure 2-5A). Of the donuts seen in the presence of GT1b, 60±1% were monomers, 17±1% were dimers, and 8±1% were trimers, with the remainder being higher-order assemblies of donuts (data from three independent experiments; total donut number = 218). In addition to increasing the percentage of particles that appeared as donuts, GT1b also supported oligo-donut formation. Specifically, in the absence of GT1b, the percentage of donut structures that were oligomers fell from 40% to 22%. Significantly, the septa between associating donuts had only a single and not a double width, suggesting that self-association resulted in a reorganization of toxin to generate unique structures. Sections through typical double and triple donuts are shown in Figure 2-5B. We found that the double-donut structures have a long axis of 65 nm and a short axis of 52 nm (n = 35); the long axis was less than twice the length of the short axis, consistent with the presence of a single

septum between the two adjoined donuts. In addition, the mean radius of the holes in the double donuts was 7 nm, identical to the value for single donuts, indicating that self-association did not generate larger holes.

We were unable to generate stable lipid bilayers for AFM imaging at pH 4.4, a pH value used in the other experiments to drive more efficient translocation (Figures 2-2B and 2-2C). As an alternative method for investigating the effect of GT1b on BoNT/B oligomerization, we incubated BoNT/B with the ganglioside (below its critical micelle concentration) at various pH values, and performed blue native-PAGE (BN-PAGE; Figures 2-5C and 2-5D). We found that in the absence of GT1b, BoNT/B behaved as a monomer (molecular mass ~150 kDa) between pH 7.4 and pH 4.4 (Figure 2-5C). In the presence of GT1b, BoNT/B remained predominantly monomeric at pH 7.4; however, when the pH was reduced to 5.0, BoNT/B behaved as a mixture of monomers and oligomers. These results are consistent with our observation, by AFM, that on GT1b-containing bilayers at pH 5.0, BoNT/B HC exists as single and multiple donut-shaped structures (Figures 2-4D and 2-5A). Interestingly, at pH 4.4, BoNT/B trimers became dominant (Figure 2-5C). In contrast to GT1b, a control ganglioside - GM1 - at the same concentration, did not induce oligomerization of BoNT/B at low pH (Figure 2-5D). These results indicate that BoNT/B holotoxin exists mainly as an oligomer, most likely a trimer, in the presence of GT1b at low pH.

2.4.5. Toosendanin Hinders BoNT/B Oligomerization and Restricts LC Translocation

The drug toosendanin (TSN) has been shown to inhibit translocation of the BoNT/A LC (Fischer et al., 2009; Li and Shi, 2006). Given the data described above suggesting that BoNT/B might assemble into multimers - and trimers in particular - at low pH, we tested whether TSN affects trimerization of BoNT/B. We first confirmed that TSN blocked BoNT/B intoxication of neurons by incubating the drug with holotoxin (20 nM) for 2 h prior to addition of the mixture to rat hippocampal neurons. We found that BoNT/B alone completely cleaved syb, and that cleavage was reduced ~50% in the presence of ≥2 μM TSN (Figure 2-6A). We then used BN-PAGE to determine whether trimerization of BoNT/B holotoxin was also disrupted by TSN. TSN prevented GT1b-promoted oligomerization of BoNT/B at pH 5.0 but not at pH 4.4 (Figures 2-6B and 2-6C); TSN also lowered the pH requirements for BoNT/B oligomerization in solution from ~pH 5.0 to ~pH 4.6 (Figure 2-S3A). Inhibition of oligomerization (at pH 5.0) occurred only when TSN was added before, or concurrently with, GT1b (Figure 2-6D). These results suggest that TSN is a moderate affinity partial antagonist of BoNT/B intoxication that might act by interfering with the assembly of oligomeric BoNT/B translocation channels. Also, the observation that TSN prevented oligomerization at pH 5.0 but not at pH 4.4 may help to explain why TSN provides only partial protection against BoNT/B in neurons (Figure 2-6A), since the effects of TSN appear to be pH dependent, and the intraluminal pH of synaptic vesicles is likely to fall transiently to relatively low values, as detailed above.

We also used AFM to test whether TSN affected the behavior of BoNT/B on GT1b-containing bilayers, and found that TSN did not significantly change the distribution of

molecular volumes of the toxin at pH 5.0. As noted above, due to the instability of the supported lipid bilayers at lower pH, we were not able to determine the effects of TSN at lower pH values via AFM; however, the drug did increase the percentage of donut-shaped structures formed by reduced BoNT/B at pH 5.0 from 28±2% to 50±1% (data from three independent experiments; total particle numbers = 463 [TSN] and 816 [control]). The significance of these observations is discussed below in the context of the single channel recordings.

Given the finding that BoNT/B might form oligomeric translocation "machines" and the fact that TSN hindered the assembly of BoNT/B oligomers in solution, we sought to determine whether the channel properties of BoNT/B are modulated by TSN. Our BN-PAGE analysis indicated that, in the presence of GT1b, BoNT/B assembles into trimers in a time-dependent manner at pH 5.0 (Figure 2-6E, left panel). When exposed at pH 5.0 to membrane patches excised from PC12 cells, BoNT/B induced a small-conductance channel (10 pS), which grew gradually over time until a maximum conductance of around 400 pS was reached (Figure 2-6F, left panel; Figure 2-6G). When TSN was present in addition to GT1b, the time-dependent assembly of trimers was inhibited (Figure 2-6E, right panel). On PC12 cell membrane patches, TSN facilitated the initial conductance growth induced by BoNT/B, but reduced the plateau conductance (Figure 6F, right panel; Figure 2-6G). Although the minimum conductance of the BoNT/B channel was unaffected by TSN (Figure 2-6H), both the maximum conductance (Figure 6I) and the $t_{1/2}$ for conductance growth (Figure 2-6J) were reduced by ~50%. Since cosedimentation assays demonstrated that TSN does not reduce binding of BoNT/B to GT1b-containing membranes at low pH (data not shown), the drug must inhibit some aspect of

translocation. Our results are consistent with the notion that TSN might inhibit translocation by preventing GT1b-dependent, low pH-induced oligomerization of BoNT/B.

2.5. DISCUSSION

A remarkable feature of the BoNTs concerns their ability to convert, in response to low pH, into membrane-associated proteins that are capable of delivering the LC into the cytosol of host neurons. This process also represents the least understood step in the action of these agents, so in the current study we carried out experiments with the goal of gaining insight into how this transformation occurs.

Initially, we found that low pH alone was unable to drive the conversion of the BoNT/B-HC into a hydrophobic, membrane-bound species that would be capable of mediating LC translocation. Further experiments revealed that the pH-triggered transformation of BoNT/B into a membrane protein requires interactions with a co-receptor molecule, the ganglioside GT1b. These findings suggest that the toxin is a coincidence detector: that is, binding to a receptor molecule, and exposure to low pH, both play a role in the conversion of the toxin into a putative translocation-competent form. Interestingly, interactions with receptors also prime some viruses for subsequent low pH-triggered fusion with host cells (Cote et al., 2009; Mothes et al., 2000; Nurani et al., 2003).

CD spectroscopy revealed that the conversion of BoNT/B into a hydrophobic species at low pH in the presence of GT1b involves a significant reduction in the α-helical content of the toxin; remarkably, this conformational change was largely reversed at neutral pH. Such

reversibility in translocation-related conformational changes appears to be a property that is shared by other bacterial toxins, including diphtheria toxin (Ladokhin et al., 2004) and *Clostridium difficile* toxin B (Qa'Dan et al., 2000), but the significance of this reversibility remains unclear.

We then turned our attention to experiments designed to gain insights into the structure of the low-pH membrane-bound form of the toxin using AFM imaging; virtually nothing is known concerning the structure of the toxin in this crucial state. We found that the low-pH membrane-bound form of BoNT/B HC resembles other protein translocation complexes that self-associate to form either double- or triple-donut structures. These include the mitochondrial TIM (Rehling et al., 2003) and TOM complexes (Ahting et al., 1999; Kunkele et al., 1998; Model et al., 2008), the endoplasmic reticulum protein Sec61p (Becker et al., 2009; Beckmann et al., 2001), and PhoE porin (Jap et al., 1991). There is some debate as to whether the assembly of these proteins into double- or triple-donut structures plays a role in translocation, or whether individual donuts are functionally active. For Sec61p, for example, early cryo-electron microscopy analysis indicated the formation of trimeric channels (Beckmann et al., 2001); however, more recent analysis led to the conclusion that the protein conducting channel consists of a single Sec61p molecule (Becker et al., 2009). In the case of BoNT/B, earlier studies are consistent with functionally relevant oligomerization of the toxin in membranes. For example, the rate of BoNT channel formation on membranes was shown to depend on the square of the toxin concentration, indicating cooperative assembly of the translocation competent form of the toxin (Donovan and Middlebrook, 1986; Hoch, 1985). Our observation that TSN inhibits BoNT/B trimerization and

in parallel truncates channel growth, lends further support to the idea that trimers may represent the optimally functional translocation unit.

We note that changes in BoNT/B conformation, and assembly into oligomers in the presence of GT1b, occurred over a very narrow pH range, and that formation of oligomers at the same pH (pH 5.0) was more efficient in solution than on membranes. In addition, the low pH requirements for BoNT/B oligomerization in solution (pH 4.8~5.0) (Figure 2-S3A) were less stringent than for effective surface entry into neurons (pH 4.4) (Figures 2-S3B and 2-S3C). These results are consistent with observations made using other pore-forming bacterial toxins, such as diphtheria toxin and anthrax toxin. Diphtheria toxin also changes conformation over a very narrow pH range (0.2 units) once the pH drops below pH 5.0 (Blewitt et al., 1985). Further, for anthrax toxin, pore formation requires a lower pH (~1 unit) on membranes than in solution (Miller et al., 1999). These findings imply that membranes also play a crucial role in shaping the behavior of bacterial toxins.

We also probed the assembly of the translocation machinery with TSN and found that this drug truncates the growth of channels formed by BoNT/B (peaking at 200 pS instead of 400 pS) and prevents trimer formation at pH 5.0. Interestingly, AFM imaging further revealed that TSN increases the proportion of toxin particles that appear as donuts following reduction. These findings are consistent with the increased rate of appearance of low-conductance BoNT/B channels in the presence of TSN. Therefore, TSN may prevent BoNT/B translocation by hindering oligomeric channel assembly, and such inhibitory effects are likely to be achieved - at least in part - by stabilizing the monomeric and low-conductance form of the toxin.

The AFM images revealed that the oligomeric BoNT/B donut structures have central holes that are similar in radius to those of single donuts, making it difficult to account for the very large increase in single-channel conductance as the pore grows on the membranes of PC12 cells (from 10 to 400 pS). However, it should be emphasized that the two structures we have imaged likely represent the beginning (membrane-associated holotoxin) and end (HC with LC removed) of the normal LC translocation process, and we have not been able to image the toxin in the act of translocation. It is possible that during translocation, three holotoxin molecules form a structure that transiently generates a very large pore, which later relaxes back to the triple-donut structure seen here when the holotoxin is reduced.

Given our finding that interactions with GT1b enable BoNT/B to sense a drop in pH, we tested whether preincubation of the toxin with GT1b, in solution at low extracellular pH, leads to premature activation of the toxin such that it enters an "off-pathway". Indeed, the action of BoNT/B on neurons was significantly reduced following such a preincubation step (data not shown). However, it should be noted that binding of exogenous GT1b to BoNT/B can also competitively inhibit binding to cellular receptors. In addition to GT1b, BoNT/B also specifically binds to the protein co-receptor, syt I/II, to undergo receptor-mediated endocytosis, prompting the question of whether syt I/II can also affect the pH-sensing activity of BoNT/B. We attempted to address this issue using P21, a soluble peptide of syt II that contains the binding site for BoNT/B (Dong et al., 2003), and failed to observe any effect. However, the lack of effect could be due to the fact that P21 binds to BoNT/B only weakly. High-affinity binding appears to require a syt I/II fragment that contains an intact transmembrane region (Dong et al., 2003), and

the presence of a hydrophobic segment precludes analysis in our partitioning and co-sedimentation assays.

In summary, the data presented here provide a glimpse into the most enigmatic state of a Clostridial neurotoxin: the low pH-induced membrane-bound form of the toxin that mediates translocation. Further studies are needed to image translocation of nascent LC. This might be achieved by arresting translocation with antibodies (Fischer and Montal, 2007a), and using cryo-electron microscopy and single particle reconstruction to gain a higher resolution view of this translocation machine. Moreover, given the function for GT1b identified here, it will be important to determine what happens when the GT1b binding domain of a BoNT is removed. In the case of BoNT/A, deletion of the receptor- binding domain results in a toxin that immediately forms large conductance channels without a requirement for low pH (Fischer et al., 2008b). Taking into account our current findings, in conjunction with previous data, the following model emerges: the receptor binding domain normally plays an inhibitory role in the conversion of the toxin into a translocation-competent form; this inhibition would be relieved by low pH and binding of GT1b, or by deletion of this domain. Hence, for the holotoxin, translocation occurs at the correct time and place.

2.6. EXPERIMENTAL PROCEDURES

Antibodies, BoNT/B and Recombinant Proteins

Monoclonal antibodies against syb II (69.1), SNAP-25 (71.1) and syntaxin (HPC-1) were kindly provided by Dr. R. Jahn (Max Planck Institute for Biophysical Chemistry, Göttingen,

Germany). BoNT/B and rabbit polyclonal anti-BoNT/B antibodies were generated as described previously (Dong et al., 2003; Dong et al., 2007; Evans et al., 1986). HCR/B was kindly provided by Dr. J.T. Barbieri (Medical College of Wisconsin, USA). Plasmids to generate recombinant full-length syb II (pTW2) and the cytoplasmic domain of syb (cd-syb; residues 1–94; pET-rsybCD) were kindly provided by Dr. J.E. Rothman (Yale University, USA). Syb II and cd-syb were purified as previously described (Bhalla et al., 2006).

Animals and Mice Lines

All procedures involving animals were performed according to US National Institutes of Health guidelines, as approved by the Animal Care and Use Committee of the University of Wisconsin, Madison. The ganglioside KO mouse line was obtained from the Consortium for Functional Glycomics, and has been described previously (Liu et al., 1999). This line is devoid of the gene encoding GM2/GD2 synthase (*Galgt1*). Genotype was verified by PCR.

Hippocampal Neuron Cultures and Preparation of Cell Lysates

Cultures of hippocampal neurons were prepared from E17-18 rats or 1 DIV WT or Gan KO mice, and plated on poly-lysine coated coverslips (12 mm, Carolina Biologicals) at a density of 50,000 cells/cm^2. Neurons were cultured in Neurobasal medium supplemented with B-27 (2%) and Glutamax (2 mM, Gibco/Invitrogen). Experiments were carried out using neurons that were 15-19 days old.

Cell lysates were prepared as previously described (Dong et al., 2007). Briefly, 120 μl of lysis buffer (PBS containing 1% Triton X-100, 0.05% SDS, and a protease inhibitor cocktail)

was added to each coverslip. Lysates were harvested, incubated for 5 min at 4°C on a shaker, and then centrifuged at 21,000 g for 10 min. Supernatants were collected for further analysis.

Off-pathway Assay

Cultures of rat hippocampal neurons and cell lysates were prepared as previously described (Dong et al., 2007); see Supplemental Experimental Procedures for further details. BoNT/B was incubated in high-K^+ buffer at pH 7.4 or pH 4.4 for 2 h at 37°C, before addition to neurons for 5 min. High-K^+ buffer stimulates recycling of synaptic vesicles, thus facilitating uptake of toxins into neurons by endocytosis. Neurons were washed with low-K^+ buffer at pH 7.4 or pH 4.4 and incubated in neuronal media at 37°C for 20 h. Cells were lysed, and cleavage of syb by BoNT/B was analyzed by SDS-PAGE and immunoblotting using anti-syb and anti-syntaxin (loading control) antibodies. The cleavage of syb was quantified using data from three independent trials.

Translocation of BoNT/B Across the Plasma Membrane

Where appropriate, hippocampal neurons were preincubated with bafilomycin A1 (1 μM, Sigma-Aldrich) for 30 min at 37°C. Unless otherwise specified, bafilomycin was added to all buffers used subsequently. Neurons were treated with high-K^+ buffer (85 mM NaCl, 60 mM KCl, 2 mM $CaCl_2$, 2 mM $MgCl_2$, 5.5 mM glucose, 10 mM Hepes, 10 mM sodium 2-(N-morpholino)ethanesulfonate (Na-MES), pH 7.4) for 5 min at 37°C, before exposure to BoNT/B (30 nM) for 10 min at 0°C. Note: with 30 nM, rather than 10 nM BoNT/B (as used in off-pathway assays), we observed reliable cleavage of syb in neurons for all batches of toxin, so this

concentration was used in all subsequent cell entry experiments. Neurons were washed and treated with low-K^+ buffer (140 mM NaCl, 5 mM KCl, 2 mM $CaCl_2$, 2 mM $MgCl_2$, 5.5 mM glucose, 10 mM Hepes, 10 mM Na-MES, pH as indicated) for 8 min at 37°C. For ganglioside KO mouse hippocampal neurons and rat hippocampal neurons treated with FB1 (25 μM, added to neurons at 4 days *in vitro*, Sigma-Aldrich), BoNT/B (30 nM; in low low-K^+ buffer, pH as indicated) was added for 10 min after high-K^+ buffer treatment (pH 7.4). The neurons were then washed and incubated without bafilomycin for 24 h. As tested by Trypan blue staining, >90% cells were viable after this 24 h incubation. Cells were harvested as described above, and cell lysates were analyzed by SDS-PAGE and immunoblotting using anti-syb, anti-SNAP-25 and anti-syntaxin antibodies. The amount of syb in each sample was normalized against SNAP-25, and cleavage of syb was quantified in three independent trials. Cells without bafilomycin treatment served as negative (minus BoNT/B) or positive (plus BoNT/B) controls for syb cleavage.

CD Spectroscopy

CD experiments were performed using an Aviv Model 202SF spectrometer. Far-UV CD spectra (197 nm to 260 nm) of BoNT/B holotoxin (0.67 μM) were obtained at pH 7.4 (5 mM citrate-phosphate buffer) or pH 4.4 (5 mM citrate buffer) at 37°C using 1-mm pathlength quartz cuvettes. GT1b (30 μM) was directly added to both samples, and spectra were again collected. The CD spectra of GT1b alone at pH 7.4 and pH 4.4 were also measured. CD data were plotted and analyzed using IGOR PRO. Spectra of buffer alone at pH 7.4 or pH 4.4 were subtracted from

sample traces for analysis. Helical content was estimated based on the ellipticity value at 222 nm, according to Chen et al. (Chen et al., 1972).

Cosedimentation Assay

The ganglioside GT1b was purchased from Matreya; all other lipids were obtained from Avanti Polar Lipids. Liposomes composed of 1-palmitoyl-2-oleoyl-*sn*-glycero-3-phosphocholine (PC) /1-palmitoyl-2-oleoyl-*sn*-glycero-3-phosphoethanolamine (PE) (70:30 by weight) or PC/PE/GT1b (60:30:10) were reconstituted as described previously (Bhalla et al., 2006; Tucker et al., 2004; Weber et al., 1998). Mixtures of BoNT/B (50 nM) and liposomes were incubated either at pH 7.4 (PBS) or at pH 4.4 (50 mM sodium acetate, 100 mM NaCl) at 37°C for 2 h, and cosedimentation assays were performed essentially as described previously (Bai et al., 2000). Briefly, samples containing both BoNT/B and liposomes were centrifuged at 163,000 x g for 40 min, and the supernatants were collected. In some experiments, pellets were analyzed immediately (below); in other experiments, pellets were resuspended in the indicated buffers and incubated for an additional 20 min at room temperature, before another round of centrifugation at 163,000 x g for 40 min. Supernatants and pellets were again collected. Samples were analyzed by SDS-PAGE and immunoblotting, using anti-BoNT/B antibodies.

Triton X-114 Partitioning Assay

Triton X-114 partitioning assays were performed as described previously (Bordier, 1981). For pH 7.4 samples, PBS was used. For pH 5.4 and 4.4 samples, the buffer was 50 mM sodium acetate and 100 mM NaCl. Final concentrations were 0.045 mg/ml for BoNT/B (300 nM) and

syb (3.5 μM), and 0.45 mg/ml for cd-syb (43 μM). Where appropriate, BoNT/B was incubated with GT1b (90 μM) for 1 h at 37°C before Triton X-114 partitioning assays were carried out. After partitioning assays, the aqueous and detergent phases of each sample were collected and analyzed by SDS-PAGE and Coomassie blue staining (for cd-syb) or immunoblotting, using anti-BoNT/B and anti-syb antibodies.

Solid-phase Binding Assay

Solid-phase binding assays were performed as described previously (Schmitt et al., 2010). Briefly, GT1b (0.1 mg/ml) in methanol was added to a 96-well, non-binding surface plate (Corning, NY), and allowed to dry overnight at room temperature. The plate was washed three times using PBS (pH 7.4) and blocked with 1% BSA in 50 mM Na_2CO_3 (pH 9.6) for 2 h at room temperature. The plate was then washed three times using PBS, and HCR/B (300 nM) in PBS (pH 7.4) or in 50 mM sodium acetate, 100 mM NaCl (pH 4.4), was added for a 1-h incubation at 4^{o}C. Wells were washed three times at pH 7.4 or pH 4.4, respectively, and anti-flag tag primary and HRP-conjugated secondary antibodies were added and incubated for 30 min at 4^{o}C. The plate was washed three times with PBS, and developed with TMB substrate (Thermo Scientific) for 30 min at room temperature. The reaction was stopped by adding H_2SO_4 (1M), and absorbance was measure at 450 nm. The absorbance of samples devoid of HCR/B was also measured as a control. Non-specific binding in the absence of GT1b was subtracted from each sample measurement.

AFM Imaging

AFM imaging was performed using a Veeco Digital Instruments Multimode instrument, controlled by a Nanoscope IIIa controller. For imaging on mica, toxin was diluted to 1 μg/ml in Hepes-buffered saline (HBS; 50 mM Hepes, pH 7.6, 150 mM NaCl) containing 1 mM Ca^{2+}, and 50 μl was placed on freshly-cleaved mica. After a 20-min incubation, samples were washed with 10 ml ultrapure water (BPC grade; Sigma-Aldrich) to remove unadsorbed protein. All imaging was carried out at room temperature. For imaging of proteins on lipid bilayers, liposomes composed of PC/PE (70:30) or PC/PE/GT1b (70:27:3) were prepared as described above. BoNT/B (10 μg/ml) in either HBS (pH 7.0) or sodium acetate (pH 5.0), was added to an equal volume of liposome suspension (lipid concentration 2.67 mM), to give a final toxin concentration of 5 μg/ml. The mixture was incubated for 15 min at 21°C before formation of supported bilayers. For imaging of reduced toxin with bilayers, toxin was first reduced by treatment with 4 mM DTT for 1 h at 37°C at pH 5.0 before incubation with liposomes, as above. In some cases, reduced toxin was incubated with liposomes at 37°C before bilayer formation. Where appropriate, TSN (Apin Chemicals, Oxon, U.K.) was present at a concentration of 40 μM. To form supported lipid bilayers, liposomes (50 μl) were deposited on freshly cleaved muscovite mica (Agar Scientific, Stansted, UK) with 50 μl of HBS containing 1 mM $CaCl_2$ for 5 min. After incubation, the unadsorbed lipids were washed away with 2 ml of buffer. Buffer (150 μl) was immediately added to the lipid bilayer and the samples were imaged.

Imaging in air was carried out using Si probes (OMCL-AC160TS-E; Olympus), with a resonance frequency of 300 kHz. Imaging under fluid was carried out using NSC-18 cantilevers

(Mikromasch) with a resonant frequency of 30-35 kHz. The actual scanning frequencies were ~5% below the maximal resonance peak. In both cases the RMS voltage was maintained at 2 V.

All AFM images were plane-fitted before any analysis to remove tilt. For dry imaging, particles were analyzed using the NanoscopeV5.31rl software. Fifty particles were first analyzed manually. These measurements were used to define the detection level in the program, which in turn defines the minimum z-value to be considered as part of the particle. After particles were thus defined, height and radius (radius of a circle fitted to data obtained for each particle) were determined. For fluid imaging, particles were first identified from the phase image and their heights and radii were measured manually using the section tool.

Bound particles assumed the approximate shape of a spherical cap. The radius and height of each particle were used to calculate its molecular volume using the formula

$$V_m = (\pi h/6)(3r^2 + h^2) \qquad (1)$$

where h is the particle height and r is the radius, as described previously (Schneider et al., 1998). For comparison, molecular volume based on molecular mass was calculated using the equation

$$V_c = (M_0/N_0)(V_1 + dV_2) \qquad (2)$$

where M_0 is the molecular mass, N_0 is Avogadro's number, V_1 and V_2 are the partial specific volumes of particle (0.74 cm^3/g) and water (1 cm^3/g), respectively, and d is the extent of protein hydration (taken as 0.4 g water/g protein).

BN-PAGE Assay of BoNT/B

The NativePAGE Novex Bis-Tris gel system for BN-PAGE was obtained from Invitrogen. BoNT/B (30 or 100 nM) was incubated alone or with the ganglioside GT1b or GM1 (10 μM, unless specifically indicated) at pH 7.4, pH 5.0 and pH 4.4 at 37°C for 2 h. For samples containing TSN, TSN (concentration as indicated) was preincubated with BoNT/B for 2 h before GT1b was added. In Figure 2-6D, TSN was either preincubated with BoNT/B for 1.5 h, added the same time as BoNT/B, or 1.5 h after BoNT/B, followed by incubation at 37 °C for 3 h. Samples were analyzed by BN-PAGE and silver staining.

Electrophysiological Recording of BoNT/B Channels

Recordings were performed essentially as described previously (Sheridan, 1998). PC12 cells were plated onto polylysine- and collagen-coated coverslips at a low density, and cultured in DMEM (Gibco/Invitrogen) supplemented with equine serum (5%) and bovine calf serum (5%) for 2-3 days.

Cells were transferred to bath solution (200 mM CsCl, 5 mM sodium 3-(N-morpholino) propanesulfonic acid (NaMOPS), 1 mM DTT or 0.25 mM Tris(2-carboxyethyl)phosphine (TCEP) hydrochloride, 1 mM tetrodotoxin (TTX), pH 7.4). BoNT/B (100 nM) with and without TSN (300 μM) was incubated in a pipette solution (200 mM CsCl, 5 mM Na·MES, 1 mM TTX, pH 5.0) and added to the pipette. The membrane potential was held at -70 mV on the cis (pipette) side of the membrane patch. After GΩ seal formation on PC12 cells, pipettes were quickly removed from the cell soma to form excised “inside-out” membrane patches. Membrane currents

were monitored over time using an EPC-10/2 amplifier (HEKA Electronics, Germany). Currents were acquired using PATCHMASTER software (HEKA), filtered at 2.9 kHz, and digitized at 10 kHz.

The BoNT/B channel conductances, in the presence and absence of TSN, were calculated by dividing the measured currents by the holding potential; the conductances were then plotted as a function of time and the data were fitted using sigmoid curves.

2.7. FIGURES AND LEGENDS

Figure 2-A1

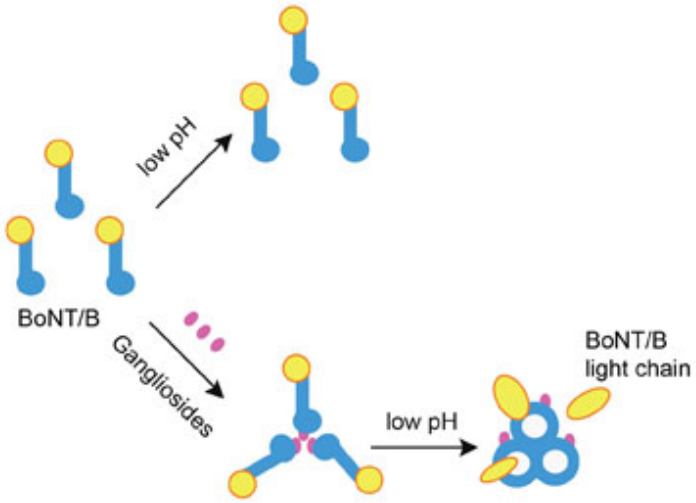

Figure 2-1

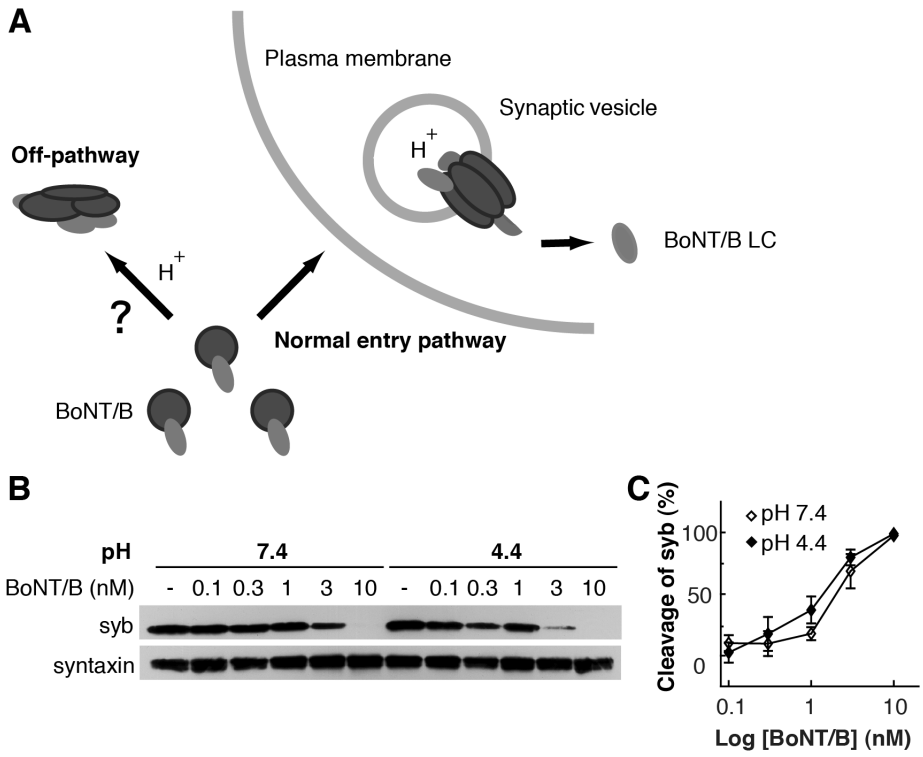
A
Plasma membrane
Synaptic vesicle
H+
Off-pathway
BoNT/B LC
H+
?
Normal entry pathway
BoNT/B
B
pH
7.4
4.4
BoNT/B (nM)
- 0.1 0.3 1 3 10 - 0.1 0.3 1 3 10
syb
syntaxin
C
pH 7.4
pH 4.4
Cleavage of syb (%)
100
50
0
0.1
1
10
Log [BoNT/B] (nM)

Figure 2-1. Low pH Pretreatment Does Not Inactivate BoNT/B

(A) Illustration of the ”off-pathway” potentially induced by low-pH pretreatment of BoNT/B. In principle, exposure to low pH in solution could transform BoNT/B into a hydrophobic protein, causing aggregation and consequent inactivation.

(B) Immunoblot analysis of syb cleavage by BoNT/B. Toxin was exposed to either pH 7.4 or pH 4.4 for 2 h before incubation with rat hippocampal neurons. Syntaxin served as a loading control.

(C) Quantitation of syb cleavage, normalized to syntaxin levels. Data are means ± SEM (n=3).

Figure 2-2

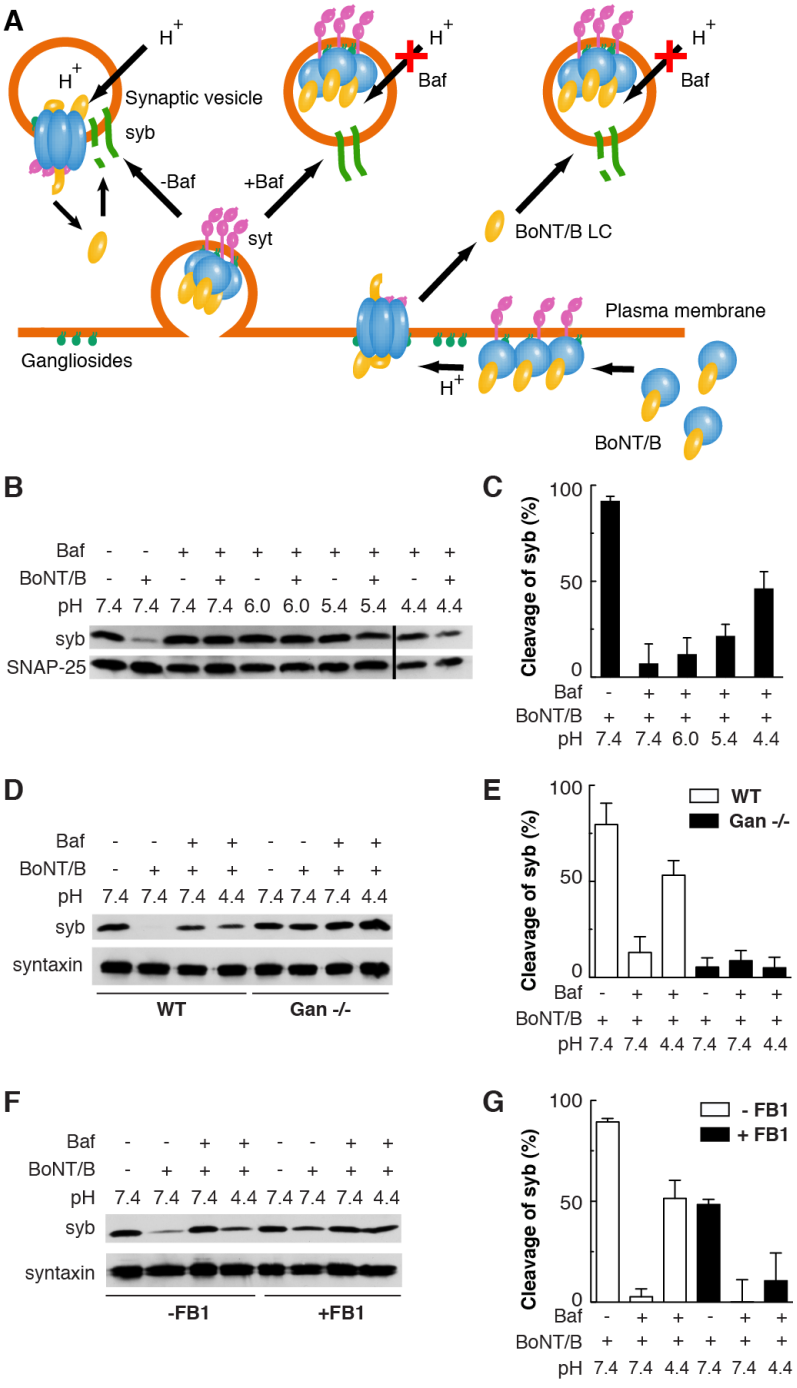
A
H+
Synaptic vesicle
syb
-Baf
+Baf
syt
Baf
BoNT/B LC
Plasma membrane
Gangliosides
BoNT/B
B
Baf
BoNT/B
pH 7.4 7.4 7.4 7.4 6.0 6.0 5.4 5.4 4.4 4.4
syb
SNAP-25
C
Cleavage of syb (%)
100
50
0
pH 7.4 7.4 6.0 5.4 4.4
D
pH 7.4 7.4 7.4 4.4 7.4 7.4 7.4 4.4
syntaxin
WT
Gan -/-
E
WT
Gan -/-
pH 7.4 7.4 4.4 7.4 7.4 4.4
F
-FB1
+FB1
G
- FB1
+ FB1

Figure 2-2. Gangliosides are Required for Efficient Cell Surface Entry of BoNT/B

(A) Illustration of potential BoNT/B LC translocation pathways. Normal translocation of BoNT/B LC across the membrane of endocytosed synaptic vesicles is blocked by bafilomycin A1 (Baf), an inhibitor of the vesicular H^+-ATPase. After BoNT/B holotoxin binds to its co-receptors, syt and gangliosides, on the neuronal plasma membrane, low extracellular pH treatment enables BoNT/B to deliver its LC directly into the neuronal cytoplasm. Translocation is monitored by assaying cleavage of syb.

(B and C) pH dependence of BoNT/B LC translocation across membranes. (B) Immunoblot analysis of syb cleavage after exposure of rat hippocampal neurons to BoNT/B for 20 h. Neurons were treated with BoNT/B with and without Baf, as indicated. SNAP-25 served as an internal loading control. The black line indicates lanes, from the same blot, that were juxtaposed. (C) Quantitation of syb cleavage in (B), normalized to SNAP-25 levels. Data are means ± SEM (n=3).

(D-G) Gangliosides are required for BoNT/B LC translocation across membranes. Hippocampal neurons from ganglioside KO ($Gan^{-/-}$) mice (D) or FB1-treated (+FB1) rat hippocampal neurons (F) were exposed to BoNT/B with and without Baf at the indicated pH for 10 min. Cleavage of syb after 20 h was analyzed by immunoblotting. Cleavage of syb in wild-type (WT) mouse neurons (D) or in rat neurons without FB1 treatment (-FB; F) was also monitored. Syntaxin served as a loading control. Cleavage of syb was quantified after normalization to the levels of syntaxin (E and G). Data are means ± SEM (n=3).

Figure 2-3

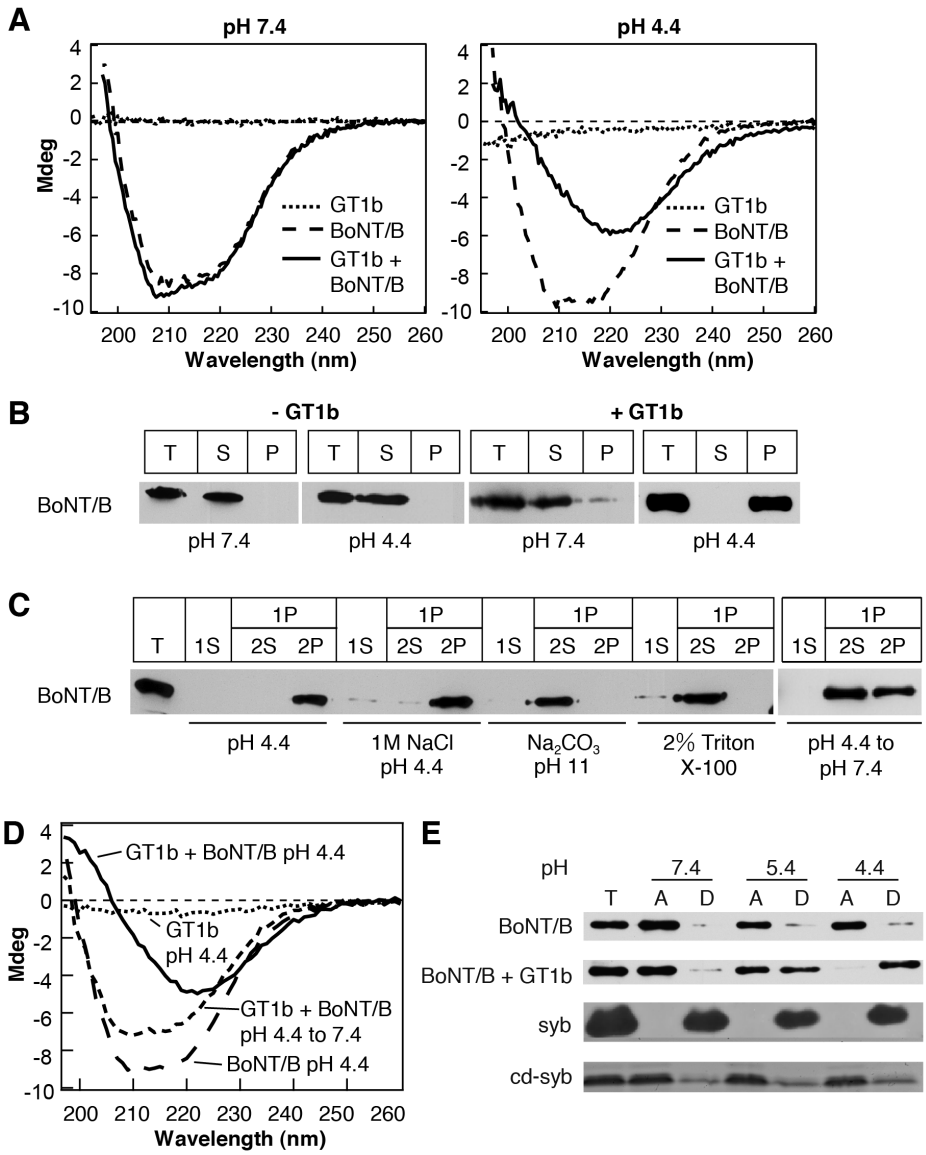
A
pH 7.4
pH 4.4
Mdeg
GT1b
BoNT/B
GT1b + BoNT/B
Wavelength (nm)
B
- GT1b
+ GT1b
T S P
BoNT/B
pH 7.4
pH 4.4
C
T 1S 1P 2S 2P
BoNT/B
pH 4.4
1M NaCl pH 4.4
Na2CO3 pH 11
2% Triton X-100
pH 4.4 to pH 7.4
D
GT1b + BoNT/B pH 4.4
GT1b pH 4.4
GT1b + BoNT/B pH 4.4 to 7.4
BoNT/B pH 4.4
Mdeg
Wavelength (nm)
E
pH
7.4
5.4
4.4
T A D A D A D
BoNT/B
BoNT/B + GT1b
syb
cd-syb

Figure 2-3. GT1b Enables BoNT/B to Undergo a Change in Secondary Structure and to Transform into a Hydrophobic Membrane-associated Protein at Low pH

(A) Low pH triggers major conformational changes in BoNT/B in the presence of GT1b. Far UV-CD spectra of BoNT/B in the absence (dashed lines) or presence (solid lines) of GT1b at pH 7.4 (*left*) and pH 4.4 (*right*). CD spectra of GT1b alone at pH 7.4 and pH 4.4 were included as controls (dotted lines).

(B) Cosedimentation of BoNT/B with liposomes. BoNT/B was incubated with liposomes that either harbored or lacked GT1b at pH 7.4 or pH 4.4. Liposomes were sedimented, and BoNT/B in the total input (T), supernatant (S) and pellet (P) fractions was assayed by immunoblotting using anti-BoNT/B antibodies.

(C) Nature of the association of BoNT/B with liposomes. BoNT/B efficiently bound to GT1b-containing liposomes at pH 4.4. The liposome-protein complexes were suspended in the indicated buffers, incubated for 20 min at room temperature and then resedimented. BoNT/B in the total input (T) and initial supernatant (1S), and in the second supernatant (2S) and pellet (2P) fractions was again assayed by immunoblotting.

(D) CD spectra showing that the GT1b-induced conformational change in BoNT/B at pH 4.4 was largely reversed at pH 7.4. Representative CD spectra of BoNT/B alone at pH 4.4 (long dashed line), BoNT/B with GT1b at pH 4.4 (solid line), and BoNT/B with GT1b after raising the pH from 4.4 to 7.4 (short dashed line), are shown. The spectrum of GT1b alone (dotted line) serves as a control.

(E) Increased hydrophobicity of BoNT/B at low pH in the presence of GT1b. Triton X-114 partitioning assays were performed at pH 7.4, pH 5.4 and pH 4.4 in the absence or presence

of GT1b. BoNT/B in the total input (T), aqueous (A) and detergent (D) phases was detected by immunoblot analysis. The behavior of full-length syb (an archetypal membrane protein) and syb cytosolic domain (cd-syb, an archetypal soluble protein) was analyzed by immunoblotting or staining with Coomassie blue, respectively.

See also Figure 2-S1.

Figure 2-4

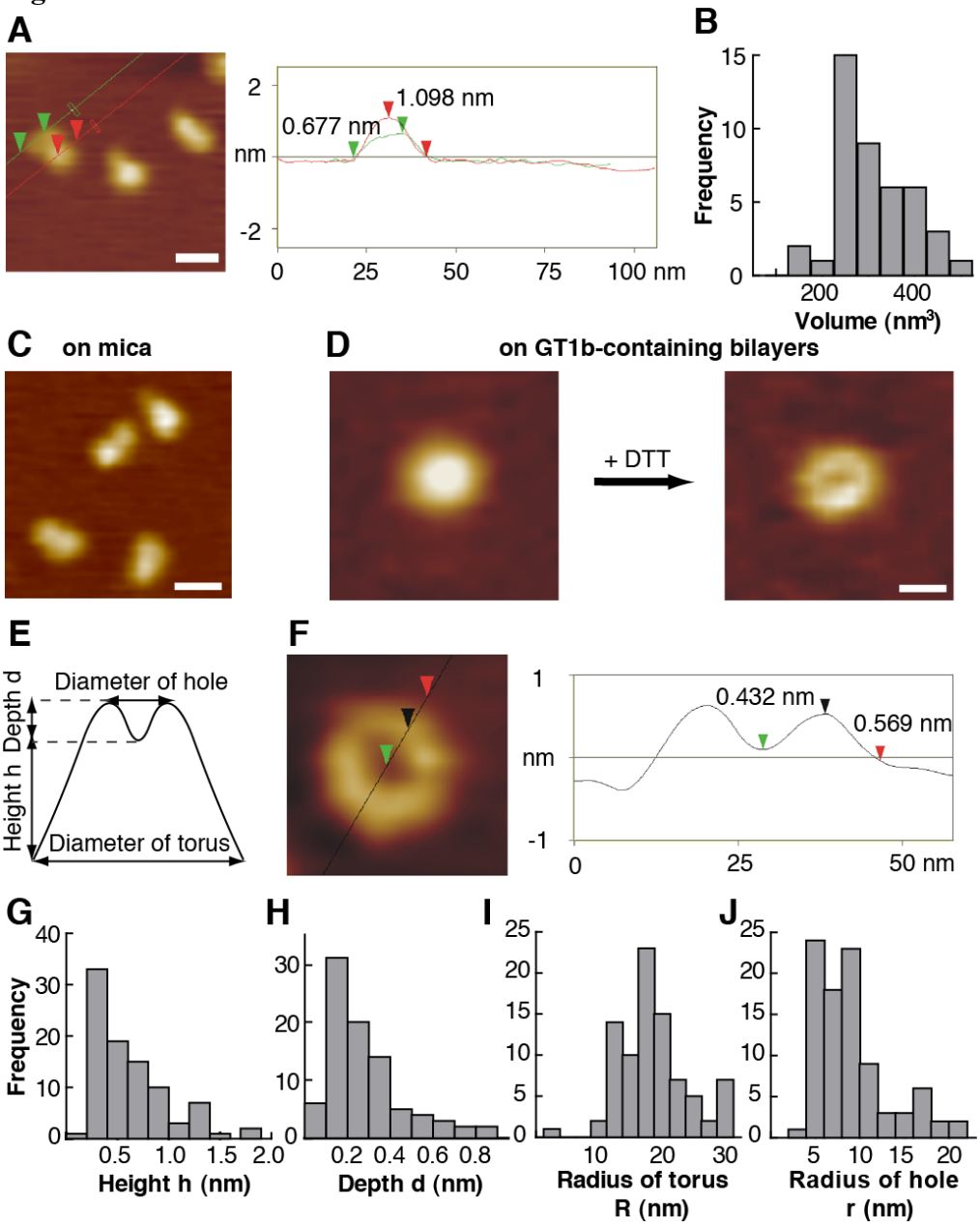
A
2
nm
-2
0.677 nm
1.098 nm
0
25
50
75
100 nm
B
15
10
5
0
Frequency
200
400
Volume (nm3)
C on mica
D on GT1b-containing bilayers
+ DTT
E
Diameter of hole
Height h Depth d
Diameter of torus
F
1
nm
-1
0.432 nm
0.569 nm
0
25
50 nm
G
40
30
20
10
0
Frequency
0.5
1.0
1.5
2.0
Height h (nm)
H
30
20
10
0
0.2
0.4
0.6
0.8
Depth d (nm)
I
25
20
15
10
5
0
10
20
30
Radius of torus
R (nm)
J
25
20
15
10
5
0
5
10
15
20
Radius of hole
r (nm)

Figure 2-4. BoNT/B HC Forms Donut-shaped Structures on GT1b-containing Bilayers at Low pH

(A) AFM image of BoNT/B holotoxin on mica, with sections taken at the positions indicated by the lines. Scale bar, 20 nm.

(B) Frequency distribution of molecular volumes of BoNT/B holotoxin on mica (*right*).

(C) Representative image of BoNT/B holotoxin on mica, showing the two-lobed structure of the LC and the HC. Scale bar, 20 nm.

(D) AFM images of non-reduced (*left*) and DTT-reduced (*right*) BoNT/B on GT1b-containing bilayers at pH 5.0. Scale bar, 15 nm.

(E) Diagram indicating the dimensions of single donuts that were measured.

(F) Dimensions of donuts. The *left-hand panel* shows an AFM image of an individual single donut. The *right-hand panel* shows a section taken at the position indicated by the lines. The height and hole depth of the donut are indicated.

(G-J) Frequency distributions of heights h (G), hole depths d (H), outer radii R (I), and hole radii r (J) for single donuts.

See also Figure 2-S2.

Figure 2-5

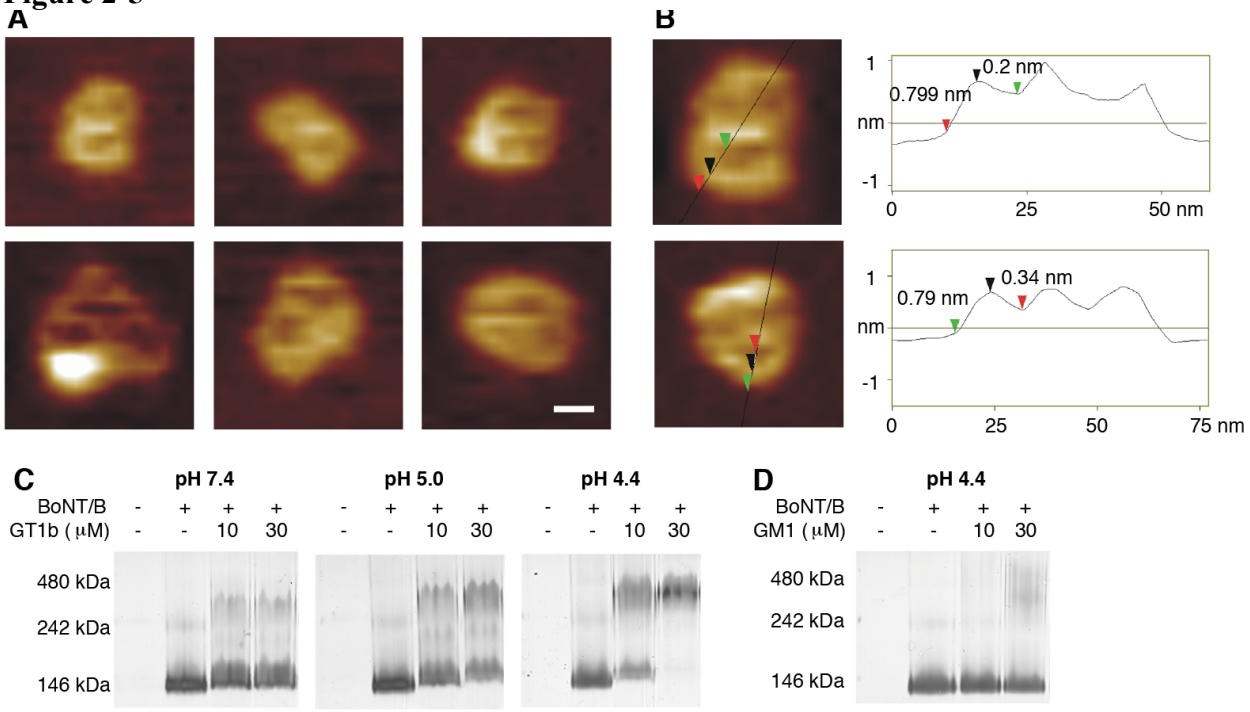
A
B
1
nm
-1
0.2 nm
0.799 nm
0 25 50 nm
0.34 nm
0.79 nm
0 25 50 75 nm
C
pH 7.4
pH 5.0
pH 4.4
BoNT/B - + + + - + + + - + + +
GT1b (μM) - - 10 30 - - 10 30 - - 10 30
480 kDa
242 kDa
146 kDa
D
pH 4.4
BoNT/B - + + +
GM1 (μM) - - 10 30
480 kDa
242 kDa
146 kDa

Figure 2-5. GT1b Triggers BoNT/B Oligomerization at Low pH

(A) Gallery of AFM images showing double (*top*) and triple (*bottom*) donut structures formed by reduced BoNT/B on GT1b-containing bilayers at pH 5.0. Scale bar, 15 nm.

(B) Dimensions of donuts. The *left-hand panels* show AFM images of individual double (*top*) and triple (*bottom*) donuts. The *right-hand panels* show sections taken at positions indicated by the lines. The height and hole depth of the donut are indicated.

(C) BN-PAGE analysis of BoNT/B holotoxin at pH 7.4, pH 5.0 and pH 4.4 in the absence and presence of GT1b. Protein was detected by silver staining.

(D) BN-PAGE analysis of BoNT/B holotoxin at pH 4.4 in the absence and presence of the control ganglioside, GM1.

Figure 2-6

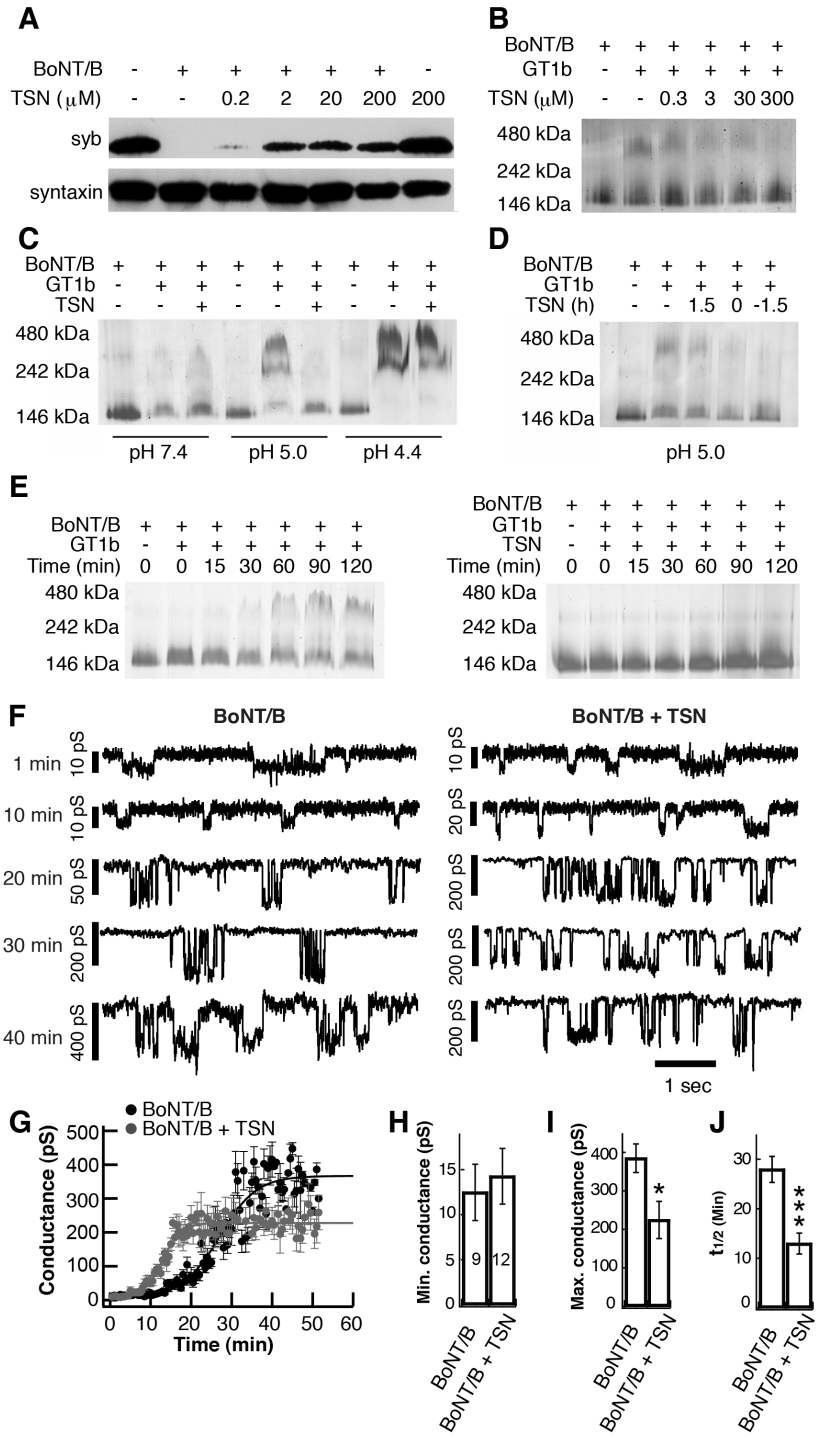
A
BoNT/B - + + + + + -
TSN (μM) - - 0.2 2 20 200 200
syb
syntaxin
B
BoNT/B + + + + + +
GT1b - + + + + +
TSN (μM) - - 0.3 3 30 300
480 kDa
242 kDa
146 kDa
C
BoNT/B + + + + + + + + +
GT1b - + + - + + - + +
TSN - - + - - + - - +
480 kDa
242 kDa
146 kDa
pH 7.4
pH 5.0
pH 4.4
D
BoNT/B + + + + +
GT1b - + + + +
TSN (h) - - 1.5 0 -1.5
480 kDa
242 kDa
146 kDa
pH 5.0
E
BoNT/B + + + + + + +
GT1b - + + + + + +
Time (min) 0 0 15 30 60 90 120
480 kDa
242 kDa
146 kDa
BoNT/B + + + + + + +
GT1b - + + + + + +
TSN - + + + + + +
Time (min) 0 0 15 30 60 90 120
480 kDa
242 kDa
146 kDa
F
BoNT/B
BoNT/B + TSN
1 min
10 min
20 min
30 min
40 min
10 pS
50 pS
200 pS
400 pS
20 pS
1 sec
G
BoNT/B
BoNT/B + TSN
Conductance (pS)
Time (min)
H
Min. conductance (pS)
I
Max. conductance (pS)
J
t1/2 (Min)
BoNT/B
BoNT/B + TSN

Figure 2-6. TSN Hinders BoNT/B Translocation and Assembly Into Oligomers

(A) Immunoblot analysis of syb cleavage after exposure of rat hippocampal neurons to BoNT/B in the presence of TSN. Syntaxin served as a loading control.

(B-E) TSN hinders the oligomerization of BoNT/B. (B) BN-PAGE analysis of BoNT/B holotoxin with GT1b at pH 5.0 in the presence of TSN. Proteins were detected by silver staining. (C) BN-PAGE analysis of BoNT/B holotoxin with GT1b at pH 7.4, pH 5.0 and pH 4.4 in the absence and presence of TSN. (D) BN-PAGE analysis of the time-course of the effect of TSN at pH 5.0. TSN was added either before (-1.5 h), at the same time (0 h) or after (1.5 h) incubation of BoNT/B with GT1b. (E) BN-PAGE analysis of BoNT/B holotoxin at various times after addition of GT1b, in the absence (*left*) and presence (*right*) of TSN.

(F-J) TSN modulates BoNT/B channel activity at pH 5.0. BoNT/B channel activity in PC12 cell membranes in the absence (*left*) or the presence (*right*) of TSN at pH 5.0. BoNT/B was added to the pipette and channel activity was recorded in 'inside-out' membrane patches (F). Effect of TSN on the time-course of BoNT/B channel conductance growth. Conductances in the absence (black symbols) and presence (gray symbols) of TSN were plotted against time and fitted using sigmoid curves (G). Effect of TSN on minimum conductance (H), maximum conductance (I) and $t_{1/2}$ of channel conductance growth (J). Data are means ± SEM.

See also Figure 2-S3.

Figure 2-S1

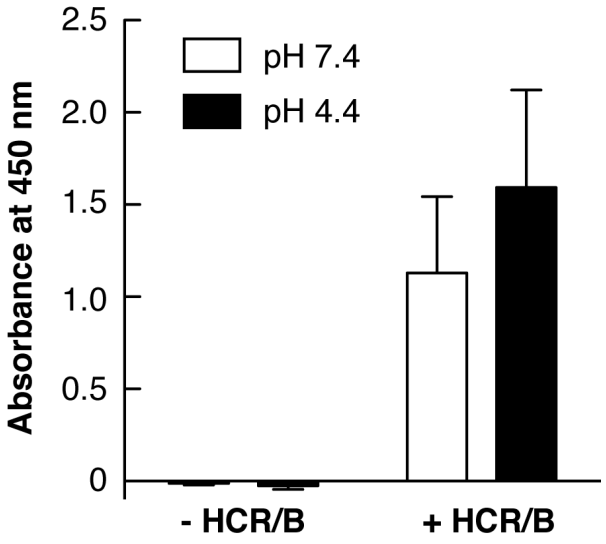

Figure 2-S1. Solid-phase binding assay showing that HCR/B has similar ganglioside binding activity at pH 7.4 and pH 4.4. Related to Figure 2-3.

Non-binding microtiter plates were coated with GT1b (10 μg) overnight, and incubated with HCR/B (300 nM) for 1 h at pH 7.4 or pH 4.4. Wells were washed, and bound material was detected using HRP-conjugated anti-FLAG antibodies, and ultra-TMB, by measuring the absorbance at 450 nm. The absorbances of GT1b-free samples were subtracted, and the absorbances of minus-HCR/B samples were included as control. Data are means ± SEM (n=3).

Figure 2-S2

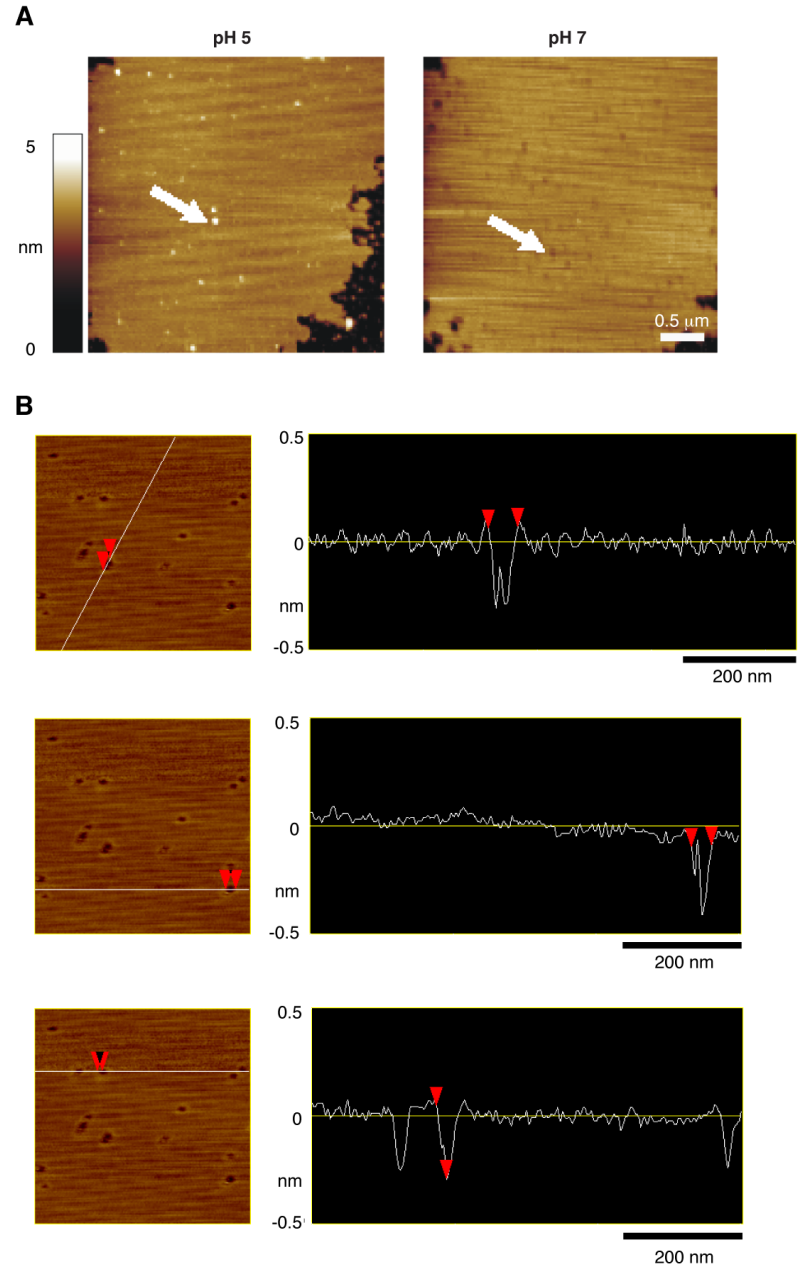
A
pH 5
pH 7
5
nm
0
0.5 μm
B
0.5
0
nm
-0.5
200 nm
0.5
0
nm
-0.5
200 nm
0.5
0
nm
-0.5
200 nm
C
Frequency
40
30
20
10
0
0.2
0.4
0.6
0.8
Depth of indentations (nm)
D
30
25
20
15
10
5
0
10
20
30
Radius of indentations (nm)

Figure 2-S2. Indentations appear as BoNT/B dissociates from GT1b-containing bilayers when pH is switched from 5.0 to 7.0. Related to Figure 2-4

(A) BoNT/B bound to GT1b-containing bilayers at pH 5.0 (*left,* white arrows indicating BoNT/B particles); BoNT/B dissociated from bilayers and left indentations on membranes when the pH was adjusted from pH 5.0 to pH 7.0 (*right*, white arrows indicating indentations). Scale bar, 0.5 μm.

(B) Dimensions of indentations. Sections taken at positions indicated by lines, showing the diameters and depths of representative indentations (red arrowheads).

(C) Frequency distributions of the depths (*left*) and radii (*right*) of the indentations.

Figure 2-S3

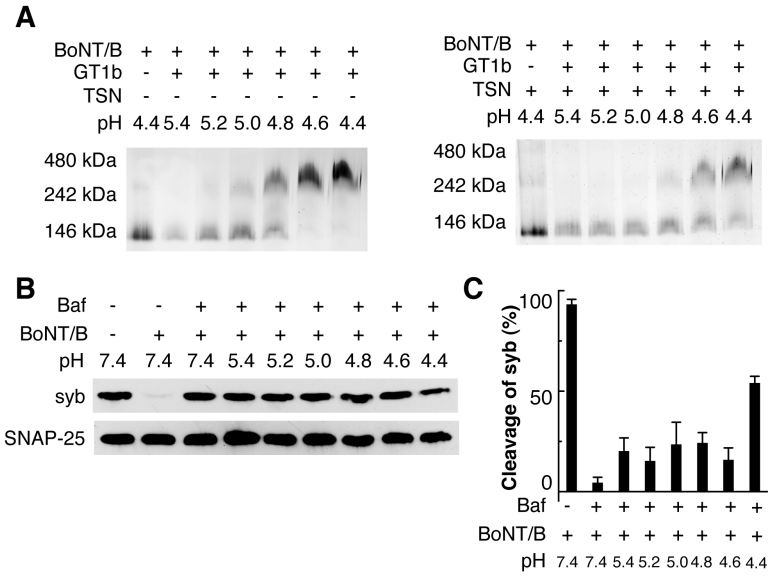
A
BoNT/B + + + + + + +
GT1b - + + + + + +
TSN - - - - - - -
pH 4.4 5.4 5.2 5.0 4.8 4.6 4.4
480 kDa
242 kDa
146 kDa
BoNT/B + + + + + + +
GT1b - + + + + + +
TSN + + + + + + +
pH 4.4 5.4 5.2 5.0 4.8 4.6 4.4
480 kDa
242 kDa
146 kDa
B
Baf - - + + + + + + +
BoNT/B - + + + + + + + +
pH 7.4 7.4 7.4 5.4 5.2 5.0 4.8 4.6 4.4
syb
SNAP-25
C
Cleavage of syb (%)
100
50
0
Baf - + + + + + + +
BoNT/B + + + + + + + +
pH 7.4 7.4 5.4 5.2 5.0 4.8 4.6 4.4

Figure 2-S3. Oligomerization and cell surface entry of BoNT/B at low pH. Related to Figure 2-6

(A) BN-PAGE analysis of BoNT/B (30 nM) after incubation with GT1b (10 μM) in the absence (*left*) and presence (*right*) of TSN (30 μM) for 2 h at the indicated pH.

(B) pH dependence of BoNT/B translocation across cellular membranes. Neurons (incubated with or without bafilomycin as indicated) were exposed to BoNT/B (30 nM) for 10 min on ice, washed and incubated at the indicated pH at 37°C for 8 min. Neurons were then incubated in neuronal media for 20 h, before cleavage of syb was analyzed by immunoblotting. SNAP-25 served as an internal loading control.

(C) Quantification of syb cleavage in (B), normalized against SNAP-25 levels. Data are means ± SEM (n=3).

2.8. APPENDIX

1) We thank M. Dong for helpful discussions, D. Wang for helping to prepare rat hippocampal neurons, and the Chapman lab for critical comments regarding this manuscript. We also acknowledge J.T. Barbieri for preparing HCR/B, with support from the GLRCE U54 AI057153. This work was supported by a grant from the NIH (AI057744) to E.R.C. S. Suresh was supported by a Cambridge Nehru Fellowship and a Cambridge Overseas Research Studentship. E.R.C. is an Investigator of the Howard Hughes Medical Institute.

2) Work in this chapter has been published in Cell Host & Microbe*:*

Receptor binding enables botulinum neurotoxin B to sense low pH for translocation channel assembly.

Sun S, Suresh S, Liu H, Tepp WH, Johnson EA, Edwardson JM, Chapman ER. Cell Host Microbe. 2011 Sep 15;10 (3): 237-47.

Highlighted in: Lencer, W.I., Tweten, R.K.. (2011) To translocate or not: that is the problem. Cell Host & Microbe. 2011 Sep 15;10 (3): 179-80.

Chapter 3

Mechanisms of Botulinum Neurotoxin E Translocation

3.1. SUMMARY

Botulinum neurotoxins (BoNTs, serotypes A-G) are the most deadly substances known. Here, we investigated how BoNT/E, a serotype that causes human botulism, translocates into the cytosol of neurons. Analogous to BoNT/B, BoNT/E required binding to the co-receptor, GT1b, to undergo significant secondary structural changes and transform into a hydrophobic protein at low pH. These data indicate that both serotypes act as coincidence detectors for both GT1b and low pH, in order to undergo translocation. However, BoNT/E translocated much more rapidly than BoNT/B. Also, BoNT/E required only GT1b, and not low pH, to oligomerize, whereas BoNT/B required both. In further contrast to BoNT/B, low pH alone altered the secondary structure of BoNT/E to some degree and resulted in its premature inactivation. Hence, comparison of two BoNT serotypes revealed that these agents exhibit both convergent and divergent responses to receptor interactions, and pH, in the translocation pathway.

3.2. INTRODUCTION

Botulinum neurotoxins (BoNTs, serotypes A-G) are the most potent toxins known to humankind (Schiavo et al., 2000). They target presynaptic nerve terminals with high specificity, causing a severe disease termed botulism. These toxins are produced as 150 kDa proteins by bacteria belonging to the genus *Clostridium*. Each toxin consists of a heavy chain (HC, 100 kDa) and a light chain (LC, 50 kDa). The HC binds to receptors on the neuronal surface and mediates toxin uptake, often via recycling synaptic vesicles (SVs) (Dong et al., 2008a; Dong et al., 2003; Dong et al., 2007; Dong et al., 2006; Mahrhold et al., 2006; Nishiki et al., 1994; Nishiki et al., 1996c; Peng et al., 2011; Rummel et al., 2007a; Rummel et al., 2004a). The HC also mediates

the translocation of the LC from the SV/endosomal lumen into the cytosol (Montal, 2010). The LC then acts as a specific protease that cleaves SNARE (soluble NSF attachment protein receptor) proteins, thereby inhibiting neurotransmitter release. Such blockade results in flaccid paralysis at the neuromuscular junction, and can result in respiratory failure and death (Schiavo et al., 2000). Due to their extreme potency (lethal dose ranging from 0.1-1 ng/kg), BoNTs are listed as Category A bioterrorism agents by the Centers for Disease Control (CDC) (Arnon et al., 2001; Rotz et al., 2002). Paradoxically, BoNTs are also widely used to treat a variety of diseases, and are also used cosmetically to treat wrinkles (Montecucco and Molgo, 2005).

The mechanism by which BoNTs translocate their LCs from the lumen of SVs/endosomes into the cytosol remains the least understood step in intoxication (Montal, 2010). Previous studies indicate that low pH in the endosomal lumen is required for the translocation step: neutralizing the pH with chloroquine, ammonium chloride, or methylamine hydrochloride, or blocking endosomal acidification by specific vacuolar H^+-ATPase inhibitors, abolished the action of all of the BoNTs (Keller et al., 2004; Simpson, 1982, 1983; Simpson et al., 1994a). Electrophysiological studies revealed that addition of BoNTs to the low pH, oxidizing side of a membrane resulted in single channel formation *in vitro*; the channel activity was restricted to the HC (Fischer et al., 2012; Hoch, 1985; Montal, 2010; Sheridan, 1998). These data led to the hypothesis that low endosomal pH triggers the HC to form a membrane channel that mediates LC translocation. Since BoNTs are synthesized as soluble proteins, transforming them into membrane channels must involve major structural rearrangements; however, low pH alone failed to trigger any structural changes in BoNT/B, and this serotype was structurally stable from pH 7 to pH 4 (Eswaramoorthy et al., 2004).

Recent studies have shed new light on this apparent paradox (Sun et al., 2011). It was found that BoNT/B is a coincidence detector: binding to the co-receptor molecule, the ganglioside GT1b, enables the toxin to sense low pH and transform into oligomeric hydrophobic membrane-associated channels. The simultaneous requirement for both receptor binding and low pH ensure that translocation occurs at the right time and place. However, whether the concept of coincidence detection applies to any other BoNT serotype has yet to be determined: the underlying mechanisms that mediate their conversion into membrane channels remain elusive, and whether receptor molecules play a role in shaping the behavior of these toxins for translocation has not been addressed.

To begin to address these questions, we studied how BoNT/E senses low pH to transform into a hydrophobic protein. In contrast to BoNT/B, which has a slow onset (e.g. 27% of subjects exhibit symptoms in ≤ 1 day), BoNT/E causes human botulism rapidly, and has the shortest onset time (97% of subjects exhibit symptoms in ≤ 1 day) (Simpson, 1980; Simpson and Dasgupta, 1983; Woodruff et al., 1992). In the current study, we have compared these two serotypes with the goal of gaining novel insights into the means by which translocation is triggered. The ganglioside GT1b serves as a co-receptor (in conjunction with protein receptors) for both BoNT/B and E (Dong et al., 2008b; Kamata et al., 1986; Kozaki et al., 1998b; Nishiki et al., 1996b; Rummel et al., 2007b; Rummel et al., 2009). We found that while both toxins act as coincidence detectors for receptor (GT1b) and low pH, they also exhibit striking differences regarding how they respond to each of these signals. We speculate that these differences might underlie the distinct kinetics of translocation of these two toxin serotypes to affect the time course of intoxication.

3.3. RESULTS

3.3.1. Time Courses for Blocking the Action of BoNT/E and B in Neurons by Concanamycin A (Con A).

Translocation is a key step during BoNT intoxication (Montal, 2010), and the kinetics of this step can potentially impact the time course for the onset of botulism on host organisms. Current evidence indicates that BoNT/E translocates faster than BoNT/A in neurons (Keller et al., 2004; Wang et al., 2008), but we still lack a general understanding of the translocation rates for other BoNT serotypes. Specifically, BoNT/B is also a common cause of human botulism (Schiavo et al., 2000), and is used clinically (Montecucco and Molgo, 2005), but the time course for translocation of this serotype remains completely unknown.

To estimate the rate of BoNT/B translocation, we used con A, a specific inhibitor of vacuolar H^+-ATPase (Keller et al., 2004), in rat hippocampal neurons. BoNT LC translocation requires low endosomal pH (Montal, 2010; Schiavo et al., 2000); after toxins are internalized into SVs/endosomes via endocytosis, blockade of acidification at different time points by con A traps the remaining LCs within the SVs/endosomes, thereby preventing SNARE cleavage by LCs in the cytosol. Thus, assaying for SNARE cleavage under these conditions provides a straightforward way to estimate BoNT translocation rates (Keller et al., 2004; Wang et al., 2008). Experiments utilizing BoNT/E were performed as controls.

Without con A, treating neurons with 10 nM BoNT/E or B in high K^+ buffer (to stimulate SV recycling) for 5 min resulted in approximately 75-80% substrate cleavage during a subsequent 12 hr incubation. Substrate cleavage was monitored by immunoblot analysis using antibodies against SNAP-25 (cleaved by BoNT/E) or synaptobrevin II (syb, cleaved by BoNT/B)

(Figure 3-1). Cleavage was completely blocked when con A was added to cells 10 min before toxin treatment. When con A was applied 10 min after BoNT/E, ~50% cleavage of SNAP-25 was observed; BoNT/E became completely insensitive to con A when con A was added 1 hr after toxin internalization (Figure 3-1A and 3-1B). In accordance with previous studies, these data suggest that BoNT/E completes translocation within 1 hr after toxin internalization (Keller et al., 2004; Wang et al., 2008). In contrast, application of con A 1 hr after BoNT/B addition severely hindered BoNT/B translocation, as less than ~25% cleavage of syb was observed; and BoNT/B did not become completely insensitive to con A until con A was added more than 6 hr after toxin treatment (Figure 3-1C and 3-1D). These results are unlikely due to slow cell surface binding and internalization of BoNT/B into SV/endosomes; analogous to BoNT/E (Dong et al., 2008b; Keller et al., 2004), the majority of BoNT/B was already internalized into SVs/endosomes during the 5 min high K^+ stimulation, and remaining toxin molecules on cell surface after high K^+ treatment were removed by extensive washing (Dong et al., 2003; Dong et al., 2007). As con A only affects translocation, our data suggest that BoNT/B translocates much more slowly than BoNT/E.

3.3.2. Binding to GT1b Enables BoNT/E to Form Oligomers at Neutral pH.

We then investigated the prerequisite factors for BoNT/E and B translocation, which might underlie different translocation rates. As noted above, previous studies revealed that BoNT/B is a coincidence detector for low pH and the co-receptor GT1b; both are simultaneously required for BoNT/B to transform into an oligomeric membrane-bound channel-like structure (Sun et al., 2011). Moreover, low pH and GT1b also drive the oligomerization of BoNT/B, and this oligomerization step might contribute to efficient translocation, as suggested by studies of other bacterial toxins (Menestrina et al., 1994; Young and Collier, 2007). To address whether

BoNT/E also responds to low pH and GT1b by forming oligomers, we subjected this serotype to blue native-PAGE (BN-PAGE) under a variety of conditions. Oligomerization of BoNT/B was monitored as a control. Similar to BoNT/B, BoNT/E alone remained monomeric at pH 7.4 and 4.4 (Figure 3-2A and Figure 3-S1; note that the toxin did not stain well with silver staining at pH 4.4, but immunoblot analysis revealed that the toxin remained monomeric at this pH value). In the presence of GT1b, BoNT/B assembled into oligomers when the pH was < 5.4 (Figure 3-2B, see also (Sun et al., 2011)). Surprisingly, binding of GT1b enabled BoNT/E to efficiently form oligomers at all pH values examined, even at pH 8 (Figure 3-2A). These data indicate that while the oligomerization of BoNT/B can only occur in acidic SVs/endosomes after internalization, BoNT/E may already undergo oligomerization upon binding to GT1b on the cell surface, potentially contributing to fast translocation.

3.3.3. BoNT/E Changes Conformation and Becomes Hydrophobic in the Presence of GT1b at Low pH.

BoNTs have the remarkable ability to transform from soluble proteins into membrane-bound channels that mediate translocation (Montal, 2010; Sun et al., 2011). We reiterate that for BoNT/B, both oligomerization and transformation into a membrane protein require the presence of GT1b and low pH. However, this question has not been addressed for BoNT/E or any other serotype. We therefore carried out circular dichroism (CD) spectroscopy measurements, to probe structural changes in BoNT/E, at different pH values in the presence and absence of GT1b. Far-ultraviolet (UV) CD spectra were collected from 197 nm to 260 nm (Figure 3-3), and helical content was estimated based on molar ellipticity at 222 nm (Chen et al., 1972). BoNT/E alone at pH 7.4 had a helical content of ~27.5% (Figure 3-3A), consistent with a value of ~26% as

determined via crystallography (Kumaran et al., 2009). Lowering the pH from pH 7.4 to pH 5.4 did not significantly affect the shape of the spectra (Figure 3-3B and 3-3C), and the helical content of BoNT/E at pH 6.4 and pH 5.4 was ~27.3% and ~29.9% respectively. However, at pH 4.4, the peak of the BoNT/E spectrum was slightly shifted to the right (Figure 3-3D), but the helical content remained ~27.6%. When pH ≥ 5.4, addition of GT1b did not significantly change the spectra of BoNT/E (Figure 3-3A to 3-3C); the helical content was ~28.1% at pH 7.4, ~28.9% at pH 6.4, ~28.8% at pH 5.4, respectively. However, similar to BoNT/B (Sun et al., 2011), addition of GT1b to BoNT/E samples at pH 4.4 resulted in a major change in the shape of the spectrum (Figure 3-3D) that was associated with a reduction in helical content to ~11.7%.

To further test whether the observed structural changes in BoNT/E triggered by GT1b at low pH were associated with its conversion into a hydrophobic protein, we performed Triton X-114 partitioning assays. The detergent Triton X-114 remains homogenous in solution at low temperature, but partitions into aqueous and detergent phases at room temperature. This provides a convenient way to distinguish integral or lipid-anchored proteins (partitioning in the detergent phase) from soluble or peripheral proteins (partitioning in the aqueous phase) (Bordier, 1981; Sun et al., 2011). Parallel experiments using BoNT/B were included as controls (Figure 3-4A*, lower panel*, Figure 3-4B, see also (Sun et al., 2011)). Similar to BoNT/B, BoNT/E alone partitioned largely in the aqueous phase at both pH 7.4 and pH 4.4 (Figure 3-4A, *higher panel,* Figure 3-4B). Binding to GT1b at pH 7.4 did not cause a significant increase in the partitioning of BoNT/E into the detergent phase. However, upon lowering the pH to 4.4, in the presence of GT1b, ~80% of BoNT/E partitioned into the detergent phase. This was not due to tighter binding of BoNT/E at lower pH, since BoNT/E binds GT1b much less avidly at acid pH than neutral pH

(Kamata et al., 1988). Overall, the data reported in this section indicate that BoNT/E requires a similar change in pH as BoNT/B in order to undergo the GT1b-dependent conversion into a hydrophobic protein.

3.3.4. BoNT/E Enters an Off-Pathway at Low pH.

As shown in the above section, BoNT/E alone exhibited a slight right shift in its CD spectra when the pH was lowered from pH 7.4 to pH 4.4 (Figure 3-3D). This behavior is clearly different from BoNT/B, which is structurally stable from pH 7.4 to pH 4.4 (Eswaramoorthy et al., 2004; Sun et al., 2011). It appears that low pH may be able to alter the structure of isolated BoNT/E in solution to some degree, even in the absence of GT1b.

To assess the functional impact of the low-pH induced structural changes in BoNT/E, we carried out an "off-pathway" assay, again using cultured neurons as the target (Sun et al., 2011). This assay was devised to determine whether incubating the toxin, free in solution, at low pH, would result in premature conformational changes that result in unfolding and inactivation (i.e. entry into an "off-pathway"). Such pathways exist for some bacterial toxins, including anthrax toxin (Sun et al., 2007), but not for BoNT/B (Figure 3-5A, see also (Sun et al., 2011)). In sharp contrast to BoNT/B, preincubation of BoNT/E at pH 4.4 for 2 hr abolished its ability to enter neurons and cleave SNAP-25 (Figure 3-5A and 3-5B). We also reversed the preincubation pH back to 7.4 - after a 2 hr incubation at pH 4.4 - before applying toxins to neurons, and found that the cleavage of SNAP-25 was only partially recovered (~40%) (Figure 3-5C and 3-5D), so the off-pathway appears to be largely irreversible. These data indicate that unlike BoNT/B, low pH alone disrupts the structure of BoNT/E, leading it to enter an "off-pathway".

3.4. DISCUSSION

Many pathogenic bacteria produce protein toxins that alter the function of host cells. Among these toxins, BoNTs are the most deadly (Schiavo et al., 2000). BoNTs act by targeting presynaptic nerve terminals; however, the mechanism by which these agents translocate into the cytosol of host cells to exert their effects remains elusive (Montal, 2010). The current study is focused on the translocation of BoNT/E, the serotype with the fastest onset for causing human botulism (Simpson, 1980; Simpson and Dasgupta, 1983; Woodruff et al., 1992).

Recent studies have provided new insights into the factors the trigger translocation of BoNT/B, and revealed that this serotype requires both binding to the co-receptor molecule GT1b, and low pH, in order to transform into an oligomeric membrane protein (Sun et al., 2011). In the current study we found that oligomerization of BoNT/E is dependent only on GT1b, and does not require low pH. In addition, oligomerization of BoNT/E was not associated with significant secondary structural changes (Figure 3-3 and Figure 3-4) (Sun et al., 2011), and was not blocked by toosendanin (data not shown), a BoNT translocation inhibitor that hinders BoNT/B oligomerization (Sun et al., 2011). These findings indicate that while BoNT/B can only oligomerize after internalization and acidification of the organelle that mediated uptake, BoNT/E might undergo oligomerization on the cell surface, possibly contributing to its fast translocation. This is reminiscent of other bacterial toxins, such as anthrax toxin, whereby oligomerization occurs upon receptor binding on the cell surface, and the soluble oligomer is further converted into a membrane channel by low endosomal pH (Miller et al., 1999; Young and Collier, 2007).

Structural studies revealed that the domain arrangement of BoNT/E at neutral pH is different from BoNT/A and B (Fischer and Montal, 2007b; Kumaran et al., 2009; Lacy et al.,

1998b; Swaminathan and Eswaramoorthy, 2000). In BoNT/E, the receptor-binding domain is on the same side of the translocation domain of the HC as the LC, and all three domains have mutual interfaces. This is different from BoNT/A and B, in which the LC and receptor-binding domain are on opposite sides of the translocation domain. The unique domain arrangement within BoNT/E has been proposed to contribute to the rapid kinetics of translocation of this serotype (Kumaran et al., 2009). Thus, it will be interesting to determine whether the unique domain arrangement with BoNT/E underlies its ability to oligomerize in a pH-independent manner upon binding GT1b.

In addition, it has been hypothesized that BoNT/E might have a less stringent requirement in low pH, and that this might also contribute to fast translation (Wang et al., 2008). However, we found that BoNT/E has a similar pH-dependence for transforming into a hydrophobic protein, in the presence of GT1b, as BoNT/B, a serotype that translocates with relatively slow kinetics. Hence, the rapid translocation of the BoNT/E LC does not appear to be due to a greater sensitivity of this serotype to low pH.

For bacterial toxins that require low pH for translocation, such as diphtheria toxin (Blewitt et al., 1985), histidine residues within the translocation domain serves as pH sensors: protonation of histidines at low pH triggers conformational changes that result in channel formation (Kyrychenko et al., 2009; Perier et al., 2007; Rodnin et al., 2011). While histidines serve as common low pH sensors for a number of processes involving protein-membrane interactions (Kampmann et al., 2006; Mason et al., 2006; Perier et al., 2007) and/or molten globule formation (Jamin et al., 2000; Wei and Song, 2005), BoNT/E only has one histidine within the translocation domain, and there are no histidines in the translocation domain of

BoNT/B. These findings indicate that BoNTs either use different sensors within the translocation domain, or pH-sensing is mediated by other regions of these proteins. Moreover, recent studies revealed that deletion of the receptor-binding domain of BoNT/A alone (or together with the LC), disrupted low-pH sensing activity, that the mutant (composed of the translocation domain-LC or the translocation domain alone) was constitutively active for channel formation, even at neutral pH (Fischer et al., 2008b; Fischer et al., 2012). These findings, in conjunction with our observations that BoNT/B and E require binding to GT1b to transform into hydrophobic proteins at low pH, indicate that the receptor-binding domain somehow plays a crucial role in sensing low pH for translocation. In this regard, it is notable that histidines are enriched in the receptor binding domains of BoNT/E and B.

In summary, the current work suggests that BoNT/E, similar to BoNT/B, is a coincidence detector for the co-receptor GT1b and low pH for translocation, and that the receptor-binding domain within these toxins may play a crucial role in sensing the low pH for translocation. Nonetheless, BoNT/E exhibited some striking differences from BoNT/B: 1) it translocates much more rapidly that BoNT/B, 2) low pH alone disrupts the structure of BoNT/E to some degree and drives the toxin into an off pathway, 3) GT1b alone triggered BoNT/E oligomerization even at neutral pH. So, though these toxins operate in similar ways, comparison of two serotypes has revealed marked differences in their responses to the factors that trigger translocation, raising the possibility that these differences contribute to the distinct translocation rates of different serotypes.

3.5. EXPERIMENTAL PROCEDURES

Toxins and Antibodies - BoNT/E and B, rabbit polyclonal anti-BoNT/E and anti-BoNT/B antibodies were prepared as described previously (Dong et al., 2008a; Schmidt and Siegel, 1986; Sun et al., 2011). Monoclonal antibodies against SNAP-25 (71.1), syntaxin (HPC-1) and syb (69.1) were kindly provided by Dr. R. Jahn (Max Planck Institute for Biophysical Chemistry, Göttingen, Germany).

Con A Resistant Assay - All procedures involving animals were carried out according to US National Institutes of Health guidelines, as approved by the Animal Care and Use Committee of the University of Wisconsin, Madison. Cultures of rat embryonic (E17-18) hippocampal neurons were prepared as previously described (Sun et al., 2011). Experiments were performed on neurons that were 15-20 days old. Neurons were treated with BoNT/E or B (10 nM) in high-K^+ buffer (85 mM NaCl, 60 mM KCl, 2 mM $CaCl_2$, 2 mM $MgCl_2$, 5.5 mM glucose, 10 mM 4-(2-hydroxyethyl)-1-piperazineethanesulfonic acid (HEPES), 10 mM sodium 2-(N-morpholino)ethanesulfonate (NaMES), pH 7.4) for 5 min. Toxins were washed off using low-K^+ buffer (140 mM NaCl, 5 mM KCl, 2 mM $CaCl_2$, 2 mM $MgCl_2$, 5.5 mM glucose, 10 mM HEPES, 10 mM NaMES, pH 7.4). Where appropriate, con A (0.05 μM, Sigma-Aldrich) was added to the culture media before, with or after toxin exposure at indicated time. Neurons were incubated for 12 hr, and cells were lysed as described previously (Sun et al., 2011). Cleavage of SNAP-25 by BoNT/E, or syb by BoNT/B, was monitored via immunoblot analysis. Syntaxin served as an

internal loading control. Cleavage of SNAP-25 or syb was quantified using data obtained from at least eight independent trials.

BN-PAGE Assay - BN-PAGE assays were performed as previously described (Sun et al., 2011), using the NativePAGE Novex Bis-Tris gel system (Invitrogen). BoNT/E or B (100 nM) was incubated alone or with the ganglioside GT1b (10 μM) at indicated pH at 37 °C for 2 h. Samples were analyzed by BN-PAGE followed by either silver staining (Figure 3-2), or via immunoblot using anti-BoNT/E antibodies (Figure 3-S1).

CD Spectroscopy - CD experiments were performed using an Aviv Model 202SF spectrometer as described previously (Sun et al., 2011). Far-UV CD spectra (197 nm to 260 nm) of BoNT/E (0.67 μM) were obtained at the indicated pH at 37 °C using 1-mm path length quartz cuvettes. GT1b (30 μM) was then directly added to samples, and spectra were measured again. All spectra were corrected by subtracting spectra of buffer alone. Helical content was estimated based on molar ellipticity value at 222 nm as described previously (Sun et al., 2011).

Triton X-114 Partitioning Assay - Triton X-114 partitioning assays were performed as described previously (Bordier, 1981; Sun et al., 2011). BoNT/E or B (0.045 mg/ml, 300 nM) was incubated with or without GT1b (90 μM) at the indicated pH for 1 h at 37 °C before Triton X-114 partitioning assays were performed. The buffer composition was 10 mM HEPES, 10 mM NaMES, 10 mM sodium acetate and 150 mM NaCl, with pH adjusted to the desired values. Triton X-114 was added to samples to a final concentration of 1% (v/v), samples were vortexed

15 min at 4 °C and centrifuged at 3000 × g for 5 min to remove insoluble material. The supernatants were collected, incubated at 30 °C for 5 min, laid on top of a sucrose cushion (containing 6% (w/v) sucrose, 0.06% Triton X-114 in the above buffer, pH as indicated) and centrifuged at 830 × g for 3 min at room temperature. The detergent phase and aqueous phases were separated, and the aqueous phase was re-extracted with Triton X-114 as detailed above. The detergent phases were combined, and all samples were precipitated with 4 volumes of acetone overnight at -30 °C. The pellets were dissolved in SDS sample buffer and subjected to immunoblot analysis using anti-BoNT/E or anti-BoNT/B antibodies. The fraction of each protein in the detergent phase was quantified using data obtained from three independent trials.

Off-pathway Assay - Off-pathway assays were performed as descried previously (Sun et al., 2011). Briefly, BoNT/E (concentration as indicated) was incubated in high-K^+ buffer at pH 7.4 or pH 4.4 for 2 h at 37 °C. Where appropriate, the pH of samples containing BoNT/E at pH 4.4 was reversed to pH 7.4, and BoNT/E was incubated at 37 °C for the indicated time. Toxins were then incubated with cultured rat hippocampal neurons for 5 min. Neurons were washed and incubated in neuronal media at 37 °C for 20 h. Off-pathway assays of BoNT/B (10 nM) were also performed as controls. Cells were harvested, and cleavage of SNAP-25 by BoNT/E, or cleavage of syb by BoNT/B, was monitored via immunoblot analysis using anti-SNAP-25 or anti-syb antibodies. The cleavage of SNAP-25 was quantified using data obtained from at least three independent trials.

3.6. FIGURES AND LEGENDS

Figure 3-1

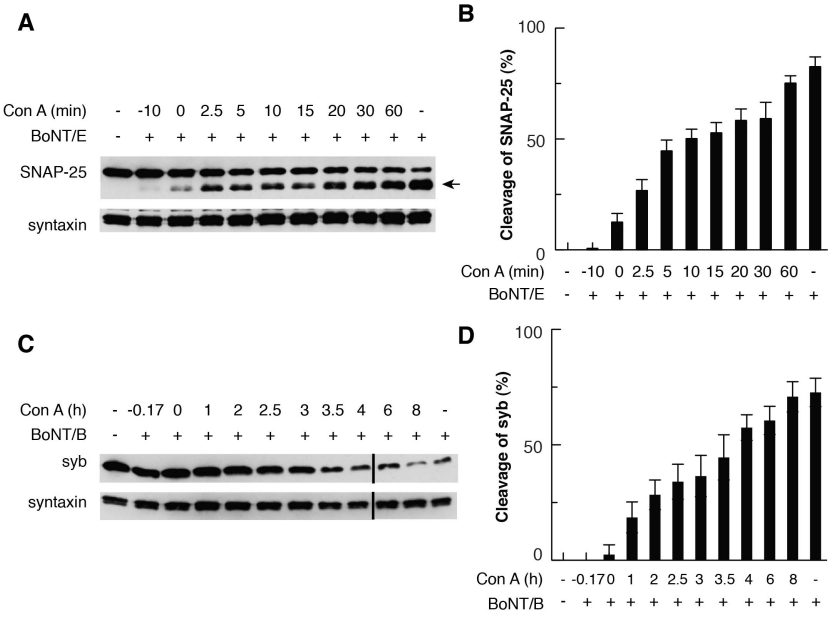

Figure 3-1. Time Courses For Blocking the Action of BoNT/E and B in Neurons by Con A.

(A-D) Immunoblot analysis of SNAP-25 cleavage by BoNT/E (A, quantified in B), or syb cleavage by BoNT/B (C, quantified in D) in cultured rat hippocampal neurons. Con A was added to neurons at the indicated time, either before, during, or after toxin exposure. SNARE cleavage was assayed 12 hr after toxin exposure. The arrow indicates the cleaved form of SNAP-25. Syntaxin served as an internal loading control. Data are means ± SEM (n = 8 in B, n = 9 in D).

Figure 3-2

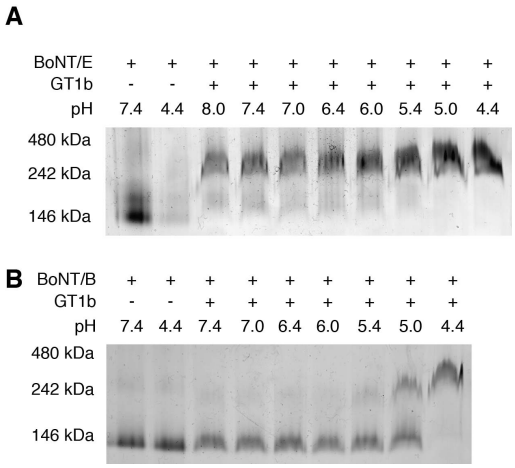
A
BoNT/E + + + + + + + + + +
GT1b - - + + + + + + + +
pH 7.4 4.4 8.0 7.4 7.0 6.4 6.0 5.4 5.0 4.4
480 kDa
242 kDa
146 kDa
B
BoNT/B + + + + + + + + +
GT1b - - + + + + + + +
pH 7.4 4.4 7.4 7.0 6.4 6.0 5.4 5.0 4.4
480 kDa
242 kDa
146 kDa

Figure 3-2. GT1b enables oligomerization of BoNT/E at neutral pH.

BN-PAGE analysis of BoNT/E (*top*) at the indicated pH in the absence and presence of GT1b. BN-PAGE analysis of BoNT/B (*bottom*) was included as a control. Representative gels, from three independent trials, are shown.

Figure 3-3

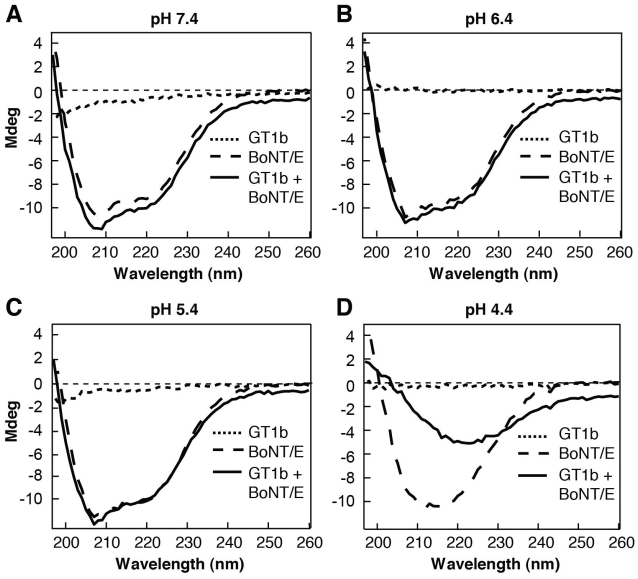
A
pH 7.4
B
pH 6.4
C
pH 5.4
D
pH 4.4
Mdeg
Wavelength (nm)
GT1b
BoNT/E
GT1b +
BoNT/E

Figure 3-3. GT1b triggers major conformational changes in BoNT/E at low pH.

(A-D) Far UV-CD spectra of BoNT/E in the absence (dashed lines) and presence (solid lines) of GT1b at pH 7.4 (A), 6.4 (B), 5.4 (C) and 4.4 (D). CD spectra of GT1b alone were included as controls (dotted lines).

Figure 3-4

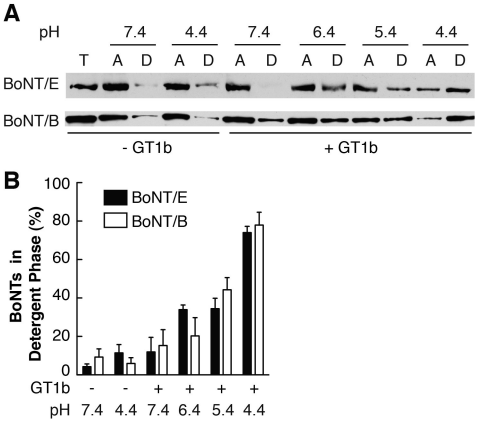
A
pH
7.4
4.4
7.4
6.4
5.4
4.4
T A D A D A D A D A D A D
BoNT/E
BoNT/B
- GT1b
+ GT1b
B
BoNTs in Detergent Phase (%)
100
80
60
40
20
0
BoNT/E
BoNT/B
GT1b - - + + + +
pH 7.4 4.4 7.4 6.4 5.4 4.4

Figure 3-4. BoNT/E becomes hydrophobic at low pH only in the presence of GT1b.

(A-B) Triton X-114 partitioning assays were carried out at the indicated pH in the absence or presence of GT1b, and BoNT/E in the total input (T), aqueous (A) and detergent (D) phase was detected by immunoblot analysis. Partitioning of BoNT/E was quantified and plotted (B). Triton X-114 partitioning assays using BoNT/B were performed as controls (Sun et al., 2011). Data are means ± SEM (n = 3).

Figure 3-5

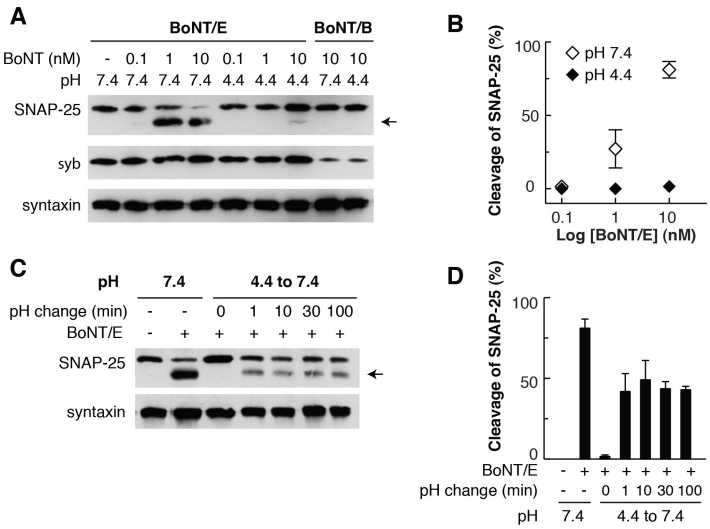
A
BoNT/E
BoNT/B
BoNT (nM) - 0.1 1 10 0.1 1 10 10 10
pH 7.4 7.4 7.4 7.4 4.4 4.4 4.4 7.4 4.4
SNAP-25
syb
syntaxin
B
Cleavage of SNAP-25 (%)
100
50
0
pH 7.4
pH 4.4
0.1
1
10
Log [BoNT/E] (nM)
C
pH
7.4
4.4 to 7.4
pH change (min) - - 0 1 10 30 100
BoNT/E - + + + + + +
SNAP-25
syntaxin
D
Cleavage of SNAP-25 (%)
100
50
0
BoNT/E - + + + + + +
pH change (min) - - 0 1 10 30 100
pH 7.4 4.4 to 7.4

Figure 3-5. Low pH pretreatment inactivates BoNT/E.

(A-B) BoNT/E was incubated at indicated pH for 2 hr at 37 °C, before being added to rat hippocampal neurons. Neurons were lysed after 20 hr, and cleavage of SNAP-25 by BoNT/E was monitored by immunoblot analysis (A, quantified in B). Cleavage of syb by BoNT/B, under the same conditions, was measured as a control. Syntaxin served as an internal loading control. (C-D) BoNT/E was incubated at pH 4.4 for 2 hr, before the pH of the samples was reversed back to pH 7.4 for the indicated period of time. BoNT/E was then incubated with neurons, and cleavage of SNAP-25 was monitored by immunoblot analysis (C, and quantified in D). The effect of BoNT/E, that had not been pretreated with low pH buffer, was analyzed as a control. Arrows indicate the cleaved form of SNAP-25. Data are means ± SEM from at least three independent trials.

Figure 3-S1

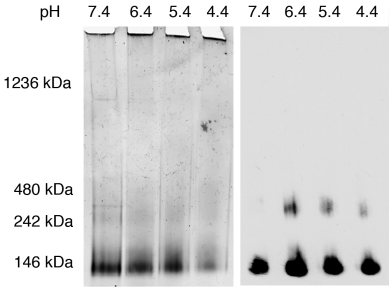

Figure 3-S1 BN-PAGE followed by silver staining (*left*) or immunoblot analysis (*right*) of BoNT/E at the indicated pH value.

3.7. APPENDEX

1) We thank A. Figueroa Bernier for helping to prepare rat hippocampal neurons. This work was supported by a grant from the NIH (AI057744) to E.R.C. E.R.C. is an Investigator of the Howard Hughes Medical Institute.

2) Work in this chapter is in submission for publication:

Botulinum Neurotoxins B and E Translocate at Different Rates and Exhibit Divergent Responses to GT1b and Low pH.

Sun S, Tepp WH, Johnson EA, Chapman ER. (2012).

Chapter 4

Conclusions and Future Perspectives

4.1. CONCLUSIONS

BoNTs are the most deadly substances known (Schiavo et al., 2000); they cause a fetal disease termed botulism in human and animals, and are listed as Category A bioterrorism agents by CDC (Arnon et al., 2001; Rotz et al., 2002). Ironically, BoNT/A and B, two of the BoNT serotypes that cause human botulism, are approved by FDA for treatment of human diseases and wrinkles (Jankovic, 2004b), sharing a multi-billion US dollar market globally. How BoNTs can be poisons that cure has puzzled scientists and physicians for centuries, and elucidation of how BoNTs intoxicate neurons, the sites of BoNT action, is key for resolving this puzzle. To date, receptors mediating entry of BoNTs have been largely resolved with the exception of BoNT/C and F (Peng et al., 2011), targets for all BoNTs in neurons are identified as SNARE proteins (Schiavo et al., 2000) (Table 1-1), however, how BoNTs translocate from neuronal endosomes into the cytosol, one critical step during their actions in neurons, is still the least understood process and remains largely unknown.

This thesis is dedicated to challenge this question, one of the biggest puzzles in the field of BoNT studies, and uncovered a novel mechanism of BoNT translocation (Lencer and Tweten, 2011). We used two serotypes of BoNTs in the current studies, BoNT/B (as shown in Chapter 2) and BoNT/E (as shown in Chapter 3), which have the slowest and fastest onset of human botulism, respectively (Woodruff et al., 1992), and examined the mechanisms underlying their translocations. The main conclusions of the thesis are summarized as below.

We found that both BoNT/B and BoNT/E are coincidence detectors for translocation. Besides the well-known requirements of low pH, as indicated by numerous previous studies (Montal, 2010), these toxins may also require binding of their coreceptor molecule, the

ganglioside GT1b, for translocation. We demonstrated that presence of GT1b facilitates cell surface translocation of BoNT/B, and binding to GT1b enables soluble BoNTs to sense low pH to conduct significant structure rearrangements to form membrane channels. These observations also help to resolve the puzzle that despite of the general belief that structure rearrangements in BoNTs at low pH are required to transform these deadly toxins into membrane channels, the crystal structures of BoNT/B at neutral and low pH remain the same, arguing against existence of putative structure changes at low pH (Eswaramoorthy et al., 2004). Our studies suggested a novel role of the receptor molecule, the function of which was largely explored as mediating the binding and entry of BoNTs as shown in previous studies (Schiavo et al., 2000), in the translocation process. BoNTs have a long journey in host bodies, and potentially the toxins may get exposed to low pH environments (such as acidic stomachs in hosts), before reaching its action site, the presynaptic nerve terminals. How BoNTs know when to translocate is a puzzle, and studies in the thesis lead to the model that binding to coreceptor GT1b and low pH ensures the translocation happens at the right time and place.

In the current studies, we also revealed the first glimpse into the molecular architecture of the potential BoNT translocation machineries in its membrane-bound state in solution at low pH. Although crystal structures of several BoNTs in their soluble states are characterized (Swaminathan, 2011), little is known regarding the structures of the translocation-competent states of the toxins. We utilized AFM, which provides single particle resolution of BoNTs at near-physiological conditions (i.e. under fluid) (Saslowsky et al., 2002; Suresh and Edwardson, 2010), and found that BoNT/B formed channel-like structures on GT1b-containing membranes at low pH upon removal of LCs. Remarkably, some of the toxins assembled into double- and triple-

donuts structures, and these oligomeric channels resemble several translocation machineries, such as the mitochondria TIM (Rehling et al., 2003) and TOM complexes (Ahting et al., 1999; Kunkele et al., 1998; Model et al., 2008), endoplasmic reticulum protein Sec61p (Becker et al., 2009; Beckmann et al., 2001), and PhoE porin (Jap et al., 1991).

TSN, the BoNT translocation inhibitor (Fischer et al., 2009; Li and Shi, 2006), hindered oligomerization of BoNT/B in solution, as well as prevented BoNT/B to form large conductance channels.

We also found that BoNT/B and BoNT/E exhibited different features regarding translocation. We revealed that translocation of BoNT/E is much faster than BoNT/B in neurons. Distinct from BoNT/B, oligomerization of BoNT/E in only dependent on GT1b, not low pH; but both toxins require the same low pH to transform into membrane protein. These data indicate that fast translocation of BoNT/E is not likely attributed to BoNT/E requiring less stringent pH to translocate, as previously hypothesized (Wang et al., 2008); alternatively, oligomerization at neutral pH may facilitate fast BoNT/E translocation. For bacterial toxins such as anthrax toxin (Miller et al., 1999; Young and Collier, 2007), binding to receptors on the cell surface allows them to assemble into oligomeric prepores, and low endosomal pH further triggers conformational changes in prepores to convert them into hydrophobic membrane channels (pores). Our data suggest that BoNT/E may follow a similar pathway, but future study is needed to further confirm this hypothesis.

In summary, data presented in this thesis gain us insights into mechanisms underlying BoNT translocation, the most mysterious process during action of these deadly toxins in neurons. We found that BoNT/B and E are coincidence detectors for translocation, that binding to the

coreceptor GT1b enables the toxins to sense low pH to transform into oligomeric membrane channels, a novel role of receptors in BoNT translocation. We also revealed the first glimpse of BoNT/B regarding its membrane channel state for translocation. The molecular architecture of BoNTs at this crucial state remained completely unknown previously, and we found that BoNT/B form oligomeric membrane channels on the GT1b-contaning membrane at low pH that resembled other translocation machineries. BoNT/E exhibited some unique features from BoNT/B regarding translocation, and these features potentially contribute its fast translocation.

4.2. FUTURE PESPECTIVES

The studies in this thesis indicate that receptor binding may be crucial for translocation of BoNTs, and an interesting question is: what if receptor-binding domain (RBD) of BoNTs are removed? In the case of BoNT/A, removal of RBD resulted in formation of large conductance channels even at neutral pH (Fischer et al., 2008b); in conjunction of data in this thesis, a novel model emerges: RBD play an inhibitory role of BoNTs translocation, such inhibition can be removed by deletion of RBD or by binding to GT1b at low pH, thus ensuring the temporal and spatial accuracy of BoNT translocation. Future studies, using RBD-devoid BoNT mutants in assays as carried out in this thesis, will give this model a further validation.

All BoNTs need two receptors for entry, gangliosides and protein receptors. As studies in this thesis indicate a role for gangliosides in the translocation of BoNT/B and E, another question is whether protein receptors play any role in translocation. Previous studies indicate that BoNT/B may remain bound to syt II, its protein receptor, at low pH (Jin et al., 2006), suggesting a possibility of such roles; we attempted to address this question using P21, a syt II peptide

containing BoNT/B binding sites (Dong et al., 2008b), and did not observe any effects. However, weak binding of P21 to BoNT/B may explain lack of effects in above assays, and roles of protein receptors in translocation need to be elucidated in future studies.

Our studies revealed that BoNT/B and E oligomerize in the presence of GT1b, and such oligomeric channels reassembled other protein translocation machineries. However, it should be noted that whether such oligomeric channels represent the minimal translocation machinery still need further validation. As oligomerization of BoNT/E was only GT1b-, not low pH- dependent, it is also essential to test whether the unique domain arrangement in BoNT/E (Fischer et al., 2008a) facilitates this process for its fast translocation.

Our studies revealed the first glimpse into the most mysterious state of BoNTs: the membrane-bound state at low pH that mediate BoNT translocation. The structures that we obtained likely represent the beginning and the end states of translocation process; future studies that image the toxins during translocation will further advance our knowledge of these deadly toxins.

References

Ahsan, C.R., Hajnoczky, G., Maksymowych, A.B., and Simpson, L.L. (2005). Visualization of binding and transcytosis of botulinum toxin by human intestinal epithelial cells. The Journal of pharmacology and experimental therapeutics *315*, 1028-1035.

Ahting, U., Thun, C., Hegerl, R., Typke, D., Nargang, F.E., Neupert, W., and Nussberger, S. (1999). The TOM core complex: the general protein import pore of the outer membrane of mitochondria. J Cell Biol *147*, 959-968.

Ando, S. (1983). Gangliosides in the nervous system. Neurochem Int *5*, 507-537.

Aquino, D.A., Bisby, M.A., and Ledeen, R.W. (1985). Retrograde axonal transport of gangliosides and glycoproteins in the motoneurons of rat sciatic nerve. Journal of neurochemistry *45*, 1262-1267.

Arnon, S.S. (1997). Human Tetanus and Human Botulism. In The Clostridia: Molecular Biology and Pathogenesis, J.I. Rood, McClane, B. A., Songer, J. G., Titball, R. W., ed. (Academic Press), pp. 96-115.

Arnon, S.S., Schechter, R., Inglesby, T.V., Henderson, D.A., Bartlett, J.G., Ascher, M.S., Eitzen, E., Fine, A.D., Hauer, J., Layton, M.*, et al.* (2001). Botulinum toxin as a biological weapon: medical and public health management. JAMA *285*, 1059-1070.

Aureli, P., Fenicia, L., Pasolini, B., Gianfranceschi, M., McCroskey, L.M., and Hatheway, C.L. (1986). Two cases of type E infant botulism caused by neurotoxigenic Clostridium butyricum in Italy. The Journal of infectious diseases *154*, 207-211.

Bai, J., Earles, C.A., Lewis, J.L., and Chapman, E.R. (2000). Membrane-embedded synaptotagmin penetrates cis or trans target membranes and clusters via a novel mechanism. J Biol Chem *275*, 25427-25435.

Becker, T., Bhushan, S., Jarasch, A., Armache, J.P., Funes, S., Jossinet, F., Gumbart, J., Mielke, T., Berninghausen, O., Schulten, K.*, et al.* (2009). Structure of monomeric yeast and mammalian Sec61 complexes interacting with the translating ribosome. Science *326*, 1369-1373.

Beckmann, R., Spahn, C.M., Eswar, N., Helmers, J., Penczek, P.A., Sali, A., Frank, J., and Blobel, G. (2001). Architecture of the protein-conducting channel associated with the translating 80S ribosome. Cell *107*, 361-372.

Bhalla, A., Chicka, M.C., Tucker, W.C., and Chapman, E.R. (2006). Ca(2+)-synaptotagmin directly regulates t-SNARE function during reconstituted membrane fusion. Nat Struct Mol Biol *13*, 323-330.

Bigalke, H., Muller, H., and Dreyer, F. (1986). Botulinum A neurotoxin unlike tetanus toxin acts via a neuraminidase sensitive structure. Toxicon : official journal of the International Society on Toxinology *24*, 1065-1074.

Binz, T., Blasi, J., Yamasaki, S., Baumeister, A., Link, E., Sudhof, T.C., Jahn, R., and Niemann, H. (1994). Proteolysis of SNAP-25 by types E and A botulinal neurotoxins. The Journal of biological chemistry *269*, 1617-1620.

Binz, T., and Rummel, A. (2009a). Cell entry strategy of clostridial neurotoxins. Journal of neurochemistry *109*, 1584-1595.

Binz, T., and Rummel, A. (2009b). Cell entry strategy of clostridial neurotoxins. J Neurochem *109*, 1584-1595.

Black, J.D., and Dolly, J.O. (1986a). Interaction of 125I-labeled botulinum neurotoxins with nerve terminals. I. Ultrastructural autoradiographic localization and quantitation of distinct membrane acceptors for types A and B on motor nerves. The Journal of cell biology *103*, 521-534.

Black, J.D., and Dolly, J.O. (1986b). Interaction of 125I-labeled botulinum neurotoxins with nerve terminals. II. Autoradiographic evidence for its uptake into motor nerves by acceptor-mediated endocytosis. The Journal of cell biology *103*, 535-544.

Blasi, J., Chapman, E.R., Link, E., Binz, T., Yamasaki, S., De Camilli, P., Sudhof, T.C., Niemann, H., and Jahn, R. (1993a). Botulinum neurotoxin A selectively cleaves the synaptic protein SNAP-25. Nature *365*, 160-163.

Blasi, J., Chapman, E.R., Yamasaki, S., Binz, T., Niemann, H., and Jahn, R. (1993b). Botulinum neurotoxin C1 blocks neurotransmitter release by means of cleaving HPC-1/syntaxin. The EMBO journal *12*, 4821-4828.

Blasi, J., Egea, G., Castiella, M.J., Arribas, M., Solsona, C., Richardson, P.J., and Marsal, J. (1992). Binding of botulinum neurotoxin to pure cholinergic nerve terminals isolated from the electric organ of Torpedo. J Neural Transm Gen Sect *90*, 87-102.

Blewitt, M.G., Chung, L.A., and London, E. (1985). Effect of pH on the conformation of diphtheria toxin and its implications for membrane penetration. Biochemistry *24*, 5458-5464.

Bordier, C. (1981). Phase separation of integral membrane proteins in Triton X-114 solution. J Biol Chem *256*, 1604-1607.

Brunger, A.T., Breidenbach, M.A., Jin, R., Fischer, A., Santos, J.S., and Montal, M. (2007). Botulinum neurotoxin heavy chain belt as an intramolecular chaperone for the light chain. PLoS Pathog *3*, 1191-1194.

Ceccarelli, B., Hurlbut, W.P., and Mauro, A. (1973). Turnover of transmitter and synaptic vesicles at the frog neuromuscular junction. The Journal of cell biology *57*, 499-524.

Chai, Q., Arndt, J.W., Dong, M., Tepp, W.H., Johnson, E.A., Chapman, E.R., and Stevens, R.C. (2006). Structural basis of cell surface receptor recognition by botulinum neurotoxin B. Nature *444*, 1096-1100.

Chapman, E.R. (2002). Synaptotagmin: a Ca(2+) sensor that triggers exocytosis? Nat Rev Mol Cell Biol *3*, 498-508.

Chapman, E.R. (2008). How does synaptotagmin trigger neurotransmitter release? Annual review of biochemistry *77*, 615-641.

Chen, Y.H., Yang, J.T., and Martinez, H.M. (1972). Determination of the secondary structures of proteins by circular dichroism and optical rotatory dispersion. Biochemistry *11*, 4120-4131.

Cheng, Y., Sequeira, S.M., Malinina, L., Tereshko, V., Sollner, T.H., and Patel, D.J. (2004). Crystallographic identification of Ca2+ and Sr2+ coordination sites in synaptotagmin I C2B domain. Protein science : a publication of the Protein Society *13*, 2665-2672.

Cote, M., Zheng, Y.M., and Liu, S.L. (2009). Receptor binding and low pH coactivate oncogenic retrovirus envelope-mediated fusion. Journal of virology *83*, 11447-11455.

de Chaves, E.I., Bussiere, M., Vance, D.E., Campenot, R.B., and Vance, J.E. (1997). Elevation of ceramide within distal neurites inhibits neurite growth in cultured rat sympathetic neurons. The Journal of biological chemistry *272*, 3028-3035.

de Paiva, A., Poulain, B., Lawrence, G.W., Shone, C.C., Tauc, L., and Dolly, J.O. (1993). A role for the interchain disulfide or its participating thiols in the internalization of botulinum neurotoxin A revealed by a toxin derivative that binds to ecto-acceptors and inhibits transmitter release intracellularly. The Journal of biological chemistry *268*, 20838-20844.

Dong, M., Liu, H., Tepp, W.H., Johnson, E.A., Janz, R., and Chapman, E.R. (2008a). Glycosylated SV2A and SV2B mediate the entry of botulinum neurotoxin E into neurons. Molecular biology of the cell *19*, 5226-5237.

Dong, M., Liu, H., Tepp, W.H., Johnson, E.A., Janz, R., and Chapman, E.R. (2008b). Glycosylated SV2A and SV2B mediate the entry of botulinum neurotoxin E into neurons. Mol Biol Cell *19*, 5226-5237.

Dong, M., Richards, D.A., Goodnough, M.C., Tepp, W.H., Johnson, E.A., and Chapman, E.R. (2003). Synaptotagmins I and II mediate entry of botulinum neurotoxin B into cells. J Cell Biol *162*, 1293-1303.

Dong, M., Tepp, W.H., Liu, H., Johnson, E.A., and Chapman, E.R. (2007). Mechanism of botulinum neurotoxin B and G entry into hippocampal neurons. J Cell Biol *179*, 1511-1522.

Dong, M., Yeh, F., Tepp, W.H., Dean, C., Johnson, E.A., Janz, R., and Chapman, E.R. (2006). SV2 is the protein receptor for botulinum neurotoxin A. Science *312*, 592-596.

Donovan, J.J., and Middlebrook, J.L. (1986). Ion-conducting channels produced by botulinum toxin in planar lipid membranes. Biochemistry *25*, 2872-2876.

Erbguth, F.J. (2004). Historical notes on botulism, Clostridium botulinum, botulinum toxin, and the idea of the therapeutic use of the toxin. Movement disorders : official journal of the Movement Disorder Society *19 Suppl 8*, S2-6.

Eswaramoorthy, S., Kumaran, D., Keller, J., and Swaminathan, S. (2004). Role of metals in the biological activity of Clostridium botulinum neurotoxins. Biochemistry *43*, 2209-2216.

Evans, D.M., Williams, R.S., Shone, C.C., Hambleton, P., Melling, J., and Dolly, J.O. (1986). Botulinum neurotoxin type B. Its purification, radioiodination and interaction with rat-brain synaptosomal membranes. Eur J Biochem *154*, 409-416.

Fischer, A., Garcia-Rodriguez, C., Geren, I., Lou, J., Marks, J.D., Nakagawa, T., and Montal, M. (2008a). Molecular architecture of botulinum neurotoxin E revealed by single particle electron microscopy. J Biol Chem *283*, 3997-4003.

Fischer, A., and Montal, M. (2006). Characterization of Clostridial botulinum neurotoxin channels in neuroblastoma cells. Neurotox Res *9*, 93-100.

Fischer, A., and Montal, M. (2007a). Crucial role of the disulfide bridge between botulinum neurotoxin light and heavy chains in protease translocation across membranes. J Biol Chem *282*, 29604-29611.

Fischer, A., and Montal, M. (2007b). Single molecule detection of intermediates during botulinum neurotoxin translocation across membranes. Proc Natl Acad Sci U S A *104*, 10447-10452.

Fischer, A., Mushrush, D.J., Lacy, D.B., and Montal, M. (2008b). Botulinum neurotoxin devoid of receptor binding domain translocates active protease. PLoS Pathog *4*, e1000245.

Fischer, A., Nakai, Y., Eubanks, L.M., Clancy, C.M., Tepp, W.H., Pellett, S., Dickerson, T.J., Johnson, E.A., Janda, K.D., and Montal, M. (2009). Bimodal modulation of the botulinum neurotoxin protein-conducting channel. Proc Natl Acad Sci U S A *106*, 1330-1335.

Fischer, A., Sambashivan, S., Brunger, A.T., and Montal, M. (2012). Beltless translocation domain of botulinum neurotoxin A embodies a minimum ion-conductive channel. The Journal of biological chemistry *287*, 1657-1661.

Foran, P., Lawrence, G.W., Shone, C.C., Foster, K.A., and Dolly, J.O. (1996). Botulinum neurotoxin C1 cleaves both syntaxin and SNAP-25 in intact and permeabilized chromaffin cells: correlation with its blockade of catecholamine release. Biochemistry *35*, 2630-2636.

Frischknecht, F. (2003). The history of biological warfare. Human experimentation, modern nightmares and lone madmen in the twentieth century. EMBO Rep *4 Spec No*, S47-52.

Fujiki, Y., Hubbard, A.L., Fowler, S., and Lazarow, P.B. (1982). Isolation of intracellular membranes by means of sodium carbonate treatment: application to endoplasmic reticulum. J Cell Biol *93*, 97-102.

Gasnier, B. (2000). The loading of neurotransmitters into synaptic vesicles. Biochimie *82*, 327-337.

Gill, D.M. (1982). Bacterial toxins: a table of lethal amounts. Microbiol Rev *46*, 86-94.

Gillard, B.K., Thurmon, L.T., and Marcus, D.M. (1993). Variable subcellular localization of glycosphingolipids. Glycobiology *3*, 57-67.

Global Industry Analyst, I. (2012). Botulinum Toxin - A Global Strategic Business Report (Global Industry Analyst, Inc.), pp. 225.

Gupta, P., Singh, S., Tiwari, A., Bhat, R., and Bhatnagar, R. (2001). Effect of pH on stability of anthrax lethal factor: correlation between denaturation and activity. Biochem Biophys Res Commun *284*, 568-573.

Habermann, B., and Dreyer, F. (1986). Clostridial neurotoxins: handling and action at the cellular and molecular level. Curr Top Microbiol Immunol *129*, 93-179.

Hall, J.D., McCroskey, L.M., Pincomb, B.J., and Hatheway, C.L. (1985). Isolation of an organism resembling Clostridium barati which produces type F botulinal toxin from an infant with botulism. Journal of clinical microbiology *21*, 654-655.

Hatheway, C.L. (1989). Bacterial Sources of Clostridial Neurotoxins. In Botulinum Neurotoxin and Tetanus Toxin, L.L. Simpson, ed. (San Diago, New York, Berkely, Boston, London, Sydney, Tokyo, Toronto, Academic Press, INC.), pp. 3-24.

Hatheway, C.L. (1990). Toxigenic clostridia. Clin Microbiol Rev *3*, 66-98.

Heuser, J.E., and Reese, T.S. (1981). Structural changes after transmitter release at the frog neuromuscular junction. J Cell Biol *88*, 564-580.

Hill, K.K., Smith, T.J., Helma, C.H., Ticknor, L.O., Foley, B.T., Svensson, R.T., Brown, J.L., Johnson, E.A., Smith, L.A., Okinaka, R.T.*, et al.* (2007). Genetic diversity among Botulinum Neurotoxin-producing clostridial strains. Journal of bacteriology *189*, 818-832.

Hines, H.B., Lebeda, F., Hale, M., and Brueggemann, E.E. (2005). Characterization of botulinum progenitor toxins by mass spectrometry. Applied and environmental microbiology *71*, 4478-4486.

Hoch, D.H. (1985). Botulinum, tetanus, and diphtheria toxin channels in planar lipid bilayers. Doctoral Dissertation (Albert Einstein College of Medicine).

Hoch, D.H., Romero-Mira, M., Ehrlich, B.E., Finkelstein, A., DasGupta, B.R., and Simpson, L.L. (1985). Channels formed by botulinum, tetanus, and diphtheria toxins in planar lipid bilayers: relevance to translocation of proteins across membranes. Proc Natl Acad Sci U S A *82*, 1692-1696.

Hughes, R., and Whaler, B.C. (1962). Influence of nerve-ending activity and of drugs on the rate of paralysis of rat diaphragm preparations by Cl. botulinum type A toxin. J Physiol *160*, 221-233.

Inui, K., Ito, H., Miyata, K., Matsuo, T., Horiuchi, R., Ikeda, T., Watanabe, T., Ohyama, T., and Niwa, K. (2010). Involvement of sialic acid in transport of serotype C1 botulinum toxins through rat intestinal epithelial cells. The Journal of veterinary medical science / the Japanese Society of Veterinary Science *72*, 1251-1255.

Jamin, M., Antalik, M., Loh, S.N., Bolen, D.W., and Baldwin, R.L. (2000). The unfolding enthalpy of the pH 4 molten globule of apomyoglobin measured by isothermal titration calorimetry. Protein science : a publication of the Protein Society *9*, 1340-1346.

Jankovic, J. (2004a). Botulinum toxin in clinical practice. Journal of neurology, neurosurgery, and psychiatry *75*, 951-957.

Jankovic, J. (2004b). Botulinum toxin in clinical practice. J Neurol Neurosurg Psychiatry *75*, 951-957.

Jap, B.K., Walian, P.J., and Gehring, K. (1991). Structural architecture of an outer membrane channel as determined by electron crystallography. Nature *350*, 167-170.

Jin, R., Rummel, A., Binz, T., and Brunger, A.T. (2006). Botulinum neurotoxin B recognizes its protein receptor with high affinity and specificity. Nature *444*, 1092-1095.

Johnson, E.A. (2000). Neurotoxigenic Clostridia. In Gram-positive pathogens, V.A. Fischetti, Novick, R. P., Ferretti, J. J., Portnoy, D. A., Rood, J. I., ed. (Washington, DC, American Society of Microbiology), pp. 540-562.

Kamata, Y., Kozaki, S., and Sakaguchi, G. (1988). Effects of pH on the binding of Clostridium botulinum type E derivative toxin to gangliosides and phospholipids FEMS Microbiol Lett *55*, 71-76.

Kamata, Y., Kozaki, S., Sakaguchi, G., Iwamori, M., and Nagai, Y. (1986). Evidence for direct binding of Clostridium botulinum type E derivative toxin and its fragments to gangliosides and free fatty acids. Biochemical and biophysical research communications *140*, 1015-1019.

Kampmann, T., Mueller, D.S., Mark, A.E., Young, P.R., and Kobe, B. (2006). The Role of histidine residues in low-pH-mediated viral membrane fusion. Structure *14*, 1481-1487.

Keller, J.E., Cai, F., and Neale, E.A. (2004). Uptake of botulinum neurotoxin into cultured neurons. Biochemistry *43*, 526-532.

Kerner, J. (1817). Vergiftung durch verdorbene Wu¨rste. Tu¨binger Bla¨tter fu¨r Naturwissenschaften und Arzneykunde *3*, 1-25

.

Kintzer, A.F., Sterling, H.J., Tang, II, Abdul-Gader, A., Miles, A.J., Wallace, B.A., Williams, E.R., and Krantz, B.A. (2010). Role of the protective antigen octamer in the molecular mechanism of anthrax lethal toxin stabilization in plasma. J Mol Biol *399*, 741-758.

Kitamura, M., Iwamori, M., and Nagai, Y. (1980). Interaction between Clostridium botulinum neurotoxin and gangliosides. Biochimica et biophysica acta *628*, 328-335.

Kitamura, M., Takamiya, K., Aizawa, S., and Furukawa, K. (1999). Gangliosides are the binding substances in neural cells for tetanus and botulinum toxins in mice. Biochimica et biophysica acta *1441*, 1-3.

Koh, T.W., and Bellen, H.J. (2003). Synaptotagmin I, a Ca2+ sensor for neurotransmitter release. Trends Neurosci *26*, 413-422.

Koriazova, L.K., and Montal, M. (2003). Translocation of botulinum neurotoxin light chain protease through the heavy chain channel. Nat Struct Biol *10*, 13-18.

Kozaki, S., Kamata, Y., Watarai, S., Nishiki, T., and Mochida, S. (1998a). Ganglioside GT1b as a complementary receptor component for Clostridium botulinum neurotoxins. Microbial pathogenesis *25*, 91-99.

Kozaki, S., Kamata, Y., Watarai, S., Nishiki, T., and Mochida, S. (1998b). Ganglioside GT1b as a complementary receptor component for Clostridium botulinum neurotoxins. Microb Pathog *25*, 91-99.

Kumaran, D., Eswaramoorthy, S., Furey, W., Navaza, J., Sax, M., and Swaminathan, S. (2009). Domain organization in Clostridium botulinum neurotoxin type E is unique: its implication in faster translocation. Journal of molecular biology *386*, 233-245.

Kunkele, K.P., Heins, S., Dembowski, M., Nargang, F.E., Benz, R., Thieffry, M., Walz, J., Lill, R., Nussberger, S., and Neupert, W. (1998). The preprotein translocation channel of the outer membrane of mitochondria. Cell *93*, 1009-1019.

Kurokawa, Y. (1987). [Binding and degenerative effect of Clostridium botulinum type A, C and E toxins on cultured neurons]. Hokkaido Igaku Zasshi *62*, 381-391.

Kurokawa, Y., Oguma, K., Yokosawa, N., Syuto, B., Fukatsu, R., and Yamashita, I. (1987). Binding and cytotoxic effects of Clostridium botulinum type A, C1 and E toxins in primary neuron cultures from foetal mouse brains. J Gen Microbiol *133*, 2647-2657.

Kyrychenko, A., Posokhov, Y.O., Rodnin, M.V., and Ladokhin, A.S. (2009). Kinetic intermediate reveals staggered pH-dependent transitions along the membrane insertion pathway of the diphtheria toxin T-domain. Biochemistry *48*, 7584-7594.

Lacy, D.B., Tepp, W., Cohen, A.C., DasGupta, B.R., and Stevens, R.C. (1998a). Crystal structure of botulinum neurotoxin type A and implications for toxicity. Nature structural biology *5*, 898-902.

Lacy, D.B., Tepp, W., Cohen, A.C., DasGupta, B.R., and Stevens, R.C. (1998b). Crystal structure of botulinum neurotoxin type A and implications for toxicity. Nat Struct Biol *5*, 898-902.

Ladokhin, A.S., Legmann, R., Collier, R.J., and White, S.H. (2004). Reversible refolding of the diphtheria toxin T-domain on lipid membranes. Biochemistry *43*, 7451-7458.

Lalli, G., Herreros, J., Osborne, S.L., Montecucco, C., Rossetto, O., and Schiavo, G. (1999). Functional characterisation of tetanus and botulinum neurotoxins binding domains. Journal of cell science *112 (Pt 16)*, 2715-2724.

Ledeen, R.W. (1985). Gangliosides of the neuron. Trends Neurosci *8*, 169-174.

Ledeen, R.W., Parsons, S.M., Diebler, M.F., Sbaschnig-Agler, M., and Lazereg, S. (1988). Ganglioside composition of synaptic vesicles from Torpedo electric organ. Journal of neurochemistry *51*, 1465-1469.

Lencer, W.I., and Tweten, R.K. (2011). To translocate or not: that is the problem. Cell Host Microbe *10*, 179-180.

Li, F., Pincet, F., Perez, E., Eng, W.S., Melia, T.J., Rothman, J.E., and Tareste, D. (2007). Energetics and dynamics of SNAREpin folding across lipid bilayers. Nature structural & molecular biology *14*, 890-896.

Li, M.F., and Shi, Y.L. (2006). Toosendanin interferes with pore formation of botulinum toxin type A in PC12 cell membrane. Acta Pharmacol Sin *27*, 66-70.

Liu, Y., Wada, R., Kawai, H., Sango, K., Deng, C., Tai, T., McDonald, M.P., Araujo, K., Crawley, J.N., Bierfreund, U.*, et al.* (1999). A genetic model of substrate deprivation therapy for a glycosphingolipid storage disorder. J Clin Invest *103*, 497-505.

Mahrhold, S., Rummel, A., Bigalke, H., Davletov, B., and Binz, T. (2006). The synaptic vesicle protein 2C mediates the uptake of botulinum neurotoxin A into phrenic nerves. FEBS letters *580*, 2011-2014.

Maksymowych, A.B., and Simpson, L.L. (1998). Binding and transcytosis of botulinum neurotoxin by polarized human colon carcinoma cells. The Journal of biological chemistry *273*, 21950-21957.

Marxen, P., Fuhrmann, U., and Bigalke, H. (1989). Gangliosides mediate inhibitory effects of tetanus and botulinum A neurotoxins on exocytosis in chromaffin cells. Toxicon : official journal of the International Society on Toxinology *27*, 849-859.

Mason, A.J., Gasnier, C., Kichler, A., Prevost, G., Aunis, D., Metz-Boutigue, M.H., and Bechinger, B. (2006). Enhanced membrane disruption and antibiotic action against pathogenic bacteria by designed histidine-rich peptides at acidic pH. Antimicrobial agents and chemotherapy *50*, 3305-3311.

Matsumura, T., Jin, Y., Kabumoto, Y., Takegahara, Y., Oguma, K., Lencer, W.I., and Fujinaga, Y. (2008). The HA proteins of botulinum toxin disrupt intestinal epithelial intercellular junctions to increase toxin absorption. Cell Microbiol *10*, 355-364.

May, A.J., and Whaler, B.C. (1958). The absorption of Clostridium botulinum type A toxin from the alimentary canal. British journal of experimental pathology *39*, 307-316.

McCroskey, L.M., and Hatheway, C.L. (1988). Laboratory findings in four cases of adult botulism suggest colonization of the intestinal tract. Journal of clinical microbiology *26*, 1052-1054.

McCroskey, L.M., Hatheway, C.L., Fenicia, L., Pasolini, B., and Aureli, P. (1986). Characterization of an organism that produces type E botulinal toxin but which resembles Clostridium butyricum from the feces of an infant with type E botulism. Journal of clinical microbiology *23*, 201-202.

Melia, T.J., Weber, T., McNew, J.A., Fisher, L.E., Johnston, R.J., Parlati, F., Mahal, L.K., Sollner, T.H., and Rothman, J.E. (2002). Regulation of membrane fusion by the membrane-proximal coil of the t-SNARE during zippering of SNAREpins. The Journal of cell biology *158*, 929-940.

Menestrina, G., Schiavo, G., and Montecucco, C. (1994). Molecular mechanisms of action of bacterial protein toxins. Mol Aspects Med *15*, 79-193.

Miesenbock, G., De Angelis, D.A., and Rothman, J.E. (1998). Visualizing secretion and synaptic transmission with pH-sensitive green fluorescent proteins. Nature *394*, 192-195.

Miller, C.J., Elliott, J.L., and Collier, R.J. (1999). Anthrax protective antigen: prepore-to-pore conversion. Biochemistry *38*, 10432-10441.

Model, K., Meisinger, C., and Kuhlbrandt, W. (2008). Cryo-electron microscopy structure of a yeast mitochondrial preprotein translocase. J Mol Biol *383*, 1049-1057.

Montal, M. (2010). Botulinum neurotoxin: a marvel of protein design. Annu Rev Biochem *79*, 591-617.

Montecucco, C., and Molgo, J. (2005). Botulinal neurotoxins: revival of an old killer. Curr Opin Pharmacol *5*, 274-279.

Montecucco, C., Schiavo, G., Brunner, J., Duflot, E., Boquet, P., and Roa, M. (1986). Tetanus toxin is labeled with photoactivatable phospholipids at low pH. Biochemistry *25*, 919-924.

Mothes, W., Boerger, A.L., Narayan, S., Cunningham, J.M., and Young, J.A. (2000). Retroviral entry mediated by receptor priming and low pH triggering of an envelope glycoprotein. Cell *103*, 679-689.

Muraro, L., Tosatto, S., Motterlini, L., Rossetto, O., and Montecucco, C. (2009). The N-terminal half of the receptor domain of botulinum neurotoxin A binds to microdomains of the plasma membrane. Biochemical and biophysical research communications *380*, 76-80.

Nishi, T., and Forgac, M. (2002). The vacuolar (H+)-ATPases--nature's most versatile proton pumps. Nat Rev Mol Cell Biol *3*, 94-103.

Nishiki, T., Kamata, Y., Nemoto, Y., Omori, A., Ito, T., Takahashi, M., and Kozaki, S. (1994). Identification of protein receptor for Clostridium botulinum type B neurotoxin in rat brain synaptosomes. The Journal of biological chemistry *269*, 10498-10503.

Nishiki, T., Tokuyama, Y., Kamata, Y., Nemoto, Y., Yoshida, A., Sato, K., Sekiguchi, M., Takahashi, M., and Kozaki, S. (1996a). The high-affinity binding of Clostridium botulinum type B neurotoxin to synaptotagmin II associated with gangliosides GT1b/GD1a. FEBS letters *378*, 253-257.

Nishiki, T., Tokuyama, Y., Kamata, Y., Nemoto, Y., Yoshida, A., Sato, K., Sekiguchi, M., Takahashi, M., and Kozaki, S. (1996b). The high-affinity binding of Clostridium botulinum

type B neurotoxin to synaptotagmin II associated with gangliosides GT1b/GD1a. FEBS Lett *378*, 253-257.

Nishiki, T., Tokuyama, Y., Kamata, Y., Nemoto, Y., Yoshida, A., Sekiguchi, M., Takahashi, M., and Kozaki, S. (1996c). Binding of botulinum type B neurotoxin to Chinese hamster ovary cells transfected with rat synaptotagmin II cDNA. Neuroscience letters *208*, 105-108.

Niwa, K., Koyama, K., Inoue, S., Suzuki, T., Hasegawa, K., Watanabe, T., Ikeda, T., and Ohyama, T. (2007). Role of nontoxic components of serotype D botulinum toxin complex in permeation through a Caco-2 cell monolayer, a model for intestinal epithelium. FEMS Immunol Med Microbiol *49*, 346-352.

Niwa, K., Yoneyama, T., Ito, H., Taira, M., Chikai, T., Kouguchi, H., Suzuki, T., Hasegawa, K., Miyata, K., Inui, K.*, et al.* (2010). Sialic acid-dependent binding and transcytosis of serotype D botulinum neurotoxin and toxin complex in rat intestinal epithelial cells. Vet Microbiol *141*, 312-320.

Nurani, G., Lindqvist, B., and Casasnovas, J.M. (2003). Receptor priming of major group human rhinoviruses for uncoating and entry at mild low-pH environments. Journal of virology *77*, 11985-11991.

Ochanda, J.O., Syuto, B., Ohishi, I., Naiki, M., and Kubo, S. (1986). Binding of Clostridium botulinum neurotoxin to gangliosides. Journal of biochemistry *100*, 27-33.

Ogasawara, J., Kamata, Y., Sakaguchi, G., and Kozaki, S. (1991). Properties of a protease-sensitive acceptor component in mouse brain synaptosomes for Clostridium botulinum type B neurotoxin. FEMS microbiology letters *63*, 351-355.

Ohishi, I., and Sakaguchi, G. (1980). Oral toxicities of Clostridium botulinum type C and D toxins of different molecular sizes. Infection and immunity *28*, 303-309.

Ohishi, I., Sugii, S., and Sakaguchi, G. (1977). Oral toxicities of Clostridium botulinum toxins in response to molecular size. Infection and immunity *16*, 107-109.

Peng, L., Tepp, W.H., Johnson, E.A., and Dong, M. (2011). Botulinum neurotoxin D uses synaptic vesicle protein SV2 and gangliosides as receptors. PLoS pathogens *7*, e1002008.

Perier, A., Chassaing, A., Raffestin, S., Pichard, S., Masella, M., Menez, A., Forge, V., Chenal, A., and Gillet, D. (2007). Concerted protonation of key histidines triggers membrane interaction of the diphtheria toxin T domain. The Journal of biological chemistry *282*, 24239-24245.

Poirier, M.A., Xiao, W., Macosko, J.C., Chan, C., Shin, Y.K., and Bennett, M.K. (1998). The synaptic SNARE complex is a parallel four-stranded helical bundle. Nature structural biology *5*, 765-769.

Qa'Dan, M., Spyres, L.M., and Ballard, J.D. (2000). pH-induced conformational changes in Clostridium difficile toxin B. Infection and immunity *68*, 2470-2474.

Rehling, P., Model, K., Brandner, K., Kovermann, P., Sickmann, A., Meyer, H.E., Kuhlbrandt, W., Wagner, R., Truscott, K.N., and Pfanner, N. (2003). Protein insertion into the mitochondrial inner membrane by a twin-pore translocase. Science *299*, 1747-1751.

Rodnin, M.V., Kyrychenko, A., Kienker, P., Sharma, O., Vargas-Uribe, M., Collier, R.J., Finkelstein, A., and Ladokhin, A.S. (2011). Replacement of C-terminal histidines uncouples

membrane insertion and translocation in diphtheria toxin T-domain. Biophysical journal *101*, L41-43.

Rossetto, O., Schiavo, G., Montecucco, C., Poulain, B., Deloye, F., Lozzi, L., and Shone, C.C. (1994). SNARE motif and neurotoxins. Nature *372*, 415-416.

Rotz, L.D., Khan, A.S., Lillibridge, S.R., Ostroff, S.M., and Hughes, J.M. (2002). Public health assessment of potential biological terrorism agents. Emerg Infect Dis *8*, 225-230.

Rummel, A., Eichner, T., Weil, T., Karnath, T., Gutcaits, A., Mahrhold, S., Sandhoff, K., Proia, R.L., Acharya, K.R., Bigalke, H.*, et al.* (2007a). Identification of the protein receptor binding site of botulinum neurotoxins B and G proves the double-receptor concept. Proceedings of the National Academy of Sciences of the United States of America *104*, 359-364.

Rummel, A., Eichner, T., Weil, T., Karnath, T., Gutcaits, A., Mahrhold, S., Sandhoff, K., Proia, R.L., Acharya, K.R., Bigalke, H.*, et al.* (2007b). Identification of the protein receptor binding site of botulinum neurotoxins B and G proves the double-receptor concept. Proc Natl Acad Sci U S A *104*, 359-364.

Rummel, A., Hafner, K., Mahrhold, S., Darashchonak, N., Holt, M., Jahn, R., Beermann, S., Karnath, T., Bigalke, H., and Binz, T. (2009). Botulinum neurotoxins C, E and F bind gangliosides via a conserved binding site prior to stimulation-dependent uptake with botulinum neurotoxin F utilising the three isoforms of SV2 as second receptor. Journal of neurochemistry *110*, 1942-1954.

Rummel, A., Karnath, T., Henke, T., Bigalke, H., and Binz, T. (2004a). Synaptotagmins I and II act as nerve cell receptors for botulinum neurotoxin G. The Journal of biological chemistry *279*, 30865-30870.

Rummel, A., Mahrhold, S., Bigalke, H., and Binz, T. (2004b). The HCC-domain of botulinum neurotoxins A and B exhibits a singular ganglioside binding site displaying serotype specific carbohydrate interaction. Mol Microbiol *51*, 631-643.

Saito, M., and Sugiyama, K. (2002). Characterization of nuclear gangliosides in rat brain: concentration, composition, and developmental changes. Arch Biochem Biophys *398*, 153-159.

Saslowsky, D.E., Lawrence, J., Ren, X., Brown, D.A., Henderson, R.M., and Edwardson, J.M. (2002). Placental alkaline phosphatase is efficiently targeted to rafts in supported lipid bilayers. J Biol Chem *277*, 26966-26970.

Schantz, E.J., and Johnson, E.A. (1992). Properties and use of botulinum toxin and other microbial neurotoxins in medicine. Microbiol Rev *56*, 80-99.

Schiavo, G. (2006). Structural biology: dangerous liaisons on neurons. Nature *444*, 1019-1020.

Schiavo, G., Benfenati, F., Poulain, B., Rossetto, O., Polverino de Laureto, P., DasGupta, B.R., and Montecucco, C. (1992). Tetanus and botulinum-B neurotoxins block neurotransmitter release by proteolytic cleavage of synaptobrevin. Nature *359*, 832-835.

Schiavo, G., Matteoli, M., and Montecucco, C. (2000). Neurotoxins affecting neuroexocytosis. Physiol Rev *80*, 717-766.

Schiavo, G., Rossetto, O., Catsicas, S., Polverino de Laureto, P., DasGupta, B.R., Benfenati, F., and Montecucco, C. (1993a). Identification of the nerve terminal targets of botulinum neurotoxin serotypes A, D, and E. The Journal of biological chemistry *268*, 23784-23787.

Schiavo, G., Santucci, A., Dasgupta, B.R., Mehta, P.P., Jontes, J., Benfenati, F., Wilson, M.C., and Montecucco, C. (1993b). Botulinum neurotoxins serotypes A and E cleave SNAP-25 at distinct COOH-terminal peptide bonds. FEBS letters *335*, 99-103.

Schiavo, G., Shone, C.C., Bennett, M.K., Scheller, R.H., and Montecucco, C. (1995). Botulinum neurotoxin type C cleaves a single Lys-Ala bond within the carboxyl-terminal region of syntaxins. The Journal of biological chemistry *270*, 10566-10570.

Schiavo, G., Shone, C.C., Rossetto, O., Alexander, F.C., and Montecucco, C. (1993c). Botulinum neurotoxin serotype F is a zinc endopeptidase specific for VAMP/synaptobrevin. The Journal of biological chemistry *268*, 11516-11519.

Schmidt, J.J., and Siegel, L.S. (1986). Purification of type E botulinum neurotoxin by high-performance ion exchange chromatography. Analytical biochemistry *156*, 213-219.

Schmitt, J., Karalewitz, A., Benefield, D.A., Mushrush, D.J., Pruitt, R.N., Spiller, B.W., Barbieri, J.T., and Lacy, D.B. (2010). Structural analysis of botulinum neurotoxin type G receptor binding. Biochemistry *49*, 5200-5205.

Schneider, S.W., Larmer, J., Henderson, R.M., and Oberleithner, H. (1998). Molecular weights of individual proteins correlate with molecular volumes measured by atomic force microscopy. Pflugers Arch *435*, 362-367.

Sheridan, R.E. (1998). Gating and permeability of ion channels produced by botulinum toxin types A and E in PC12 cell membranes. Toxicon *36*, 703-717.

Simpson, L.L. (1980). Kinetic studies on the interaction between botulinum toxin type A and the cholinergic neuromuscular junction. The Journal of pharmacology and experimental therapeutics *212*, 16-21.

Simpson, L.L. (1981). The origin, structure, and pharmacological activity of botulinum toxin. Pharmacol Rev *33*, 155-188.

Simpson, L.L. (1982). The interaction between aminoquinolines and presynaptically acting neurotoxins. J Pharmacol Exp Ther *222*, 43-48.

Simpson, L.L. (1983). Ammonium chloride and methylamine hydrochloride antagonize clostridial neurotoxins. J Pharmacol Exp Ther *225*, 546-552.

Simpson, L.L. (2004). Identification of the major steps in botulinum toxin action. Annu Rev Pharmacol Toxicol *44*, 167-193.

Simpson, L.L., Coffield, J.A., and Bakry, N. (1994a). Inhibition of vacuolar adenosine triphosphatase antagonizes the effects of clostridial neurotoxins but not phospholipase A2 neurotoxins. J Pharmacol Exp Ther *269*, 256-262.

Simpson, L.L., Coffield, J.A., and Bakry, N. (1994b). Inhibition of vacuolar adenosine triphosphatase antagonizes the effects of clostridial neurotoxins but not phospholipase A2 neurotoxins. The Journal of pharmacology and experimental therapeutics *269*, 256-262.

Simpson, L.L., and Dasgupta, B.R. (1983). Botulinum neurotoxin type E: studies on mechanism of action and on structure-activity relationships. The Journal of pharmacology and experimental therapeutics *224*, 135-140.

Simpson, L.L., and Rapport, M.M. (1971a). The binding of botulinum toxin to membrane lipids: sphingolipids, steroids and fatty acids. Journal of neurochemistry *18*, 1751-1759.

Simpson, L.L., and Rapport, M.M. (1971b). Ganglioside inactivation of botulinum toxin. Journal of neurochemistry *18*, 1341-1343.

Sonnino, S., Ghidoni, R., Marchesini, S., and Tettamanti, G. (1979). Cytosolic gangliosides: occurrence in calf brain as ganglioside--protein complexes. Journal of neurochemistry *33*, 117-121.

Steinbuch, J.G. (1817). Vergiftung durch verdorbene Wu¨rste. Tu¨binger Bla¨tter fu¨r Naturwissenschaften und Arzneykunde *3*, 26-52.

Stenmark, P., Dupuy, J., Imamura, A., Kiso, M., and Stevens, R.C. (2008). Crystal structure of botulinum neurotoxin type A in complex with the cell surface co-receptor GT1b-insight into the toxin-neuron interaction. PLoS pathogens *4*, e1000129.

Suen, J.C., Hatheway, C.L., Steigerwalt, A.G., and Brenner, D.J. (1988). Genetic confirmation of identities of neurotoxigenic Clostridium baratii and Clostridium butyricum implicated as agents of infant botulism. Journal of clinical microbiology *26*, 2191-2192.

Sun, J., Vernier, G., Wigelsworth, D.J., and Collier, R.J. (2007). Insertion of anthrax protective antigen into liposomal membranes: effects of a receptor. J Biol Chem *282*, 1059-1065.

Sun, S., Suresh, S., Liu, H., Tepp, W.H., Johnson, E.A., Edwardson, J.M., and Chapman, E.R. (2011). Receptor binding enables botulinum neurotoxin B to sense low pH for translocation channel assembly. Cell Host Microbe *10*, 237-247.

Suresh, S., and Edwardson, J.M. The endophilin N-BAR domain perturbs the structure of lipid bilayers. Biochemistry *49*, 5766-5771.

Suresh, S., and Edwardson, J.M. (2010). Phase separation in lipid bilayers triggered by low pH. Biochemical and biophysical research communications *399*, 571-574.

Sutton, R.B., Ernst, J.A., and Brunger, A.T. (1999). Crystal structure of the cytosolic C2A-C2B domains of synaptotagmin III. Implications for Ca(+2)-independent snare complex interaction. The Journal of cell biology *147*, 589-598.

Sutton, R.B., Fasshauer, D., Jahn, R., and Brunger, A.T. (1998). Crystal structure of a SNARE complex involved in synaptic exocytosis at 2.4 A resolution. Nature *395*, 347-353.

Svennerholm, L. (1980). Ganglioside designation. Advances in experimental medicine and biology *125*, 11.

Swaminathan, S. (2011). Molecular structures and functional relationships in clostridial neurotoxins. Febs J *278*, 4467-4485.

Swaminathan, S., and Eswaramoorthy, S. (2000). Structural analysis of the catalytic and binding sites of Clostridium botulinum neurotoxin B. Nat Struct Biol *7*, 693-699.

Tettamanti, G., and Riboni, L. (1993). Gangliosides and modulation of the function of neural cells. Advances in lipid research *25*, 235-267.

Tsukamoto, K., Kohda, T., Mukamoto, M., Takeuchi, K., Ihara, H., Saito, M., and Kozaki, S. (2005). Binding of Clostridium botulinum type C and D neurotoxins to ganglioside and

phospholipid. Novel insights into the receptor for clostridial neurotoxins. The Journal of biological chemistry *280*, 35164-35171.

Tsukamoto, K., Kozai, Y., Ihara, H., Kohda, T., Mukamoto, M., Tsuji, T., and Kozaki, S. (2008). Identification of the receptor-binding sites in the carboxyl-terminal half of the heavy chain of botulinum neurotoxin types C and D. Microbial pathogenesis *44*, 484-493.

Tucker, W.C., Weber, T., and Chapman, E.R. (2004). Reconstitution of Ca2+-regulated membrane fusion by synaptotagmin and SNAREs. Science *304*, 435-438.

Van Ermengem, E.P. (1897). U¨ber einen neuen anaeroben Bacillus und seine Beziehung zum Botulismus. Z Hyg Infektionskrankh *26*, 1-56.

Vernier, G., Wang, J., Jennings, L.D., Sun, J., Fischer, A., Song, L., and Collier, R.J. (2009). Solubilization and characterization of the anthrax toxin pore in detergent micelles. Protein Sci *18*, 1882-1895.

Wang, J., Meng, J., Lawrence, G.W., Zurawski, T.H., Sasse, A., Bodeker, M.O., Gilmore, M.A., Fernandez-Salas, E., Francis, J., Steward, L.E.*, et al.* (2008). Novel chimeras of botulinum neurotoxins A and E unveil contributions from the binding, translocation, and protease domains to their functional characteristics. The Journal of biological chemistry *283*, 16993-17002.

Weber, T., Zemelman, B.V., McNew, J.A., Westermann, B., Gmachl, M., Parlati, F., Sollner, T.H., and Rothman, J.E. (1998). SNAREpins: minimal machinery for membrane fusion. Cell *92*, 759-772.

Wei, Z., and Song, J. (2005). Molecular mechanism underlying the thermal stability and pH-induced unfolding of CHABII. Journal of molecular biology *348*, 205-218.

Williams, R.S., Tse, C.K., Dolly, J.O., Hambleton, P., and Melling, J. (1983). Radioiodination of botulinum neurotoxin type A with retention of biological activity and its binding to brain synaptosomes. European journal of biochemistry / FEBS *131*, 437-445.

Williamson, L.C., and Neale, E.A. (1998). Syntaxin and 25-kDa synaptosomal-associated protein: differential effects of botulinum neurotoxins C1 and A on neuronal survival. J Neurosci Res *52*, 569-583.

Woodruff, B.A., Griffin, P.M., McCroskey, L.M., Smart, J.F., Wainwright, R.B., Bryant, R.G., Hutwagner, L.C., and Hatheway, C.L. (1992). Clinical and laboratory comparison of botulism from toxin types A, B, and E in the United States, 1975-1988. The Journal of infectious diseases *166*, 1281-1286.

Wu, G., Lu, Z.H., and Ledeen, R.W. (1995). GM1 ganglioside in the nuclear membrane modulates nuclear calcium homeostasis during neurite outgrowth. Journal of neurochemistry *65*, 1419-1422.

Yamasaki, S., Baumeister, A., Binz, T., Blasi, J., Link, E., Cornille, F., Roques, B., Fykse, E.M., Sudhof, T.C., Jahn, R.*, et al.* (1994a). Cleavage of members of the synaptobrevin/VAMP family by types D and F botulinal neurotoxins and tetanus toxin. The Journal of biological chemistry *269*, 12764-12772.

Yamasaki, S., Binz, T., Hayashi, T., Szabo, E., Yamasaki, N., Eklund, M., Jahn, R., and Niemann, H. (1994b). Botulinum neurotoxin type G proteolyses the Ala81-Ala82 bond of rat synaptobrevin 2. Biochemical and biophysical research communications *200*, 829-835.

Young, J.A., and Collier, R.J. (2007). Anthrax toxin: receptor binding, internalization, pore formation, and translocation. Annu Rev Biochem *76*, 243-265.